

**Comparing lightning polarity and cloud  
microphysical properties over regions of high  
ground flash density in South Africa**

by

**Lee-ann SIMPSON**

Submitted in partial fulfillment of the requirements

for the degree

**MASTER OF SCIENCE**

in the

Faculty of Natural and Agricultural Sciences

University of Pretoria

**April 2013**

## DECLARATION

I *Lee-ann Simpson*, declare that the dissertation, which I hereby submit for the degree *Master of Science* at the University of Pretoria, is my own work and has not previously been submitted by me for a degree at this or any other tertiary institution.

---

SIGNATURE

---

DATE

# **Comparing lightning polarity and cloud microphysical properties over regions of high ground flash density in South Africa**

Lee-ann SIMPSON

Promoter: Professor Cornelis Johannes de Wet Rautenbach  
Department: Geography, Geoinformatics and Meteorology  
Faculty: Faculty of Natural and Agricultural Sciences  
University: University of Pretoria

Degree: Master of Science in Meteorology

## **SUMMARY**

Positive lightning flashes are known to be more intense and cause more damage than negative flashes, although positive flashes only occur about 10% of the time. This study expounds on cloud microphysical aspects of thunderstorms and investigates the occurrence, timing and location of ice particles within thunderstorms and correlates this to the occurrence of positive cloud-to-ground lightning events.

Satellite data obtained from the Meteosat Second Generation (MSG) satellite, were used to: 1) depict Cloud Top Temperatures (CTT) by considering Infra Red (IR) radiation with a wave length of  $10.8\mu\text{m}$ , 2) compare results from the CTT with the Brightness Temperature Difference (BTD) calculated by subtracting  $IR_{10.8\mu\text{m}}$  from  $IR_{8.7\mu\text{m}}$ , 3) after the cloud particle phase was determined from the abovementioned comparison, the sum of cloud-to-ground lightning strokes over a 1-hour period around the time of a reported lightning fatality was compared with cloud microphysical properties and then 4) these results were further compared with the lightning polarity obtained from the South African Weather Service (SAWS) Lightning Detection Network (LDN) data set.

Four case studies were identified to investigate from the many available case study dates. These four cases occurred on 3 separate days namely: 1) 22 November 2007,

2) 10 February 2009 and 3) 29 October 2009. There were two fatal events reported on 22 November 2007 and therefore two case studies were compiled for this one date. On 10 February 2009 over 250 insurance damage claims were honoured but no fatality was reported. The three case studies mentioned above were classified as primary case studies. The 29 October 2009 case was classified as a secondary, more generalized case which was chosen in order to test whether the results gained from the first three cases were indeed noteworthy.

Results gathered from two of the three primary case studies showed that the fatalities occurred when the most intense part of the thunderstorm was to the east of the location where the lightning struck the victims, although actual storm properties were not considered as being particularly severe. The lightning data for the primary case studies showed that the percentage of cloud-to-ground lightning was within 10% of the total number of strokes recorded for 22 November 2007, and above 10% for 10 February 2009. In the one secondary case study of 29 October 2009 the percentage of positive lightning was only between 2% and 4% of the total number of strokes recorded, which was significantly lower than in the three primary cases. A significant difference in cloud microphysics between the primary and secondary cases was the possible occurrence of super-cooled liquid water found in Cumulonimbus (CB) clouds in the secondary case. This could have been a determining factor for the difference in percentage of positive lightning between the primary and secondary case studies.

## ACKNOWLEDGEMENTS

- I would like to thank my supervisor Professor Hannes Rautenbach for his guidance and assistance in this dissertation.
- Professor Sivakumar Venkataraman, thank you for your help and advice during the past two years, your input has been invaluable.
- A very big thank you to Dr Estelle de Coning for your advice and help, especially regarding the Meteosat Second Generation Satellite data and the programming required with it.
- Thank you Morne Gijben for all of the help with the retrieval and programming of the lightning data set.
- I would like to extend my gratitude to Charlotte McBride, Karin Marais and Anastasia Demertzis at the South African Weather Service (SAWS) who were always willing to help, even at short notice.
- To my colleagues in the Regional Training Center, thank you all for your support during the past two years.
- Thank you as well to EUMETSAT and SAWS for the satellite and lightning data sets used in this study.
- A very special thank you to my husband Ian who's constant encouragement and support carried me through many difficult days and nights.
- To my daughter Erin, a very big thank you for making me smile every time I looked up from my work while at home.

# Table of Contents

CHAPTER 1 .....	1
Introduction .....	1
1.1 Background .....	1
1.2 Motivation for the research.....	8
1.3 Aim and objectives.....	9
1.4 Organization of the report .....	11
CHAPTER 2 .....	13
Lightning and cloud microphysics.....	13
2.1 Lightning.....	13
2.2 Cloud microphysics .....	21
2.3 Cloud particles.....	22
CHAPTER 3 .....	24
Data and methodology .....	24
3.1 Data.....	25
3.2 Methodology.....	27
CHAPTER 4 .....	33
Case studies .....	33
4.1 Primary case studies .....	33
4.2 Secondary case study.....	53
CHAPTER 5 .....	67
Case study summaries and combined results.....	67
5.1 Case study summaries .....	67
5.2 Combined results .....	71
CHAPTER 6 .....	78
Conclusion and recommendations .....	78
6.1 Conclusion.....	78
6.2 Recommendations .....	82
References .....	83
APPENDIX A.....	87

APPENDIX B.....	88
APPENDIX C.....	95

## LIST OF SYMBOLS

$\mu$	$1 \times 10^{-6}$
kA	Kilo ampere
mm	Millimeter
m	Meter
km	kilometer
°	Degree
°C	Degrees Celsius
K	Degrees Kelvin
$r_e$	Effective radius
%	Percentage
T	Temperature
Z	Zulu time
y	Year



## LIST OF ACRONYMS

Absa	Amalgamated Banks of South Africa
AMS	American Meteorological Society
AMSL	Above Mean Sea Level
BMP	Bitmap Image file
BTD	Brightness Temperature Difference
CB	Cumulonimbus
CTT	Cloud Top Temperature
DAAC	Distributed Active Archive Center
EOSDIS	Earth Observing System Data and Information System
EUMETSAT	European Organisation for the Exploitation of Meteorological Satellites
GHRC	Global Hydrology Resource Center
GrAds	Grid Analysis display system
HRIT	High Resolution Image Transfer
HRV	High Resolution Visible image
IR	Infra Red image
LDN	Lightning Detection Network
LIS	Lightning Imaging Sensor
MDF	Magnetic Direction Finding
MSG	Meteosat Second Generation
NASA	National Aeronautics and Space Administration
NIC	Non-Inductive Charge transfer
NIR	Near Infra Red
PLRI	Positive Lightning Risk Index

RGB	Red Green Blue colour combination
SAST	South African Standard Time
SAWS	South African Weather Service
SCF	Science Computing Facility
SUMO	Software for the Utilization of Meteosat in Outlook activities
TOA	Time Of Arrival
USA	United States of America
UTC	Coordinated Universal Time
VIS	Visible
WV	Water Vapour

## LIST OF FIGURES

FIGURE 1.1	A topographical map of South Africa, indicating altitude Above Mean Sea Level (AMSL) in meters (m). Lesotho and the nine provinces of South Africa are indicated.	1
FIGURE 1.2	Mean annual precipitation, measured in millimeters (mm), over South Africa. From Dent <i>et al.</i> (1989)	3
FIGURE 1.3	Annual average (2006 to 2011) ground flash density, measured in flashes per square kilometer per year ( $\text{km}^{-2} \cdot \text{y}^{-1}$ ), over South Africa. From Gijben (2012)	4
FIGURE 1.4	Global annual lightning flash density measured in flashes per square kilometer per year ( $\text{km}^{-2} \cdot \text{y}^{-1}$ ), based on a $2.5^\circ$ grid from the Lightning Imaging Sensor (LIS). Courtesy: Global Hydrology Resource Center (GHRC) Distributed Active Archive Center (DAAC)/Lightning Imaging Sensor (LIS) Science Computing Facility (SCF)	5
FIGURE 2.1	Negative and positive charge distribution within a thundercloud, where N is the negative charge, P is the upper positive charge, $p$ the positive charge found at the cloud base and $gc$ the positive charge found above the surface of the earth. Adapted from Malan (1963) and incorporating ideas from Kriebhel (1986)	15
FIGURE 2.2	Location and paths of negatively and positively charged cloud-to-ground lightning strokes according to the typical charge distribution within a thunderstorm. Adapted from Rakov and Uman (2003) and Malan (1963)	19
FIGURE 2.3	Average flash multiplicity measured in number of flashes over the period 2006 to 2011 over South Africa. From Gijben (2012)	20
FIGURE 3.1	South African Weather Service (SAWS) Lightning Detection Network (LDN) sensor sites in 2012. Source: SAWS	26
FIGURE 4.1	A satellite image depicting the location of two reported fatalities caused by lightning strikes (points A and C) and one injury caused by a lightning strike (point B) for 22 November 2007. Point A represents Randfontein, point B represents Gold Reef City and point C represents Northcliff. From Google Earth (2010)	33

- FIGURE 4.2 Meteosat Second Generation (MSG) satellite imagery over the Gauteng Province at 1415Z for 22 November 2007. The High Resolution Visible (HRV) image is at the top, the inverted Infra Red (IR) 10.8 $\mu$ m is on the bottom left hand side and the convection combination is on the bottom right hand side. Copyright (2013) EUMETSAT 34
- FIGURE 4.3 Grid Analysis display system (GrAds) imagery of Infra Red (IR) 10.8 $\mu$ m data in degrees Kelvin (K) on the left hand side and Brightness Temperature Difference (BTD) of IR8.7 $\mu$ m-IR10.8 $\mu$ m measured in K on the right hand side, for 22 November 2007 at 1415Z. Copyright (2013) EUMETSAT 35
- FIGURE 4.4 Sum of the lightning strokes detected over the Gauteng Province are depicted on the left hand side and the percentage (%) of positively charged lightning strokes over the Gauteng Province are depicted on the right hand side, for 22 November 2007 between 1400Z and 1415Z. 36
- FIGURE 4.5 Meteosat Second Generation (MSG) satellite imagery over the Gauteng Province at 1500Z for 22 November 2007. The High Resolution Visible (HRV) image is at the top, the inverted Infra Red (IR) 10.8 $\mu$ m is on the bottom left hand side and the convection combination is on the bottom right hand side. Copyright (2013) EUMETSAT 37
- FIGURE 4.6 Grid Analysis display system (GrAds) imagery of Infra Red (IR)10.8 $\mu$ m data in degrees Kelvin (K) on the left hand side and Brightness Temperature Difference (BTD) of IR8.7 $\mu$ m-IR10.8 $\mu$ m measured in (K) on the right hand side, for 22 November 2007 at 1500Z. Copyright (2013) EUMETSAT 38
- FIGURE 4.7 Sum of the lightning strokes detected over the Gauteng Province are depicted on the left hand side and the percentage (%) of positively charged lightning strokes over Gauteng are depicted on the right hand side, for 22 November 2007 between 1500Z and 1515Z. 39
- FIGURE 4.8 A graph depicting the daily totals and the monthly average of honoured lightning related insurance claims from the Amalgamated banks of South Africa (Absa) for the month of February 2009 over the Highveld of South Africa. 40

- FIGURE 4.9 Meteosat Second Generation (MSG) satellite imagery over the Gauteng Province at 1300Z for 10 February 2009. The High Resolution Visible (HRV) satellite image, inverted Infra Red (IR) 10.8 $\mu$ m satellite image, convection channel combination are depicted from top left to the bottom center. Copyright (2013) EUMETSAT 41
- FIGURE 4.10 The Grid Analysis display system (GrAds) imagery of IR10.8 $\mu$ m measured in degrees Kelvin (K) is on the left hand side and the Brightness Temperature Difference (BTD) of IR8.7 $\mu$ m – IR10.8 $\mu$ m measured in K is on the right hand side for 10 February 2009 at 1300Z. Copyright (2013) EUMETSAT 42
- FIGURE 4.11 Meteosat Second Generation (MSG) satellite imagery over the Gauteng Province at 1315Z for 10 February 2009. The High Resolution Visible (HRV) satellite image, inverted Infra Red (IR) 10.8 $\mu$ m satellite image, convection channel combination are depicted from top left to the bottom center. Copyright (2013) EUMETSAT 43
- FIGURE 4.12 The Grid Analysis display system (GrAds) imagery of IR10.8 $\mu$ m measured in degrees Kelvin (K) is on the left hand side and the Brightness Temperature Difference (BTD) of IR8.7 $\mu$ m – IR10.8 $\mu$ m measured in K is on the right hand side for 10 February 2009 at 1315Z. Copyright (2013) EUMETSAT 44
- FIGURE 4.13 Meteosat Second Generation (MSG) satellite imagery over the Gauteng Province at 1330Z for 10 February 2009. The High Resolution Visible (HRV) satellite image, inverted Infra Red (IR) 10.8 $\mu$ m satellite image, convection channel combination are depicted from top left to the bottom center. Copyright (2013) EUMETSAT 45
- FIGURE 4.14 The Grid Analysis display system (GrAds) imagery of IR10.8 $\mu$ m measured in degrees Kelvin (K) is on the left hand side and the Brightness Temperature Difference (BTD) of IR8.7 $\mu$ m – IR10.8 $\mu$ m measured in K is on the right hand side, for 10 February 2009 at 1330Z. Copyright (2013) EUMETSAT 46
- FIGURE 4.15 Meteosat Second Generation (MSG) satellite imagery over the Gauteng Province at 1345Z for 10 February 2009. The High Resolution Visible (HRV) satellite image, inverted Infra Red (IR) 10.8 $\mu$ m satellite image, convection channel combination are depicted from top left to the bottom center. Copyright (2013) EUMETSAT 47

- FIGURE 4.16 The Grid Analysis display system (GrAds) imagery of IR10.8 $\mu$ m measured in degrees Kelvin (K) is on the left hand side and the Brightness Temperature Difference (BTD) of IR8.7 $\mu$ m – IR10.8 $\mu$ m measured in K is on the right hand side for 10 February 2009 at 1345Z. Copyright (2013) EUMETSAT 48
- FIGURE 4.17 Meteosat Second Generation (MSG) satellite imagery over the Gauteng Province at 1400Z for 10 February 2009. The High Resolution Visible (HRV) satellite image, inverted Infra Red (IR) 10.8 $\mu$ m satellite image, convection channel combination are depicted from top left to the bottom center. Copyright (2013) EUMETSAT 49
- FIGURE 4.18 The Grid Analysis display system (GrAds) imagery of IR10.8 $\mu$ m measured in degrees Kelvin (K) is on the left hand side and the Brightness Temperature Difference (BTD) of IR8.7 $\mu$ m – IR10.8 $\mu$ m measured in K is on the right hand side for 10 February 2009 at 1400Z. Copyright (2013) EUMETSAT 50
- FIGURE 4.19 Total lightning strokes detected over the Gauteng Province for 10 February 2009 between 1300Z and 1400Z are on the left hand side and the percentage (%) of positively charged lightning strokes detected during the corresponding time period are depicted on the right hand side. 51
- FIGURE 4.20 Total lightning strokes detected over the Gauteng Province for 10 February 2009 between 1330Z and 1400Z are on the left hand side and the percentage (%) of positively charged lightning strokes detected during the corresponding time period are depicted on the right hand side. 52
- FIGURE 4.21 Total lightning strokes detected over the Gauteng Province for 10 February 2009 between 1330Z and 1345Z are on the left hand side and the percentage (%) of positively charged lightning strokes detected during the corresponding time period are depicted on the right hand side. 52
- FIGURE 4.22 Total lightning strokes detected over the Gauteng Province for 10 February 2009 between 1345Z and 1400Z are on the left hand side and the percentage (%) of positively charged lightning strokes detected during the corresponding time period are depicted on the right hand side. 53
- FIGURE 4.23 Meteosat Second Generation (MSG) satellite imagery over the Mpumalanga Province at 1500Z for 29 October 2009. The High Resolution Visible (HRV) satellite image, inverted Infra Red (IR) 10.8 $\mu$ m satellite image, convection channel combination are depicted from top left to the bottom center. Copyright (2013) EUMETSAT 55

- FIGURE 4.24 The Grid Analysis display system (GrAds) imagery of IR10.8 $\mu$ m measured in degrees Kelvin (K) is on the left hand side and the Brightness Temperature Difference (BTD) of IR8.7 $\mu$ m – IR10.8 $\mu$ m measured in K is on the right hand side for 29 October 2009 at 1500Z. Copyright (2013) EUMETSAT 56
- FIGURE 4.25 Meteosat Second Generation (MSG) satellite imagery over the Mpumalanga Province at 1515Z for 29 October 2009. The High Resolution Visible (HRV) satellite image, inverted Infra Red (IR) 10.8 $\mu$ m satellite image, convection channel combination are depicted from top left to the bottom center. Copyright (2013) EUMETSAT 57
- FIGURE 4.26 The Grid Analysis display system (GrAds) imagery of IR10.8 $\mu$ m measured in degrees Kelvin (K) is on the left hand side and the Brightness Temperature Difference (BTD) of IR8.7 $\mu$ m – IR10.8 $\mu$ m measured in K is on the right hand side for 29 October 2009 at 1515Z. Copyright (2013) EUMETSAT 58
- FIGURE 4.27 Meteosat Second Generation (MSG) satellite imagery over the Mpumalanga Province at 1530Z for 29 October 2009. The High Resolution Visible (HRV) satellite image on the left hand side and inverted Infra Red (IR) 10.8 $\mu$ m satellite image on the right hand side. Copyright (2013) EUMETSAT 59
- FIGURE 4.28 The Grid Analysis display system (GrAds) imagery of IR10.8 $\mu$ m measured in degrees Kelvin (K) is on the left hand side and the Brightness Temperature Difference (BTD) of IR8.7 $\mu$ m – IR10.8 $\mu$ m measured in K is on the right hand side for 29 October 2009 at 1530Z. Copyright (2013) EUMETSAT 59
- FIGURE 4.29 Meteosat Second Generation (MSG) satellite imagery over the Mpumalanga Province at 1545Z for 29 October 2009. The High Resolution Visible (HRV) satellite image on the left hand side and inverted Infra Red (IR) 10.8 $\mu$ m satellite image on the right hand side. Copyright (2013) EUMETSAT 60
- FIGURE 4.30 The Grid Analysis display system (GrAds) imagery of IR10.8 $\mu$ m measured in degrees Kelvin (K) is on the left hand side and the Brightness Temperature Difference (BTD) of IR8.7 $\mu$ m – IR10.8 $\mu$ m measured in K is on the right hand side for 29 October 2009 at 1545Z. Copyright (2013) EUMETSAT 61
- FIGURE 4.31 Meteosat Second Generation (MSG) satellite imagery over the Mpumalanga Province at 1600Z for 29 October 2009. The High Resolution Visible (HRV) satellite image on the left hand side and inverted Infra Red (IR) 10.8 $\mu$ m satellite image on the right hand side. Copyright (2013) EUMETSAT 61

- FIGURE 4.32 The Grid Analysis display system (GrAds) imagery of IR10.8 $\mu$ m measured in degrees Kelvin (K) is on the left hand side and the Brightness Temperature Difference (BTD) of IR8.7 $\mu$ m – IR10.8 $\mu$ m measured in K is on the right hand side for 29 October 2009 at 1600Z. Copyright (2013) EUMETSAT 62
- FIGURE 4.33 Total lightning strokes detected over the Mpumalanga Province for 29 October 2009 between 1500Z and 1600Z are depicted on the left hand side. The percentage (%) of positively charged lightning strokes detected at the corresponding time are depicted on the right hand side. 63
- FIGURE 4.34 Total lightning strokes detected over the Mpumalanga Province for 29 October 2009 between 1500Z and 1530Z are depicted on the left hand side. The percentage (%) of positively charged lightning strokes detected at the corresponding time are depicted on the right hand side. 63
- FIGURE 4.35 Total lightning strokes detected over the Mpumalanga Province for 29 October 2009 between 1500Z and 1515Z are depicted on the left hand side. The percentage (%) of positively charged lightning strokes detected at the corresponding time are depicted on the right hand side. 64
- FIGURE 4.36 Total lightning strokes detected over the Mpumalanga Province for 29 October 2009 between 1515Z and 1530Z are depicted on the left hand side calculated in 30 minute. The percentage (%) of positively charged lightning strokes detected at the corresponding time are depicted on the right hand side. 64
- FIGURE 4.37 Total lightning strokes detected over the Mpumalanga Province for 29 October 2009 between 1530Z and 1600Z are depicted on the left hand side. The percentage (%) of positively charged lightning strokes detected at the corresponding time are depicted on the right hand side. 65
- FIGURE 4.38 Total lightning strokes detected over the Mpumalanga Province for 29 October 2009 between 1530Z and 1545Z are depicted on the left hand side. The percentage (%) of positively charged lightning strokes detected at the corresponding time are depicted on the right hand side. 66



FIGURE 4.39 Total lightning strokes detected over the Mpumalanga Province for 29 October 2009 between 1545Z and 1600Z are depicted on the left hand side of the figure. The percentage (%) of positively charged lightning strokes detected at the corresponding time are depicted on the right hand side of the figure. 66

## LIST OF TABLES

TABLE 5.1: Results based on satellite imagery obtained for Case 1 and Case 2 for 22 November 2007 at 1414Z and 1503Z respectively.	72
TABLE 5.2: Results based on satellite imagery obtained for Case 3 and Case 4 for 10 February 2009 and 29 October 2009.	73
TABLE 5.3: Results based on lightning data obtained for Case 1 and Case 2 for 22 November 2007 at 1414Z and 1503Z respectively.	75
TABLE 5.4: Results based on lightning data obtained for Case 2 and Case 3 for 10 February 2009 and 29 October 2009.	76

# CHAPTER 1

## Introduction

### 1.1 Background

South Africa is found at the southern tip of the African continent, sharing its northern and north-eastern borders with Namibia, Botswana, Zimbabwe and Mozambique. South Africa has an extensive coastline, with the warm Indian Ocean in the east, and the cold Atlantic Ocean in the west. Landlocked within the borders of South Africa is Lesotho. Swaziland is bordered to the north, west and south by South Africa and by Mozambique to the east. South Africa is located roughly between 22°S and 35°S, 16°E and 33°E (figure 1.1). This geographical position allows for both tropical and extra-tropical weather systems to have a significant impact on the country.

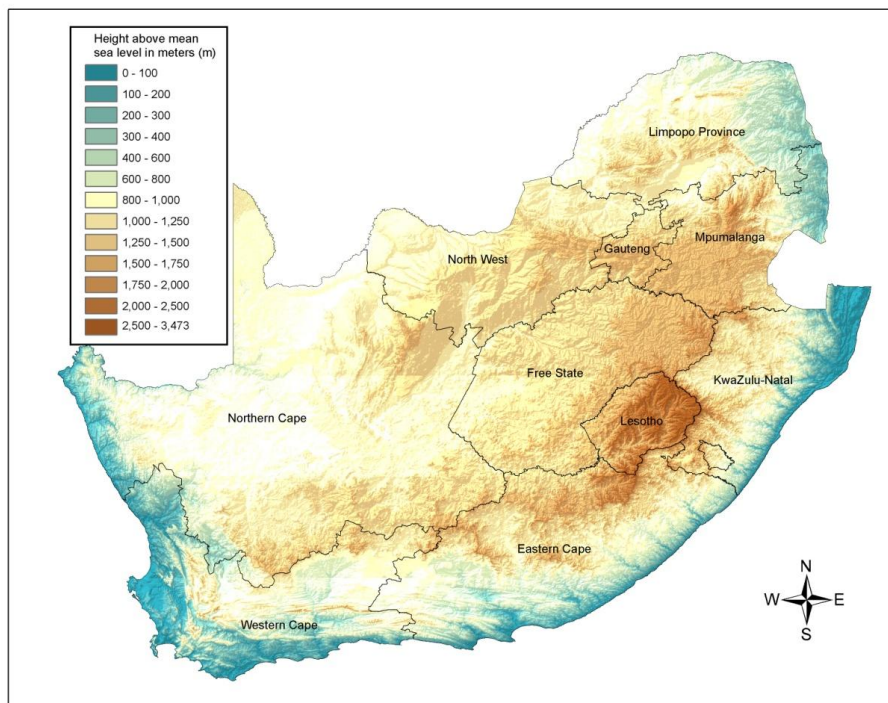


**FIGURE 1.1**

A topographical map of South Africa, indicating altitude Above Mean Sea Level (AMSL) in meters (m). Lesotho and the nine provinces of South Africa are indicated.

Kruger (2004) describes the southern African subcontinent as moderately elevated at a height of generally more than 1000m Above Mean Sea Level (AMSL), reaching heights of above 1500m AMSL over extensive areas. Kruger (2004) further states that the escarpment of South Africa, which can be found at 200km to 300km from the eastern and south-eastern coastlines, consists of mountain ranges. This escarpment encircles a central basin area which is at its lowest elevation over north-eastern Botswana.

Taljaard (1994) lists six factors which control the weather of South Africa, namely: 1) latitude, 2) position relative to the distribution of land and sea, 3) height AMSL and that of the surrounding terrain, 4) the general circulation of the atmosphere and its perturbations, 5) sea temperature and 6) the nature of the underlying surface. According to Taljaard (1996) the geographical distribution of rainfall over southern Africa is highly variable and is, to a large extent, controlled by the country's topography.

Figure 1.2 depicts annual rainfall over South Africa. Over the western interior of the region the annual rainfall is between 100mm and 200mm, with less than 100mm over the far north-western interior and coastline (Dent *et al.*, 1989). Dent *et al.* (1989) also shows the central interior regions to have annual rainfall figures of between 200mm and 600mm with the eastern interior receiving the highest annual rainfall of between 600mm and 800mm. The eastern escarpment and coastal regions receive between 800mm and 1200mm of rain with a maximum of more than 1200mm over the north-eastern escarpment (Dent *et al.*, 1989).

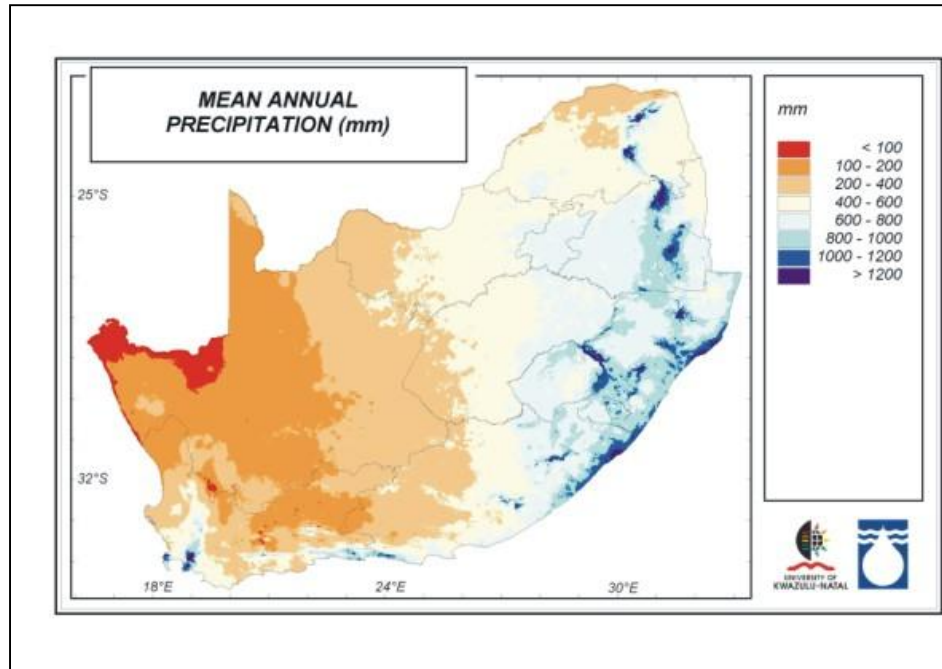


**FIGURE 1.2**

Mean annual precipitation, measured in millimeters (mm), over South Africa. From Dent *et al.* (1989)

The predominantly eastern summer rainfall region of South Africa receives most of its precipitation from thunderstorms, which are typically associated with single cell or multi-cell development (Taljaard, 1996). The basic mechanisms needed for thunderstorm development are listed by Watson *et al.* (1994) as being: 1) moisture, 2) instability and 3) a triggering mechanism.

The South African Weather Service (SAWS) installed a new Lightning Detection Network (LDN) in 2006. This network is made up of sensors which determine the time and location of a lightning flash in real-time using two methods: 1) Magnetic Direction Finding (MDF) and 2) Time Of Arrival (TOA) (VAISALA, 2004). Over the summer rainfall region, the north-eastern and eastern high ground of South Africa, including the northern Drakensberg mountains and the Highveld regions of the Gauteng and Mpumalanga Provinces, experience the highest ground flash density of lightning in the country (Gill, 2008). Ground flash density refers to the amount of lightning flashes per square kilometre (km<sup>2</sup>) over a predetermined period of time. Gijben (2012) has recently updated the ground flash density map for South Africa

(figure 1.3). In figure 1.3, the annual average ground flash density is highest over the eastern Highveld region of South Africa and to a slightly lesser extent the southern parts of Gauteng and most of Mpumalanga and western KwaZulu-Natal (figure 1.1).

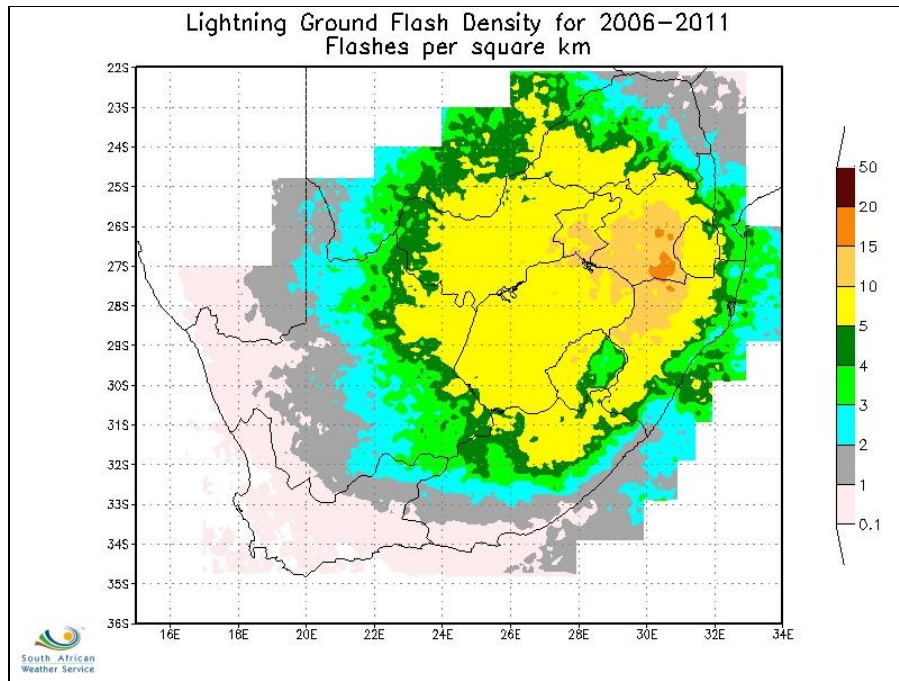


**FIGURE 1.3** Annual average (2006 to 2011) ground flash density, measured in flashes per square kilometer per year ( $\text{km}^{-2} \cdot \text{y}^{-1}$ ), over South Africa. From Gijben (2012)

Figure 1.4 shows the Lightning Imaging Sensor (LIS) global flash density map of average flashes per square kilometer per year ( $\text{km}^{-2} \cdot \text{y}^{-1}$ ) as obtained from the National Aeronautics and Space Administration (NASA) Earth Observing System Data and Information System (EOSDIS) Global Hydrology Resource Center (GHRC) Distributed Active Archive Center (DAAC), Huntsville, Alabama (<http://thunder.nsstc.nasa.gov/>). Figure 1.4 shows that the Highveld region of South Africa receives between 20 and 30 flashes. $\text{km}^{-2} \cdot \text{y}^{-1}$ . Although this ground flash density is a significant number, central Africa has by far the highest ground flash density globally. The resolution of this data is much more coarse than the new South African LDN, hence the discrepancy in the measured ground flash densities between figures 1.3 and 1.4.



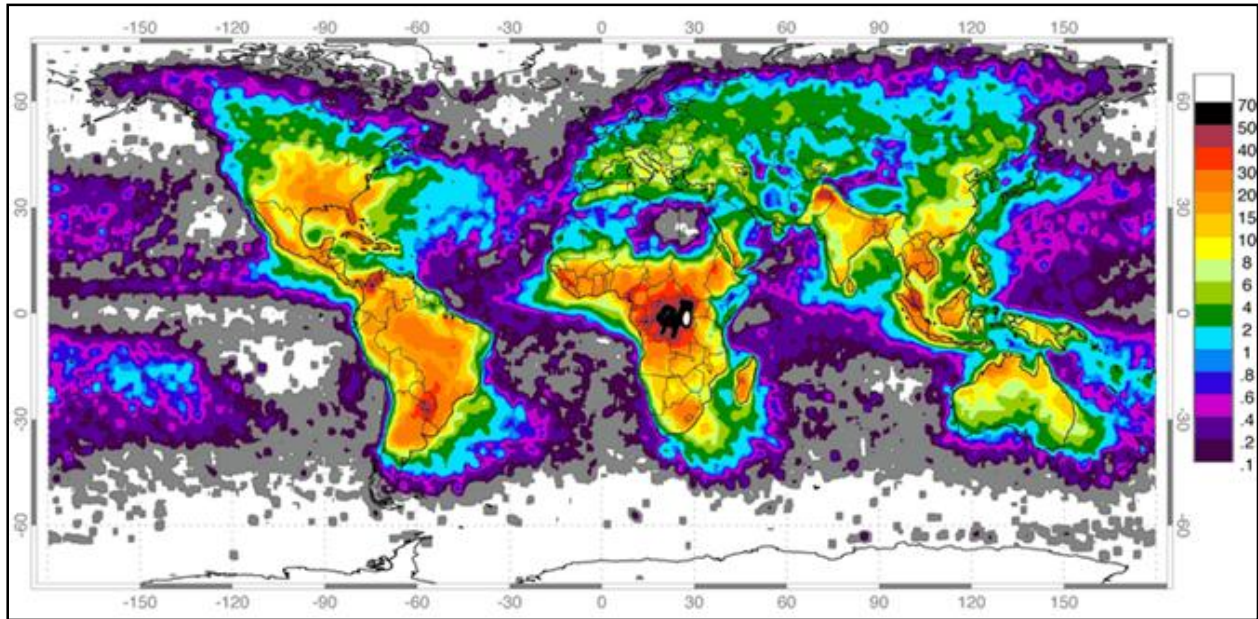


**FIGURE 1.4**

Global annual lightning flash density measured in flashes per square kilometer per year ( $\text{km}^{-2}\cdot\text{y}^{-1}$ ), based on a  $2.5^\circ$  grid from the Lightning Imaging Sensor (LIS). Courtesy: Global Hydrology Resource Center (GHRC) Distributed Active Archive Center (DAAC)/Lightning Imaging Sensor (LIS) Science Computing Facility (SCF)

The LDN is only effective in providing data after a flash of lightning has occurred. In order to limit damage and possible loss of life caused by lightning strokes, there needs to be a way to pre-determine what the severity of the resulting lightning would be from a developing thunderstorm. Lightning can either transfer a negative charge from the thundercloud to earth, which is known as a negative stroke, or it can transfer a positive charge from the thundercloud to earth, known as a positive stroke. The majority of lightning strokes are negatively charged, with a small percentage carrying a positive charge (Malan, 1963).

According to Gijben (2012), the western parts of Gauteng in South Africa received 6% to 8% positively charged lightning strokes from thunderstorms, while the Mpumalanga Province's Highveld receives a lower 4% to 6% positively charged strokes, based on accumulated data between 2006 and 2010. Gill (2008) calculated the Positive Lightning Risk Index (PLRI) for 2006, which classified the southern Highveld regions of South Africa as being under extreme risk of positively charged

lightning, while the majority of Gauteng is seen to have a lesser risk, being classified only as severe. Gijben (2012) updated this index to include data from 2006 to 2010 and thereafter classified Gauteng and Mpumalanga as both being under severe risk.

According to Uman (1969), Cumulonimbus (CB) clouds are the most common producers of lightning. Also known as thunderclouds, thunderheads or thunderstorms, CB clouds are low level convective clouds which typically contain water droplets and ice particles, the latter almost entirely in the upper parts of the cloud (Glossary of Meteorology, 2000). One of the easiest ways to identify thunderstorm development remotely is by using satellite imagery. The Meteosat Second Generation (MSG) satellite system offers its users the benefit of being able to identify cloud particle properties by being able to distinguish between ice and water droplets within a cloud, and being able to infer the current stage of development of particular storms. Considering that satellite data is invaluable in the near real-time placement of weather systems and atmospheric features, it is used very effectively as a forecasting tool when it comes to now-casting and severe storm forecasting. Since 2005 the SAWS has been using Software for the Utilization of Meteosat in Outlook activities (SUMO) software to display MSG data. Later, by 2007, the lightning detection data was integrated into the SUMO system in real time. By integrating these two data types, a user can determine which thunderstorms have developed sufficiently to produce lightning, and what is the polarity of the individual flashes. Although South Africa has the benefit of an extensive LDN and full satellite coverage via the MSG satellite, most other African countries are not as fortunate.

According to Blumenthal (2005), there were 38 victims of lightning related fatalities recorded at six medicolegal mortuaries over the Highveld region of South Africa between 1997 and 2000. This number increased to 52 victims during the period between 2001 and 2004, recorded at seven medicolegal mortuaries in the Gauteng Province alone (Blumenthal, 2007). These numbers combined, document that at least 90 people were killed from lightning alone in Gauteng and over the Highveld region



of South Africa between 1997 and 2005. According to Holle and Lopez (2003), there are about 24000 deaths and 240000 injuries caused by lightning globally each year. Holle (2008), states that in 2006, Creamer Media Engineering news reported that in South Africa there was an annual rate of 8.8 lightning related deaths per million people in rural areas, and 1.5 in urban areas. Holle (2008) further states that the annual death rate over the Highveld region of South Africa, in particular, was 6.3 fatalities per million people. Compared to the United States of America (USA) and Australia, which Holle (2008) states only had an annual death rate of 0.2 or less per million people, the South African Highveld region is certainly a high risk area for lightning related fatalities. The world-wide annual death rates resulting from lightning range between 0.2 and 1.7 per million of the population (Wetli, 1996). In countries such as Zimbabwe which according to Holle (2008) have an annual death rate of 21.3 people per million per year, there is a need to: 1) improve public awareness surrounding lightning and 2) develop a warning system based on meteorological data which can be disseminated to the public in a timely manner.

The ability to use MSG data which is widely available to predict the potential severity of lightning emanating from a CB cloud, could ultimately save lives and limit damage to property. Blumenthal (2005) found that most of the lightning strikes that resulted in deaths on the Highveld region of South Africa took place during the austral summer rainfall season of September to April, and mostly happened during the late afternoon.

Lightning strokes are most commonly negatively charged with up to 90% of downward strokes being negatively charged, the remaining being positively charged (Rakov and Uman, 2003 and Malan, 1963). These positively charged strokes are thought to cause more severe damage to objects and systems than negative strokes (Rakov and Uman, 2003), as they have a much higher electrical charge than the negative strokes. A negatively charged lightning stroke typically carries a charge of 30kA while a positively charged stroke can carry up to 300kA according to Rakov and Uman (2003). Because of the potential severity associated with positive lightning

strokes, if there is a way to determine in advance whether an above average amount of positive strokes are expected out of a thunderstorm, warnings to the public could become more informative and help to limit the damage caused by lightning. The use of satellite imagery in aiding the understanding of the lightning producing potential of a thunderstorm will also benefit those countries that make use of satellite imagery exclusively to determine storm severity and its potential impact.

## **1.2 Motivation for the research**

Each summer season in South Africa brings with it a multitude of thunderstorms, particularly over the Highveld region and north-eastern interior of the country. Each of these thunderstorms has the potential to cause damage from heavy rainfall, strong winds, hail, tornadoes and lightning. The severity of individual thunderstorms depends on the structure and development of the storm. Of the possible thunderstorm features mentioned above, lightning damage is one of the least researched topics in South Africa. Since the implementation of the new SAWS LDN in 2005, the database for lightning strokes is a reliable source of information regarding scenarios where lightning damage and lightning related fatalities have been reported.

As previously stated, at least 90 cases of lightning related fatalities were recorded between 1997 and 2005 over the Gauteng Province and the Highveld region of South Africa. Whether due to better media coverage, more public awareness regarding lightning or an increase in fatal lightning strikes, there has been much publicity over the deaths of school children, sportsmen and women as well as average people going about their daily activities.

To understand the meteorological parameters under which lightning causes fatalities can contribute to making not only weather forecasters, but the general public aware of when a thunderstorm has a higher threat than normal to deliver a fatal stroke. The

availability of satellite and lightning data over South Africa is reliable and covers the entire country with a high spatial resolution. By using these data sets, it is envisaged that the author may find common features in CB cloud properties for cases when lightning fatalities were reported, and/or when lightning caused large amounts of damage.

### **1.3 Aim and objectives**

#### *1.3.1 Aim*

The aim of this study is to determine the cloud microphysical characteristics associated with positively charged lightning strokes in high ground flash density areas in South Africa between 2006 and 2010. The study will use reports of fatalities caused by lightning as well as incidents where lightning caused large amounts of damage on the ground, to narrow down case studies for research.

The aim will be achieved by the following objectives:

#### **OBJECTIVE 1**

**The first objective of this study is to compare lightning polarity to cloud particle phases in primary case studies where fatalities and/or above normal amounts of damaged where caused.**

*Positively charged lightning strokes are known to carry a stronger charge than negatively charged strokes, and occur less frequently as well. By comparing the polarity of detected lightning strokes around the time and at the location where a fatality was reported, could provide insight as to the potential severity of resultant lightning strokes. The use of a case study where high amounts of lightning damage were reported, could clarify whether lightning polarity is indeed a factor to consider when classifying lightning as being potentially more dangerous than usual.*

- a) *Insurance claim data from Amalgamated Banks of South Africa (Absa) bank for the period 2007-2010 will be used to find dates where above average numbers of damages were reported.*
- b) *Media reports will be used to find dates on which fatalities occurred due to lightning strikes*
- c) *European Organisation for the Exploitation of Meteorological Satellites (EUMETSAT) MSG data will be used to calculate the cloud microphysical properties on the dates and times of interest.*
- d) *LDN data will be used to calculate the total amount of lightning strokes, as well as the percentage of positive polarity in lightning strokes.*
- e) *The data mentioned in points c and d above will be compared to narrow down any common factors between the primary case studies.*

## **OBJECTIVE 2**

**The second objective of this study is to determine the percentage of positive lightning strokes compared to negative strokes in the identified primary and secondary case studies**

*Determining whether more or less than the globally accepted amount of 10% positive cloud-to-ground lightning strokes were detected, will give insight as to the severity of the event.*

## **OBJECTIVE 3**

**The third and final objective of this study is to check for consistency in particle phase and lightning polarity in a secondary case study over the region of interest where neither a fatality, nor an above average amount of damaged was reported.**

*A case study will be chosen where average amounts of damages were honoured, and no fatality was reported. The satellite and lightning data will be compared as in objectives 1 and 2. This will be done in order to ascertain whether fatal and damaging*

*lightning events show any clear distinctions from non-fatal and average damage producing events.*

## **1.4 Organization of the report**

The study is comprised of three primary and one secondary case study, each containing a full set of lightning and satellite data. Data from the LDN and MSG satellite data are focused on in each of the case studies. Not only are the specific cloud and lightning properties investigated but also the movement and positioning of the thunderstorms at the time of the reported incidents.

CHAPTER 2 examines the formation of lightning as well as the characteristics of thunderstorms. The chapter is sub-divided into three sections. The first section investigates the lightning formation process within the atmosphere and within a CB cloud. The second section deals with cloud microphysical properties, and introduces the various MSG channels to be used in the study. The third and final section looks at cloud particle size and phase and how MSG satellite imagery can be used to distinguish between each phase.

CHAPTER 3 details the use of the various data sets chosen for this study. The insurance claim database acquired from Absa bank and MSG data from EUMETSAT are discussed, as well as the LDN dataset acquired from SAWS. The chapter also reveals the methodology used in acquiring, manipulating and displaying these various datasets.

In CHAPTER 4, four case studies are investigated individually. The first two case studies fall on the same day, when there were two fatalities one hour apart. The third case involves a large amount of reported damage from lightning, but no reported

fatality. The fourth and final case addressed in this chapter has no extreme damage, nor a fatality, and is used to determine whether there are any distinguishable cloud microphysical and lightning polarity features in fatal events, that are not found in cases which are seemingly unremarkable.

CHAPTER 5 contains summaries of the four case studies and research results obtained from the comparison of data sets within each case study.

The research conclusion and recommendations are found in CHAPTER 6. This chapter is followed by the references used in the study. Relevant appendices are attached at the end of the document including additional satellite and lightning data for the two case studies involving fatalities. An interpretation guide for the convection satellite channel combination is also included.

## **CHAPTER 2**

### Lightning and cloud microphysics

#### **2.1 Lightning**

The term “lightning” is used to describe a discharge of energy, either between a thundercloud and the ground, between two thunderclouds or within the same thundercloud. These various types of lightning can be defined as cloud-to-ground, inter-cloud or intra-cloud lightning. It is safe to say that not all lightning reaches the ground as a stroke or a flash. These flashes which do not make contact with the ground, or an object thereon, are harmless to people and infrastructure. The flashes that do, however, make contact with the ground, or with objects thereon, pose a direct risk to the safety of people and to the integrity of infrastructure.

Lightning is usually associated with convective cloud systems, ranging from 3km to 20km in vertical extent (Rakov and Uman, 2003). The most common convective cloud which is associated with lightning would be a CB cloud. It is important to remember, however, that not all CB clouds are associated with lightning (Rakov and Uman, 2003). Thunderstorms generally refer to more than one thundercloud or cell, and can be made up of several cells, or even of one cell with a rotating updraft, known as a super-cell (Rakov and Uman, 2003).

Malan (1963) and Cotton and Anthes (1989) divide the life cycle of a thundercloud into three stages, namely: 1) cumulus stage, 2) mature stage and 3) dissipating stage. The cumulus stage of a thunderstorm is dominated by updrafts, and there will not be any precipitation during this phase (Malan, 1963 and Cotton and Anthes, 1989). The mature stage is reached when precipitation occurs that reaches the ground. Precipitation occurs due the ice and water particles present within the cloud, which can no longer be carried to the top of the thundercloud by the updraft. In falling

through the thundercloud, the ice particles and water droplets generate the downdraft (Malan, 1963). Once the downdraft has spread throughout the thundercloud, the dissipating stage has been reached (Malan, 1963). According to Cotton and Anthes (1989), the average duration of precipitation and electrical activity from a single cell thunderstorm is approximately 30 minutes.

Saunders (1992) states that during the growth/cumulus stage of a thundercloud, positive ions can be drawn into the updraft, from the positively charged atmosphere below the cloud base. These positive ions then attach to the water droplets, and are transported to the tops of the clouds by the updrafts. This positive charge at the top of the cloud will attract a negative charge to the cloud. Such negative charge will be trapped on cloud particles, and drawn into the cloud by entrainment and transported downwards by the eventual downdrafts in the thundercloud (Saunders, 1992).

There are many theories surrounding the charge separation within a thundercloud. Malan (1963) puts forward two theories of how charge separation occurs in thunderclouds. Firstly, he has described the charge separation in terms of the size and weight of various cloud particles. The smaller, positively charged particles are transported to the top of the cloud by the updraft, while the heavier, negatively charged particles either move upwards more slowly because of their weight, they remain stationary or move downwards in the cloud. In this theory, it is essential that the oppositely charged particles are of different sizes. His second theory is based on the work done by Latham and Mason (1961), who provide evidence which suggests that separation of electric charge occurs in ice, under the influence of a temperature gradient.

The most widely accepted theory of charge separation is, however, the Non-Inductive Charge-transfer (NIC) process, or the graupel-ice mechanism. The NIC process generally occurs when cloud and precipitation particles collide within the



thundercloud (Saunders, 1992). During these collisions, charge is transferred independently of the local electric field strength. Reynolds *et al.* (1957) concluded that the charge separation which results from ice crystals colliding with a riming ice sphere (also known as graupel), is adequate to account for thunderstorm electrification. It was found that the downward moving graupel became negatively charged after colliding with the upward moving ice crystals, where the positive charge is being removed (Reynolds *et al.*, 1957). Reynolds *et al.* (1957) suggested that the charge transfer is largely due to the temperature differences between the two colliding particles, where the graupel is warmed due to the release of latent heat during droplet freezing. The findings of Reynolds *et al.* (1957) are therefore in line with the work done by Latham and Mason (1961).

According to Malan (1963), the bulk of the positive charge (P) in a thundercloud is positioned above the main accumulation of negative charge (N) within a thundercloud, as in figure 2.1.

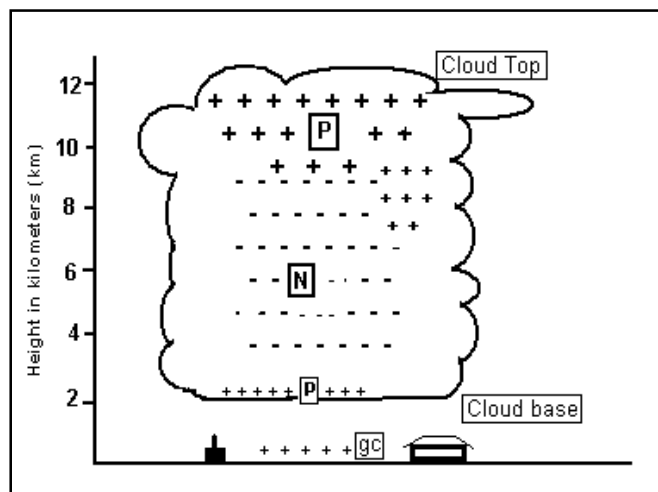


**FIGURE 2.1**

Negative and positive charge distribution within a thundercloud, where N is the negative charge, P is the upper positive charge, p the positive charge found at the cloud base and gc the positive charge found above the surface of the earth. Adapted from Malan (1963) and incorporating ideas from Kriebhel (1986)

Kriebhel (1986) and Berger (1977) agree with this depiction and name the two charge areas as the “upper positive” and the “main negative” charges, respectively. According to Malan (1963) and using figure 2.1, as the main negative charge (N) increases within the thundercloud, positive ions are released by objects on the ground (including buildings, people and vegetation) directly beneath the thundercloud. This is called “*point discharge*”. These positive ions are drawn towards the cloud base either by air flowing towards the cloud base or by the influence of the electric field. This will result in the air below the cloud base containing a positive charge (gc). Malan (1963) notes two reasons why the distribution of this positive charge below the cloud base is not always uniformly distributed: 1) points on the ground are not evenly distributed or equal in height and 2) air flowing towards the cloud base is not uniform but rather gusty.

Rakov and Uman (2003) noted that the two main charges, what Krehbiel (1986) defines as the upper positive (P) and the main negative charges (P) (figure 2.1), are equal in magnitude, and that a third region of positive charge, found at the base of the cloud, area p in figure 2.1, is not always necessarily present. The main upper positive charge (P) and the main negative charge (N) together form a vertical dipole within a thundercloud, which is said to be positive because the positive charge is found above the negative charge in the cloud (Rakov and Uman, 2003). Cotton and Anthes (1989) state that negative charges are usually found between the -10 degrees Celsius (°C) and -20°C levels, with the positively charged particles found at significantly higher levels.

Once the charge separation has occurred in the thundercloud, the charge accumulation in the upper positive region and the main negative region will continue until such time that the electric stresses are such that a lightning discharge will occur (Krehbiel, 1986). Much research has been done on the propagation of lightning from a thundercloud to the ground. The works of Malan (1963), Rakov and Uman (2003) and Proctor (1993) all explain the propagation of lightning by means of a stepped

leader, originating in the thundercloud and extending to the ground. The stepped leader is defined as the initial electrical breakdown that occurs between the thundercloud and the ground, where there is no prepared track to follow through the air (Malan, 1963).

Malan (1963) explains that a lightning discharge begins within the cloud and will progress towards the ground. The advancing discharge is known as the leader stroke, and will open a channel between the cloud and the ground through which electricity will flow once a connection has been made between cloud and ground. A stepped leader advances hesitantly from the cloud to the ground, and the length of each step to the ground is determined by the field strength in front of the leader tip (Malan, 1963). The advance of the leader stroke is not continuous but rather a hesitant process with intermittent stopping and starting in the descent. For this reason the leader stroke is also called the "stepped leader".

As the stepped leader progresses downward it is attracted to a positive point on the ground due to the surrounding electric field. When it is near the ground the stepped leader will have lowered a column of high negative potential to that point, resulting in upward moving discharges to launch from the ground towards the tip of the stepped leader, creating a connection between the cloud and the ground (Uman, 1969). Once this connection is formed the negative charge in the channel will be neutralized, and a "return stroke" will travel along this channel from the ground back up towards the cloud (Malan, 1963), (Rakov and Uman, 2003) and Proctor (1993). Multiple strokes can occur via the channel which has been formed and these strokes are collectively known as a lightning flash.

According to Rakov and Uman (2003), the high current return stroke rapidly heats the channel between the cloud and the ground to approximately 30000 Kelvin (K) and creates a pressure of 10 atmospheres ( $10 \times 1.01325 \times 10^5$  Pascal) or more,

resulting in the expansion of the channel, intense optical radiation (bright flash) and an outward propagating shock wave that is heard as thunder

Before a stepped leader can propagate from a thundercloud to the ground, the conducting region first needs to be created within the cloud. This is achieved via a process known as photo-ionization (Malan, 1963). This ionization process provides the negative charge needed for the advance of a leader from the cloud but this first leader will not drain all the negative charge from the cloud. After the first return stroke is completed, the cloud-ward end of the channel is left positively charged, leaving a strong electric field which has been established between the branched top of the channel and the remaining negative charge in the cloud. After this electric field is established positive streamers will now advance upwards and outwards and ionize the air between the negatively charged particles. These resultant streamers are called J-streamers and they serve to make more of the cloud conductive (Malan, 1963).

Once the positive charge has been neutralized and the J-streamers have spread far enough, or have reached a pocket of high density negative charge, sufficient negative charge can collect at the top of the channel to start a second leader on its way to the ground. This process will again lower the negative charge at the top of the channel, and the J-streamer process will repeat itself until there is no more negative charge or the negative charge density is too low to allow the propagation of any J-streamers (Malan, 1963).

Carey and Buffalo (2006), Malan (1963) as well as Rakov and Uman (2003) state that approximately 90% of all cloud-to-ground lightning discharges are in fact negatively charged, meaning they carry a negative charge from the cloud to the ground. Carey and Buffalo (2006) go on to state that there are some severe storms in the United States of America which can indeed result in percentages of positive lightning strokes that are comparable with the amount of negative strokes which are typically observed in an active thunderstorm. Due to the charge distribution within

mature thunderstorms, as seen in figure 2.1, most positively charged lightning strokes emanate from the anvil of the storm, while most negatively charged strokes are found directly beneath the storm cloud. A schematic diagram of this is presented in figure 2.2.

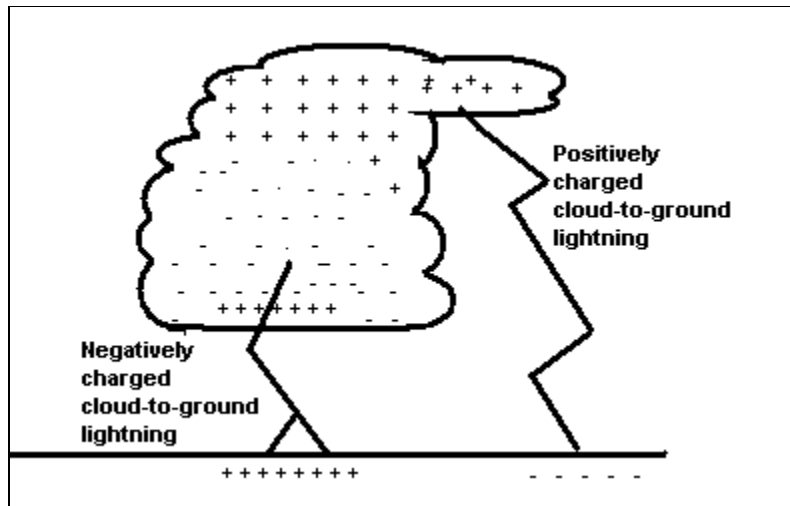


**FIGURE 2.2**

Location and paths of negatively and positively charged cloud-to-ground lightning strokes according to the typical charge distribution within a thunderstorm. Adapted from Rakov and Uman (2003) and Malan (1963)

Gill (2008) and Gijben (2012) have discussed the multiplicity of lightning flashes, which are the number of strokes within a cloud-to-ground lightning flash. Looking at figure 2.3, the highest multiplicity over South Africa is found over the Drakensberg mountain region in the western parts of the KwaZulu-Natal Province, as well as over the southern parts of the North-West Province (figure 1.1). Both of these regions receive an annual average of three strokes per flash. These areas of high multiplicity are also coincident with areas of high ground stroke flash density, particularly over the Drakensberg mountain region, as illustrated in figure 1.3. Gill (2008) showed that positive strokes over the Highveld region and high flash density regions of South Africa have a multiplicity of less than two strokes per flash. According to Malan (1963), in instances where positive flashes consist of more than one stroke, the first subsequent stroke is often a continuing current stroke. By considering the flash multiplicity on a month-by-month basis, Gill (2008) found that about 90% of

positively charged strokes over South Africa had a single multiplicity. Uman (1969) also stated that positive lightning flashes rarely contain more than one stroke.

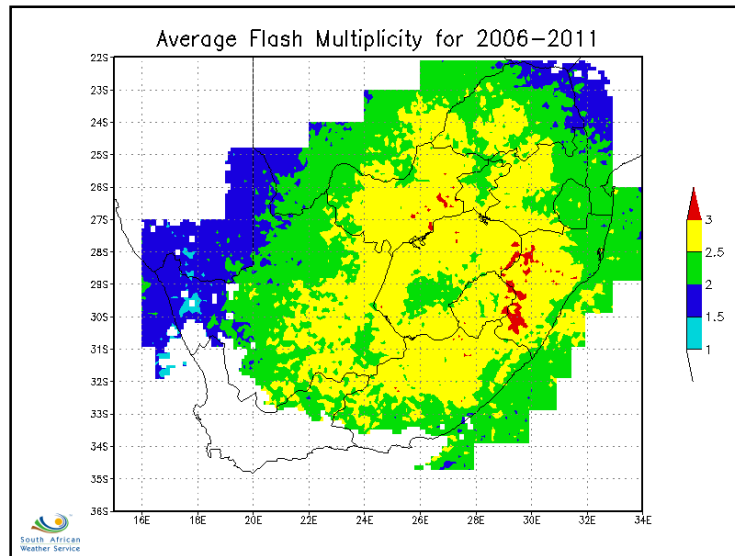


**FIGURE 2.3**

Average flash multiplicity measured in number of flashes over the period 2006 to 2011 over South Africa. From Gijben (2012)

Of all the lightning strokes that occur, it is widely believed that less than 10% of these strokes carry a positive charge (Rakov and Uman, 2003), (Mason, 1963) and (Carey and Buffalo, 2006). Rakov and Uman (2003) lists that one of the reasons why positively charged lightning strokes receive a lot of attention, is that the highest directly measured lightning currents and the largest charge transfers to the ground are thought to be associated with positively charged lightning. The occurrence of positively charged lightning does not necessarily follow the same formation process as with negatively charged lightning strokes. Zajac and Rutledge (2001) state that once a positive charge is developed at the base of the cloud it will not follow the stepped leader approach to the ground, but rather propagate in a direct channel from the cloud to the ground. These channels can last for long periods of time, and result in large amounts of energy being dissipated to the ground. Rutledge and MacGorman (1988) found that most positively charged cloud-to-ground lightning emanates from the rear of a convective storm, mostly in the trailing stratiform region of cloud. These findings are also in line with what Rakov and Uman (2003) describe as one of the situations favourable for positively charged lightning to occur, is the dissipating stage

of a thunderstorm. This will happen once most of the negative charge has been removed from the thundercloud by negative ground flashes during the mature and most active stages of the thundercloud life cycle (Rakov and Uman, 2003 and Zajac and Rutledge, 2001).

## 2.2 Cloud microphysics

### 2.2.1 *Meteosat Second Generation Satellite data*

The MSG satellite was launched in 2002 and was fully operational on 29 January 2004 (MSG-2 *Successfully launched*, 2005). This geo-stationary, meteorological satellite was an upgrade from the Meteosat 7 satellite that had been used by the SAWS for operational purposes up until that point. The MSG satellite has 11 spectral channels and one high resolution visible channel. Of the 11 spectral channels two are visible channels, found in the 0.4 $\mu\text{m}$  to 0.7 $\mu\text{m}$  wavelength, eight channels are Infra-Red (IR) channels, found in the 4.0 $\mu\text{m}$  to 14.0 $\mu\text{m}$  wavelengths and one channel is Near Infra-Red (NIR), namely NIR1.6 $\mu\text{m}$  (NIR with a wavelength of 1.6 $\mu\text{m}$ ). Of the eight IR channels two are for Water Vapour (WV). Of the IR channels, IR10.8 $\mu\text{m}$  is considered to be the “cleanest” window channel and is the preferred channel to be used when determining cloud top temperatures or even land surface temperatures. IR8.7 $\mu\text{m}$  is also a window channel, and is seen as being useful in support of the discrimination between cloud ice and liquid water (Zwartz-Meise, 2004).

By performing a channel difference (subtraction) between IR8.7 $\mu\text{m}$  and IR10.8 $\mu\text{m}$ , a user can determine optical thickness and the phase of the particles at the cloud top (Kerkmann, 2005). Kerkmann (2005) and Prieto (2008) show that the Brightness Temperature Difference (BTD) of IR8.7 $\mu\text{m}$  minus IR10.8 $\mu\text{m}$  equal to and above -1K is evidence of the presence of ice clouds. Similarly, a BTD value less than -1K of the same two channels is indicative of a liquid water cloud droplets. According to Wolters

*et al.* (2007), brightness temperature thresholding affects the cloud water phases by assuming a sudden transition from liquid water to ice clouds below a given temperature threshold. The Cloud Top Temperature (CTT) therefore is more of an indication of the prevailing cloud water phase, rather than being a direct identification of it.

### **2.3 Cloud particles**

Continental clouds generally contain many small droplets as compared to marine clouds, which tend to contain smaller concentrations of larger droplets (Rosenfeld and Lensky, 1998) and (Pruppacher and Klett, 1978). Rosenfeld and Lensky (1998) also go on to explain that ice particles tend to be smaller in size than water droplets, at the same temperature.

In the convection Red-Green-Blue (RGB) combination, the BTD between WV6.2 $\mu\text{m}$  and WV7.3 $\mu\text{m}$  (WV6.6 $\mu\text{m}$  minus WV7.3 $\mu\text{m}$ ) is allocated to the red channel, the BTD between the IR3.9 $\mu\text{m}$  and IR10.8 $\mu\text{m}$  (IR3.9 $\mu\text{m}$  minus IR10.8 $\mu\text{m}$ ) is allocated to the green channel and the reflectance difference between NIR1.6 $\mu\text{m}$  and VIS0.6 $\mu\text{m}$  (NIR1.6 $\mu\text{m}$  minus VIS0.6 $\mu\text{m}$ ) is allocated to the blue channel. These channels are combined in an attempt to locate severe convection (Kerkmann, 2005). Severe convective storms appear bright yellow when using this RGB because of the near zero BTD of WV6.2 $\mu\text{m}$  minus WV7.3 $\mu\text{m}$  found in overshooting tops in CB clouds (high red). The strong updrafts in these clouds produce small ice particles at cloud tops due to homogeneous freezing of cloud liquid water drops, resulting in large BTD IR3.9 $\mu\text{m}$  minus IR10.8 $\mu\text{m}$  (high green). Finally, large negative values of NIR1.6 $\mu\text{m}$  minus VIS0.6 $\mu\text{m}$  occur because of the large absorption at NIR1.6 $\mu\text{m}$  by ice particles results in a low feedback from blue (Kerkmann, 2005). A colour interpretation of the convection RGB is given in appendix A.

In addition to the use of the visual classification scheme, the CTT can also be used in conjunction with effective radius ( $r_e$ ) to determine the particle growth process in a



cloud. This process of using CTT can eliminate the need to use cloud top height to determine the vertical depth of a convective cloud, as it is known that clouds tops generally become colder with height (Rosenfeld and Lensky, 1998). During this growth process, it needs to be assumed that  $r_e$  is conserved for a given temperature, as long as there is no development of precipitation by that time. Arakawa and Schubert (1974) explained that particle size will increase consistently from the base of the cloud to the top of the cloud until precipitation particles are formed, which will fall downwards from the cloud top. According to Rosenfeld and Lensky (1998), droplets near the cloud base still form by condensation and grow by a diffusion process, while coalescence and ice processes are responsible for the cloud growth rate in higher reaches of the cloud. Pruppacher and Klett (1978) agree that cloud liquid water content reaches a maximum near the upper half of a convective cloud. The liquid water content will then decrease again towards the top of the cloud, where more ice is found.

Carey and Buffalo (2006) have shown that thunderstorms with higher cloud bases and smaller warm cloud depths have a higher likelihood of producing a larger amount of cloud-to-ground lightning strokes which are positively charged. Lindsey *et al.* (2006) add to the results by Carey and Buffalo (2006) by proving that similar thermodynamic conditions lead to thunderstorms with small cloud-top ice crystals. Climatologies found in both the abovementioned studies have shown the regions containing the largest amount of positively charged cloud-to-ground lightning overlap with the areas containing the smallest cloud top ice crystals. Sherwood *et al.* (2006) cited in Lindsey (2008), show that globally, areas which have a maximum total lightning flash rate, also have a minima in cloud top particle size. The study, however, does not include the breakdown in flash polarity.

## **CHAPTER 3**

### Data and methodology

Lightning is a very common feature in South Africa, and particularly over the Highveld regions. Evidence of this is given in figure 1.3 where the Mpumalanga, southern Gauteng and the western parts KwaZulu-Natal Provinces experience a far higher ground flash density per annum than any other part of the country. Cloud-to-ground lightning often results in damage occurring on the ground, and even the potential loss of human life. For this reason the area of highest flash density was chosen for this study, as this area would naturally pose the largest risk to damage of property, infrastructure and the potential loss of human life.

The data were collected and displayed in Zulu (Z) time, which is equivalent to Coordinated Universal Time (UTC). South African Standard Time (SAST) is equivalent to Z + 2 hours. Various data sets were used to determine the chosen case study dates, and eventually four cases were identified: 1) 22 November 2007 at 1414Z, 2) 22 November 2007 1503Z, 3) 10 February 2009 from 1300Z to 1400Z and 4) 29 October 2009 between 1500Z and 1600Z. Of these four cases, the first three listed were categorized as primary cases and they fell within the predetermined criteria of high lightning damage reports, reported human fatalities or a combination of both of these factors. The fourth case was regarded as a secondary case and was unremarkable in respect to lightning damage and there was no fatality reported. Such a case was chosen to test the results obtained from the three more severe primary cases.

## 3.1 Data

### 3.1.1 Insurance claim data

As lightning has the potential to cause noticeable damage when a stroke or flash makes contact with an object on the ground, the study made use of insurance claim data from a banking institution, namely Absa. The data were confined to lightning related claims that were paid out between 2006 and 2011 over South Africa. The data did not include any specific locations, only the municipal areas for which the claim was valid. This was due to confidentiality clauses from the bank. The data were received in text format, providing dates, categorization, area codes and regions of the individual incidents. There were 40388 claims nationwide over the abovementioned time period. Of these, 5249 claims were from 2007, 6137 from 2008, 7164 from 2009, 6492 from 2010 and 3736 claims from January up to May 2011 over only the Highveld areas of South Africa. This totals 28788 lightning related insurance claims, from one bank, for a period of 5.5 years over the Highveld region.

### 3.1.2 Meteosat Second Generation satellite data

In 2005 the first MSG images became available to view. The MSG satellite is a geostationary satellite, located at approximately 36000km above the Earth at latitude 0°S and longitude 0°E. The satellite comprises a series of sensors, resulting in an array of 12 channels. Of the 12 channels, 11 have a horizontal resolution of 3km at the nadir, which is the point directly below the position of the satellite. The High Resolution Visible (HRV) channel has a 1km resolution at the nadir (Schmetz *et al.*, 2003). The temporal resolution of the data from all 12 channels is 15 minutes.

The satellite imagery for this study was ordered in High Rate Information Transfer (HRIT) format directly from the EUMETSAT data archive. Data from all 12 channels were collected, although only VIS0.6 $\mu$ m, NIR16.4 $\mu$ m, NIR3.9 $\mu$ m, WV6.2 $\mu$ m,

WV7.3 $\mu$ m, IR8.7 $\mu$ m, IR10.8 $\mu$ m and HRV were used either as single channels or part of RGB combinations and BTD calculations.

### 3.1.3 Lightning data

The SAWS installed a new LDN in 2005, comprising of 19 LS7000 lightning sensors. This LDN has since been expanded to 24 locations around South Africa, as shown in figure 3.1.



**FIGURE 3.1**  
South African Weather Service (SAWS) Lightning Detection Network (LDN) sensor sites in 2012. Source: SAWS

The lightning sensors detect both lightning flash data and lightning stroke data, due to the fact that the network consists entirely of combined sensor technology (Gill, 2008). A lightning flash is classified as the total discharge from cloud-to-ground

lightning, while lightning strokes are the separate component discharges which make up a lightning flash (Uman, 1969). The detection efficiency of the LDN in 2005, with only 19 sensors, was at 95% for most of South Africa. This means that 95% of all cloud-to-ground lightning flashes could be detected over most regions of the country. The location accuracy of the lightning flashes is 0.5km over the majority of South Africa, also based on 19 sensors. During 2009 and 2010, additional sensors were added to the network, increasing the number to 24, with 23 sensors being located within South Africa, and 1 sensor installed in Swaziland (figure 3.1). With the addition of five new sensors it can be assumed that the detection efficiency and the location accuracy should have improved. For this study, no corrections have been made for the location accuracy or the detection efficiency, and all data were used as recorded by the network sensors.

## **3.2 Methodology**

### *3.2.1 Insurance claim data*

Insurance claim data were received from Absa in Microsoft Excel format. The data covered insurance claims over the whole of South Africa for the period January 2007 to May 2010. This data were separated into provincial groups, and then further separated to only include insurance claims honoured over the Highveld region of South Africa. The data were then used to create graphs depicting the total number of claims for each day of each month of the year. In total, eight graphs were created for each year from 2007 to 2010 for the months of January, February, March, April, September, October, November and December. Austral winter months were neglected as the highest occurrence of thunderstorm activity over the Highveld takes place during austral summer months.

The average number of claims was calculated for each month of each year, and then compared to the daily totals of the respective months. After this had been done, it could be seen which days of each month of each year experienced above average

insurance claims. Days on which fatalities were reported were also highlighted on each graph. It was from this information that case studies were chosen, depending on the amount of insurance claims honoured on a particular day, the occurrence of a fatality on the day, and the availability of reliable information regarding the timing of the fatality.

In cases where there was no time frame available for the lightning related fatality, the case was discarded. In cases where the exact location of the fatality was not certain, the location of the nearest town or city was used as the point of interest. For the case of 10 February 2009 no fatality was reported but the case was selected due to the well above average amount of insurance claims honoured on that particular day.

### *3.2.2 Meteosat Second Generation satellite data*

The raw HRIT data were processed through SUMO software to produce both a bitmap (BMP) image file, as well as a binary (DATA) file. The BMP images were viewed using SUMO software in order to gain the overall perspective and understanding of what was happening with thunderstorm development for each of the case studies. The DATA files were read into Fortran code, manipulated and viewed through the Grid Analysis display system (GrAds) graphical display software for interpretation.

The colour contrast settings were inverted when creating images of IR10.8 $\mu\text{m}$  to be viewed in SUMO, in order to interpret the imagery in the format by which it is primarily displayed in operational forecasting environments. The IR10.8 $\mu\text{m}$  data were also written into DATA format to be read into Fortran code and displayed using GrAds.



The HRV and VIS0.6 $\mu$ m imagery were displayed as single channels for direct interpretation in SUMO. For investigation of convection during the day, it is best to use an RGB comprised of the following channel combinations: WV0.62 $\mu$ m minus WV0.73 $\mu$ m; NIR3.9 $\mu$ m minus IR10.8 $\mu$ m; NIR1.6 $\mu$ m minus VIS0.6 $\mu$ m, which is known as the “convection” RGB. For convective activity overnight, it is best to make use of the RGB combination: IR12.0 $\mu$ m minus IR10.8 $\mu$ m; IR10.8 $\mu$ m minus NIR3.9 $\mu$ m; IR10.8 $\mu$ m, which is known as the “night microphysical” RGB. The RGB combinations were created in SUMO. The BTD DATA files were created in SUMO and then read into Fortran code before the final image was displayed through GrAds.

From these various single channels, RGB combinations and channel differences, features such as overshooting tops, cloud particle phase and cloud particle size could be identified. The IR10.8 $\mu$ m channel helped in obtaining information on the temperature based cloud features during both the day and at night. It was also used to determine the CTT of the thunderstorms identified in the various case studies. The convection RGB helped in identifying the cloud particle phase at the cloud top level, and so provided evidence of the occurrence of the updrafts and development phase of the thunderstorms. The night microphysical RGB is more limited than the convection RGB as it relies solely on IR channels to create an image. This removes the possibility to identify cloud particle phase and size at night. The RGB combination does, however, show areas of convection by looking at CTT and BTD.

Satellite imagery could be animated, zoomed into and manipulated as needed within SUMO. The IR10.8 $\mu$ m channel was viewed in order to ascertain the geographical coordinates of lowest CTT in the thunderstorms throughout their life cycle, and to determine at which times, and over what areas the storms were most intense. The IR10.8 $\mu$ m channel is well suited for this, as the imagery can be used during the day and at night, therefore maintaining continuity in the information required.

The CTT by default are displayed in °C in SUMO, and at each data point, a latitude and longitude reading is given simultaneously with the CTT. For the purpose of consistency in the units by which data are discussed, the CTT were converted from °C to K in all discussion of the case studies. The CTT values were also rounded off to the nearest whole number. The HRV and VIS0.6µm measure reflectance as a percentage (%), where the higher the reflectance the thicker the cloud. This imagery was viewed using SUMO to gain information on cloud texture, thickness and features such as overshooting tops on developing thunderstorms. The overshooting top is a good indicator of a strong and well-structured updraft within the developing thunderstorm and is also an indicator for a potentially severe thunderstorm (Bader *et al.*, 1995).

By comparing the IR10.8µm, HRV and convection RGB imagery, an overall impression of the convective development over the area of interest could be determined. It was by this method that time periods for case studies of 10 February 2009 and 29 October 2009 were narrowed down to the 60 minutes wherein the most intense convection was identified.

Once all the imagery were created by both GrAds and SUMO software, the data from each image were compared with one another to determine what the cloud phase was at the time and point of interest, as well as the intensity of the accompanying thunderstorm. As satellite data is representative only of information regarding temperature and reflectance at the very top of clouds, all discussion of MSG data refer to the cloud tops exclusively.

### *3.2.3 Lightning data*

Lightning data were obtained in text format from the SAWS LDN archive for the period 2007 to 2010. The data were for the entire LDN region over South Africa in order to



maintain continuity in the data for each date and time period of interest. The data obtained for this study appeared over a time period of 1-hour around the time of the reported fatality (30 minutes before and 30 minutes after the event). The hourly sum of lightning strokes was calculated and further separated into accumulated time intervals of 30 minutes and 15 minutes. The minimum time period of 15 minutes is chosen to coincide with the 15 minute temporal resolution of the MSG satellite imagery.

In the two cases when no fatality was reported, data were collected for the entire day. For all four case studies, data from the entire network were collected, and no buffer or boundary region was set up around the area of interest. As the complete lightning data set was retrieved, both positive and negative polarity data, as well as location data was available for processing, manipulation and interpretation. The text files were read using Fortran code in order to calculate the sum of all the strokes measured during the time period of interest. The resulting file was then written to a recognizable GrAds format. Once in this format, the visual image could be displayed through GrAds, and could also be manipulated as needed. It was during this display process that areas could be amplified and changed according to the needs of each individual case study. The lightning data were displayed in a  $0.1^\circ \times 0.1^\circ$  horizontal resolution across the entire region.

Firstly, the sum of all lightning strokes was calculated and displayed for appropriate time intervals and subsequently, the percentage of positively charged strokes was calculated during the corresponding times. To calculate the percentage of positively charged strokes, two data files were compiled using Fortran code. The first file contained the geographical coordinates, time and total amount of cloud-to-ground lightning detected during the time period of interest. The second file was similar to the first but instead of containing the total amount of cloud-to-ground lightning, it contained the amount of positively charged lightning strokes. These two files were

then used in conjunction to calculate the percentage of positively charged strokes detected and results were graphically displayed using GrAds.

## CHAPTER 4

### Case studies

#### 4.1 Primary case studies

##### 4.1.1 Primary case study: 22 November 2007 at 1414Z

On 22 November 2007, three incidents of people being struck by lightning were reported by Netcare 911 to the Road Safety and Arrive Alive blog (Netcare 911, 2007). Of these three incidents, two resulted in fatalities. According to the report, the first incident occurred at 1414Z in the Randfontein area, point A on figure 4.1. During this incident, a factory worker was struck by lightning while she was seeking shelter at a brick factory.

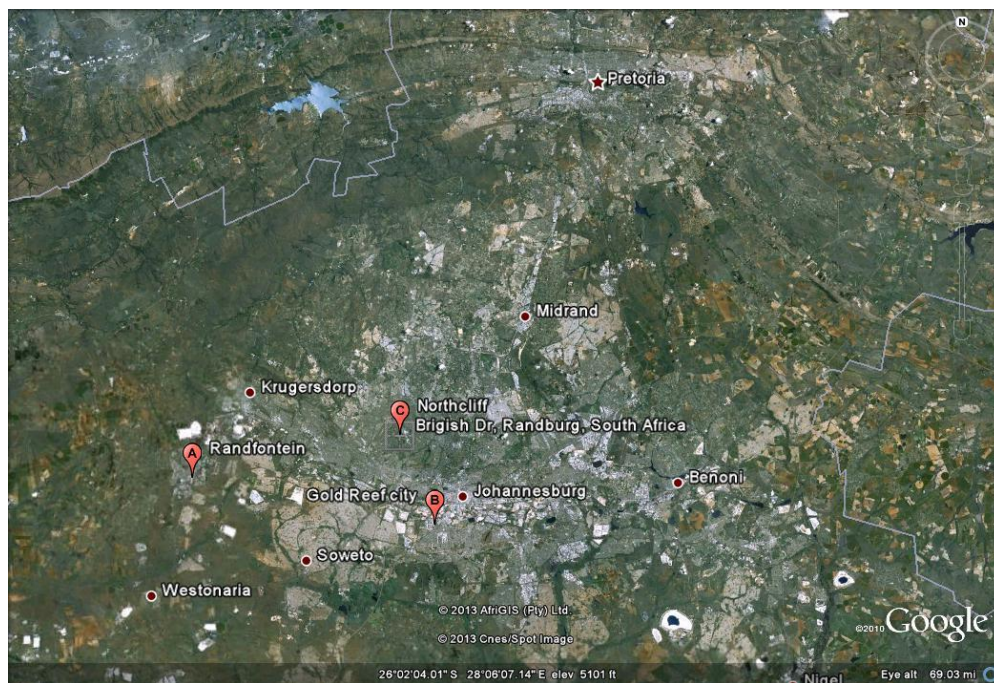


**FIGURE 4.1**

A satellite image depicting the location of two reported fatalities caused by lightning strikes (points A and C) and one injury caused by a lightning strike (point B) for 22 November 2007. Point A represents Randfontein, point B represents Gold Reef City and point C represents Northcliff. Source: Google Earth (2010)

## Satellite data

Considering the HRV image in figure 4.2, the clouds were seen as being bright white and having an irregular, clumpy texture over Gauteng, the eastern parts of the North-West Province and the northern part of the Free State. The lowest measured CTT was 204K (-68.56°C) on the IR10.8µm image in figure 4.2, in a position north-west of Randfontein. The convection RGB depicted small ice particles over and to the south-east of Randfontein. Together the three satellite images in figure 4.2 gave enough evidence to suggest that the clouds over the Randfontein area were indeed CB clouds with small ice particles at 1415Z.

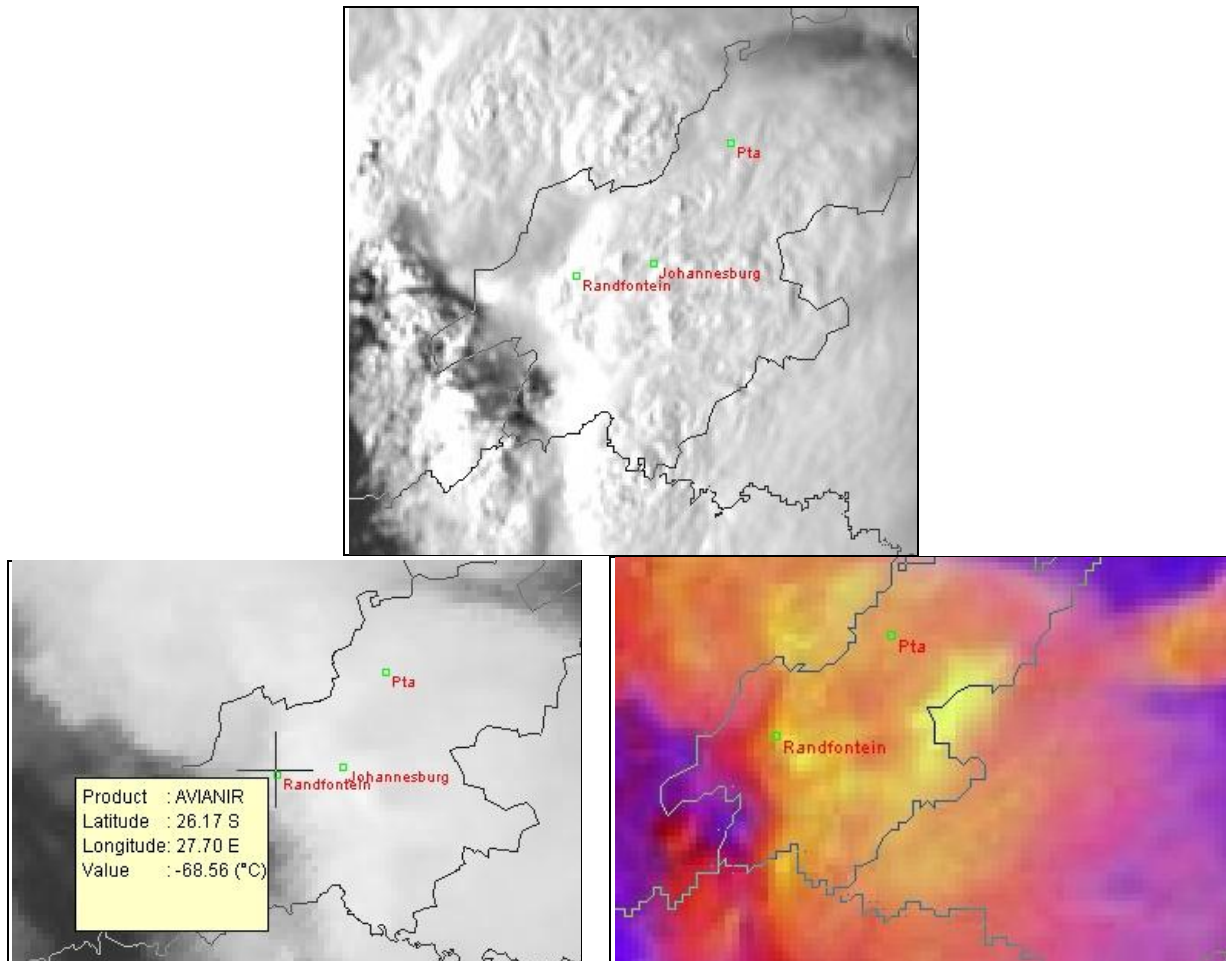


**FIGURE 4.2**

Meteosat Second Generation (MSG) satellite imagery over the Gauteng Province at 1415Z for 22 November 2007. The High Resolution Visible (HRV) image is at the top, the inverted Infra Red (IR) 10.8µm is on the bottom left hand side and the convection combination is on the bottom right hand side. Copyright (2013) EUMETSAT

The CTT values over Randfontein in figure 4.3 fell between 210K and 220K at 1415Z and the lowest CTTs were found in a north-to-south band lying east of Randfontein and were colder than 190K. The BTD of between 0K and 1K over Randfontein was further evidence of ice particles in the CB cloud over the area at 1415Z.

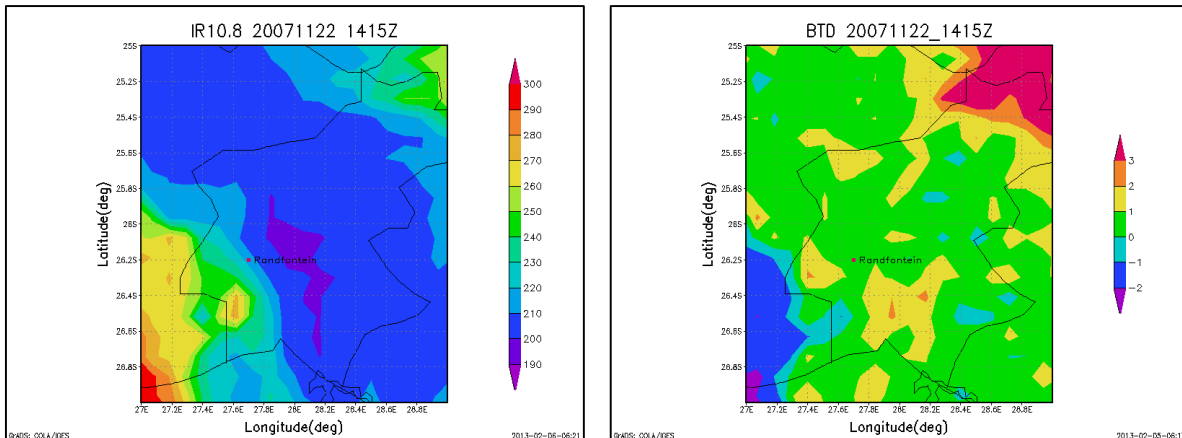


**FIGURE 4.3**

Grid Analysis display system (GrAds) imagery of Infra Red (IR) 10.8µm data in degrees Kelvin (K) on the left hand side and Brightness Temperature Difference (BTD) of IR8.7µm-IR10.8µm measured in K on the right hand side, for 22 November 2007 at 1415Z.

### *Lightning data*

The distribution of lightning strokes for the afternoon of 22 November 2007 was coincident with the area of convection which had been identified in figure 4.2. Between 15 and 25 strokes were detected between 1400Z and 1415Z over Randfontein. This was not the most active area for cloud-to-ground lightning during this time period, as between 100 and 300 strokes were detected to the east and south east of Randfontein. Between 5% and 6% of the total cloud-to-ground lightning strokes were positively charged in this case, as seen in figure 4.4. More than 10% of the total strokes were measured as having a positive polarity in a band oriented north-to-south, lying to the east of Randfontein. This area of more than 10% positively charged strokes borders the Randfontein area very closely in the east and south-east, and must be regarded as being significant.

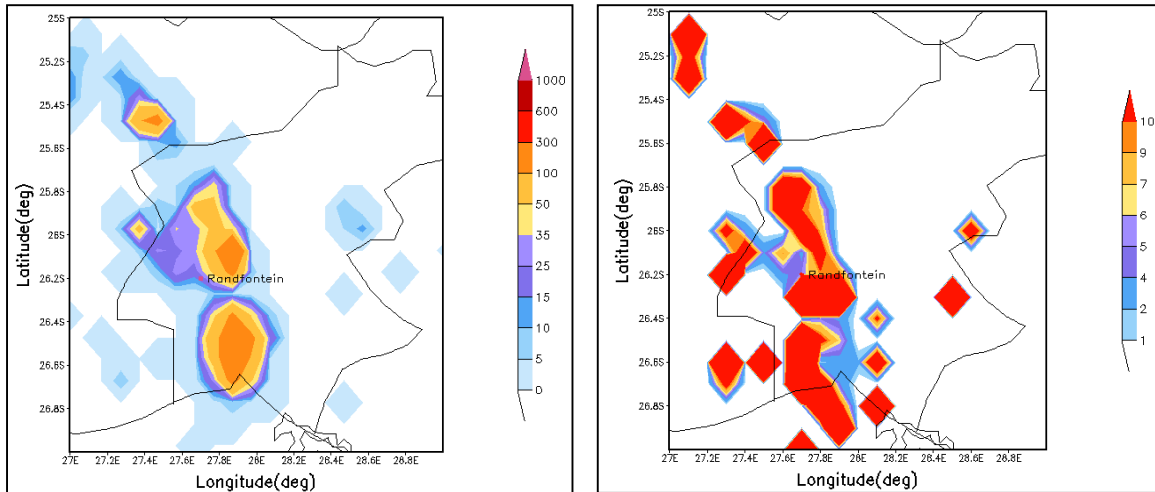


**FIGURE 4.4**

Sum of the lightning strokes detected over the Gauteng Province are depicted on the left hand side and the percentage (%) of positively charged lightning strokes over Gauteng are depicted on the right hand side, for 22 November 2007 between 1400Z and 1415Z.

The positioning and movement of the thunderstorm during the 30 minutes preceding and the 30 minutes after the event, including satellite imagery and lightning data, can be found in appendices B and C.

#### 4.1.2 Primary case study: 22 November 2007 at 1503Z

At 1503Z on 22 November 2007 a second fatality was reported in the Gauteng. This event occurred in the suburb of Northcliff, north-west of the Johannesburg city center located at point C on figure 4.1. Reports from witnesses at the scene suggested that the victim was walking under a tree while carrying an umbrella when she was struck by lightning (Netcare 911, 2007). As this incident occurred at 1503Z, 1500Z was used as the time reference for the data gathered.

#### *Satellite imagery*

In the HRV image shown in figure 4.5, reflectance over the Northcliff area was very high at 1500Z, indicating an optically thick cloud. The shadowing from the clouds to the north and north-east of Northcliff suggest the presence of an overshooting top



and hence very strong updrafts can be expected in the cloud. These clouds can be classified as CB cloud. In the IR10.8 $\mu$ m image in figure 4.5 the CTT over the Northcliff area was 202K (-70.93°C). The cloud water particle phase at 1500Z was ice according to the convection RGB in figure 4.5. The ice particles were, however, growing in size and therefore the absorption in the NIR1.6 $\mu$ m channel as part of the convection RGB was slightly less than for the small ice particles, hence the orange colour over Northcliff in figure 4.5.

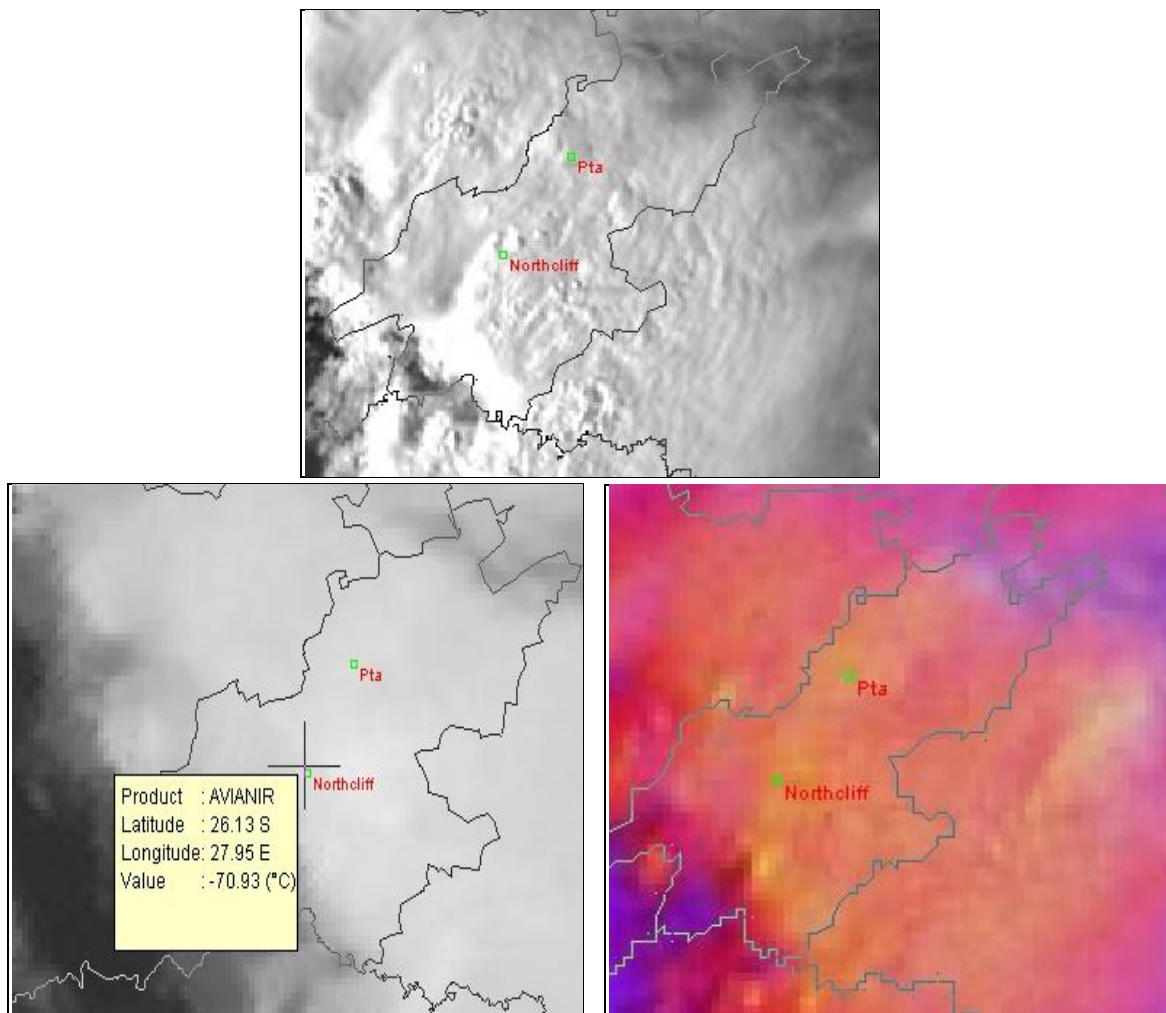


**FIGURE 4.5**

Meteosat Second Generation (MSG) satellite imagery over the Gauteng Province at 1500Z for 22 November 2007. The High Resolution Visible (HRV) image is at the top, the inverted Infra Red (IR) 10.8 $\mu$ m is on the bottom left hand side and the convection combination is on the bottom right hand side. Copyright (2013) EUMETSAT

The low angle of the setting sun in the west at 1500Z could interfere with the actual reflectance and this should be kept in mind when interpreting any satellite imagery derived from a channel within the visible light range on the electromagnetic spectrum (0.4 $\mu$ m to 0.7 $\mu$ m).

In figure 4.6 the CTT measured over Northcliff fell between 200K and 210K. The BTD values at 1500Z over Northcliff fell between 0K and 1K which is indicative of ice particles. The CTTs were well below the freezing point and so the BTD data are consistent with the CTT data and the satellite data presented in figure 4.5.

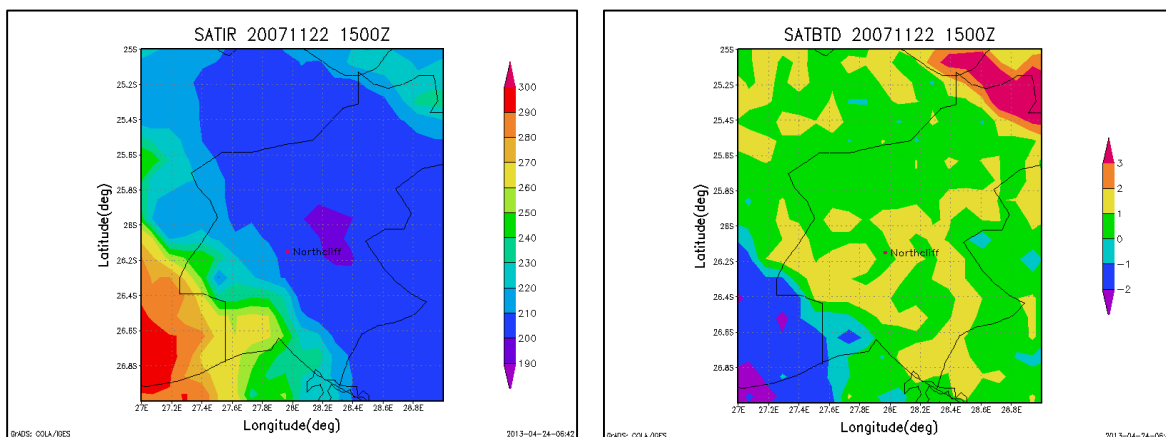


**FIGURE 4.6**

Grid Analysis display system (GrAds) imagery of Infra Red (IR)10.8 $\mu$ m data in degrees Kelvin (K) on the left hand side and Brightness Temperature Difference (BTD) of IR8.7 $\mu$ m-IR10.8 $\mu$ m measured in (K) on the right hand side, for 22 November 2007 at 1500Z.

### *Lightning data*

In figure 4.7 the total amount of cloud-to-ground lightning strokes measured between 1500Z and 1515Z on 22 November 2007 was between 5 and 10 strokes. Highest amounts of lightning during the 15 minute accumulation period totaled 50 to 100 strokes and were detected east and north-east of Northcliff. Of the total lightning strokes detected over Northcliff between 1500Z and 1515Z, 6% to 9% carried a positive charge, as seen in figure 4.7.



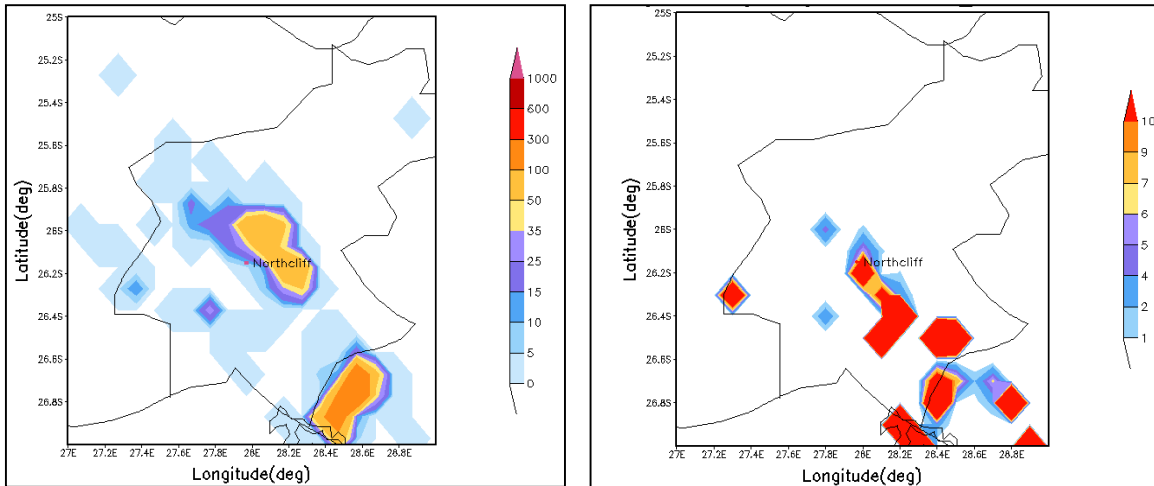


**FIGURE 4.7**

Sum of the lightning strokes detected over the Gauteng Province are depicted on the left hand side and the percentage (%) of positively charged lightning strokes over Gauteng are depicted on the right hand side, for 22 November 2007 between 1500Z and 1515Z.

The positioning of the thunderstorm, including satellite imagery and lightning stroke data for the 30 minutes preceding and the 30 minutes after the event, can be found in appendices B and C.

#### 4.1.3 Primary case study: 10 February 2009 between 1300Z and 1400Z

This case study was chosen due to the high number of insurance claims honoured on the day by Absa bank. The average amount of insurance claims listed during February 2009 was 34.2 per day. On 10 February 2009 a total of 258 claims were honoured over the Highveld area alone (figure 4.8), this was seven and a half times the monthly average. Regarding such data, it was assumed that convective activity and resultant lightning were very active on the day.

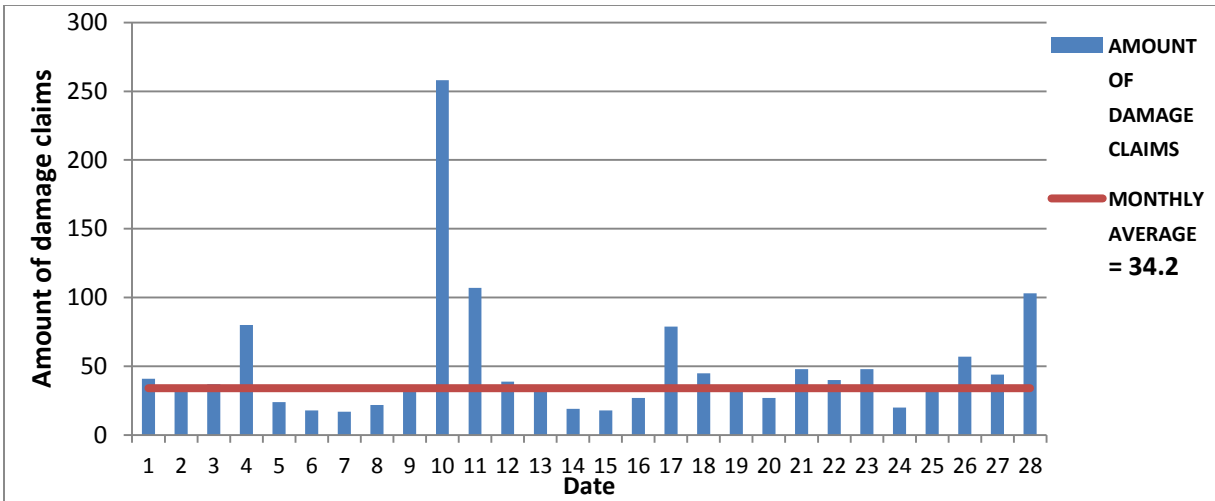


**FIGURE 4.8**

A graph depicting the daily totals and the monthly average of honoured lightning related insurance claims from Amalgamated banks of South Africa (Absa) for the month of February 2009 over the Highveld of South Africa.

Satellite and lightning data were scrutinized for 10 February 2009, and two separate time periods emerged during the day as having had the most significant convective activity. The two time periods were identified as firstly falling between 1300Z and 1400Z, a period during which the CB clouds were rapidly developing and a second period of interest between 1500Z and 1600Z with CB clouds that were already fully developed.

There were no fatalities reported for this event, which is not indicative of how intense the lightning may have been. This case study will focus on the convective activity between 1300Z and 1400Z, while the CB clouds were still in their development stages.

### *Satellite Imagery*

There were two thunderstorms over the southern parts of Gauteng at 1300Z, one over the south-western parts of the province, referred to hereafter as storm A and a second thunderstorm over Johannesburg, referred to hereafter as storm B. In figure 4.9, the HRV image depicted both CB clouds as being optically thick, while the IR10.8µm image gave the location of the lowest CTT at that time, which was found

to occur in storm A and measured as 202K. The convection RGB in figure 4.9 shows that small ice particles were present in both thunderstorms with larger particles found in the anvil of storm A, while storm B was dominated by strong updrafts and small ice. The CB clouds were positioned fairly close to one another at 1300Z, with storm A seemingly smaller in horizontal extent than storm B.

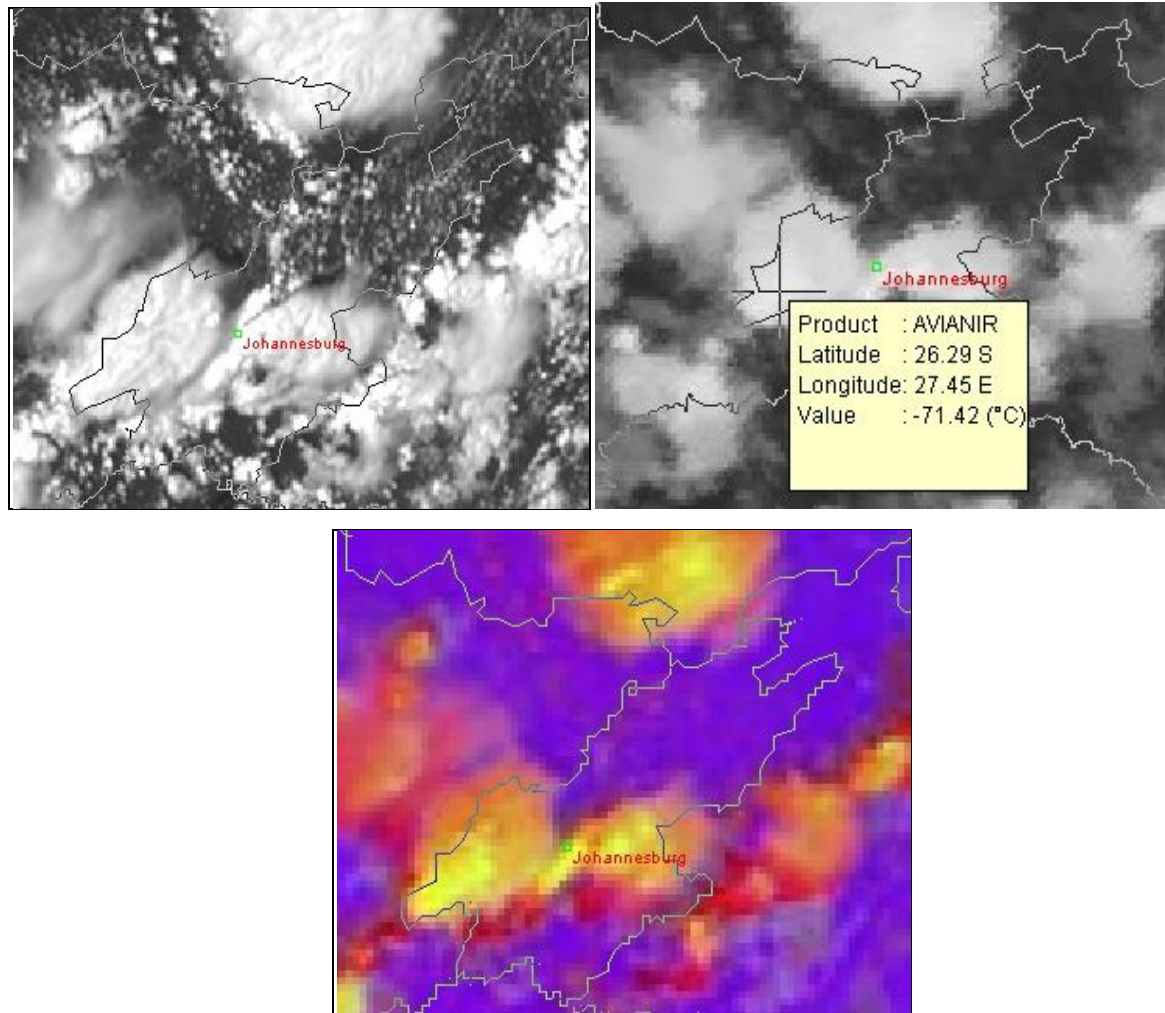


**FIGURE 4.9**

Meteosat Second Generation (MSG) satellite imagery over the Gauteng Province at 1300Z for 10 February 2009. The High Resolution Visible (HRV) satellite image, inverted Infra Red (IR) 10.8µm satellite image, convection channel combination are depicted from top left to the bottom center. Copyright (2013) EUMETSAT

The IR10.8µm image in figure 4.10 depicted a band of CTT values between 200K and 210K oriented west to east through the central parts of Gauteng, corresponding with the area of ice particles in a similar orientation in the BTD image. These data were in

agreement with the placement of lowest CTT and the CTT value measured on the IR10.8 $\mu$ m satellite image in figure 4.9.

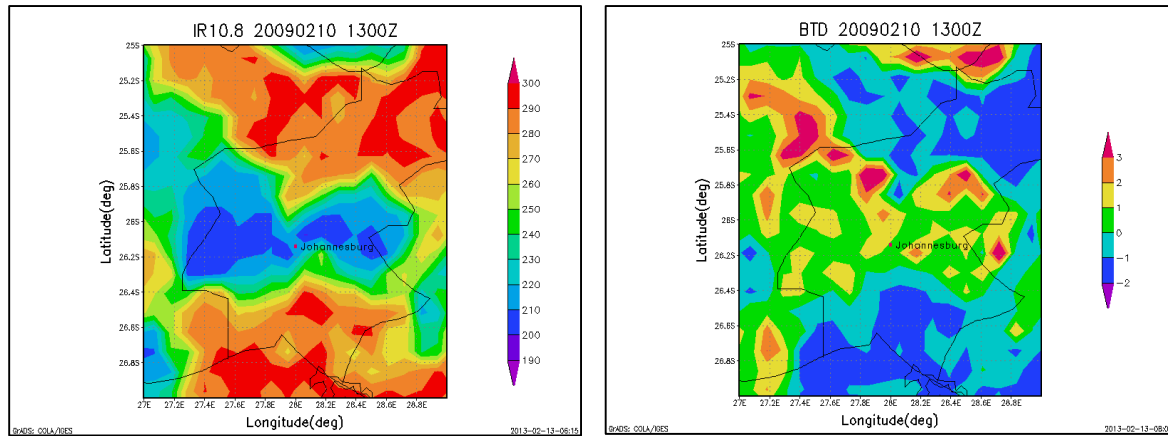


**FIGURE 4.10**

The Grid Analysis display system (GrAds) imagery of IR10.8 $\mu$ m measured in degrees Kelvin (K) is on the left hand side and the Brightness Temperature Difference (BTD) of IR8.7 $\mu$ m – IR10.8 $\mu$ m measured in K is on the right hand side for 10 February 2009 at 1300Z.

Copyright (2013) EUMETSAT

The satellite imagery depicted in figure 4.11 showed storm A and storm B to be in a similar position at 1315Z as they were at 1300Z in figure 4.9. The optical thickness from the HRV image was still high for both CB clouds with the lowest CTT located in storm B over Johannesburg. According to the IR10.8 $\mu$ m image in figure 4.11 ice particles still dominated as the phase of the cloud water in both CB clouds at 1315Z, with larger ice particles still found in the anvil of storm A. From figure 4.11, storm B seemed to have increased in horizontal extent since the previous time step in figure 4.9.

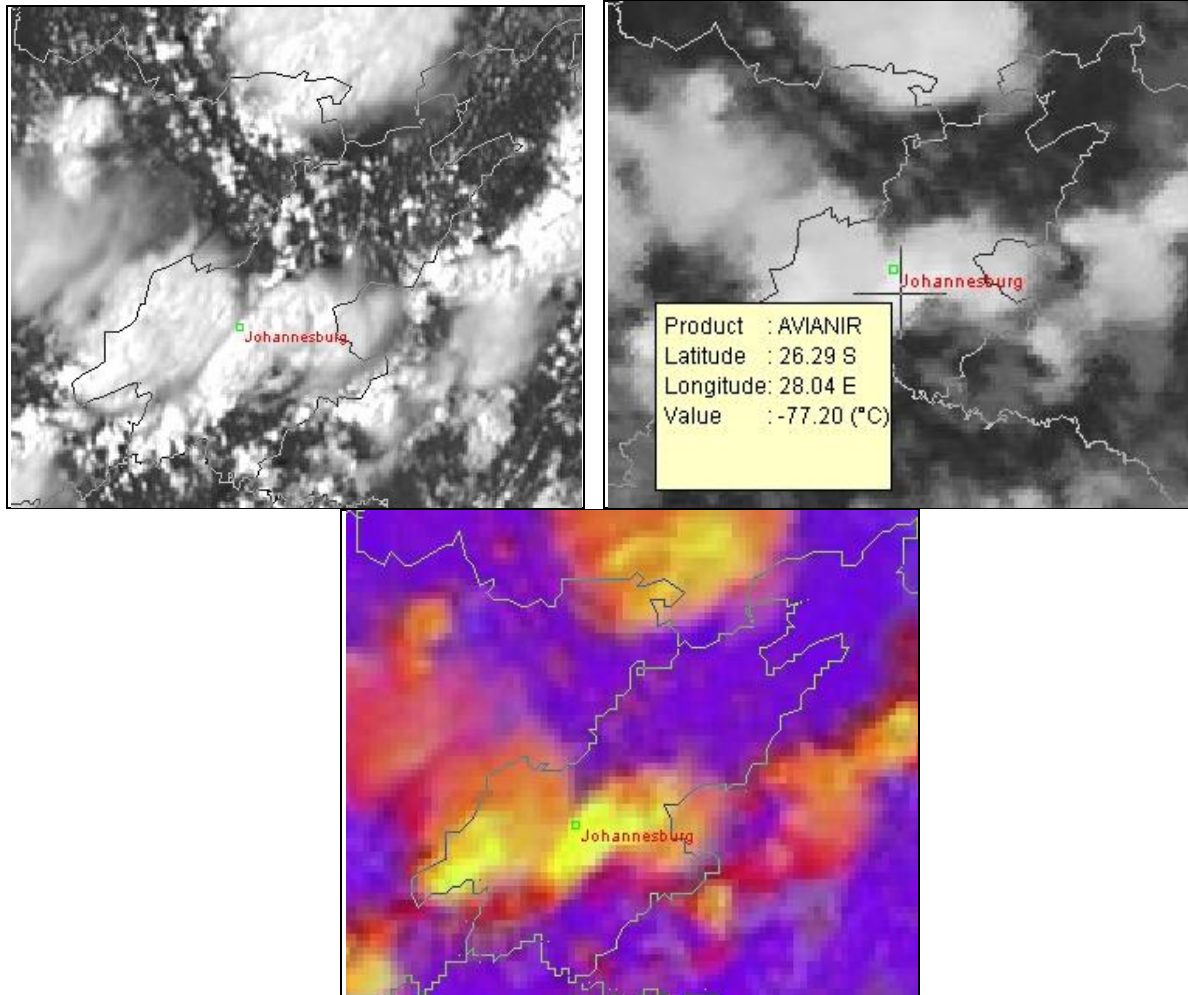


**FIGURE 4.11**

Meteosat Second Generation (MSG) satellite imagery over the Gauteng Province at 1315Z for 10 February 2009. The High Resolution Visible (HRV) satellite image, inverted Infra Red (IR) 10.8µm satellite image, convection channel combination are depicted from top left to the bottom center. Copyright (2013) EUMETSAT

The data displayed on the IR10.8µm image in figure 4.12 is consistent with the findings from the IR10.8µm satellite image, where the lowest CTTs are now located in storm B with values dropping to below 200K. Ice particles dominate in both CB clouds with a small pocket of liquid water found to the east of Johannesburg. Water clouds were present to the north and south of the two identified thunderstorms.

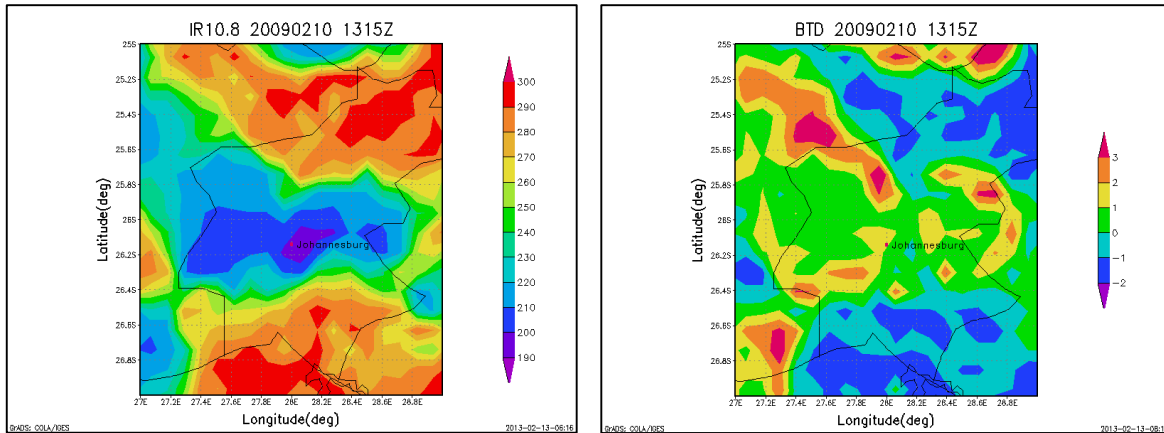


**FIGURE 4.12**

The Grid Analysis display system (GrAds) imagery of IR10.8 $\mu\text{m}$  measured in degrees Kelvin (K) is on the left hand side and the Brightness Temperature Difference (BTD) of IR8.7 $\mu\text{m}$  – IR10.8 $\mu\text{m}$  measured in K is on the right hand side for 10 February 2009 at 1315Z.

Copyright (2013) EUMETSAT

By 1330Z storm B had become the most active thunderstorm of the two, with the higher optical thickness, a lowest CTT of close to 190K and a large area of small ice particles as seen in figure 4.13. From the HRV image in figure 4.13, the texture of storm B was much more uneven while storm A in the west had become much smoother and taking on a grey colour, suggesting a lowering in optical thickness and lack of active updraft.

Storm B was still growing in horizontal and vertical extent at 1330Z indicating that the storm was in its development stage and not yet fully mature. This is when most lightning activity is expected from a thunderstorm. Storm A was showing signs of maturity and dissipation by 1330Z.



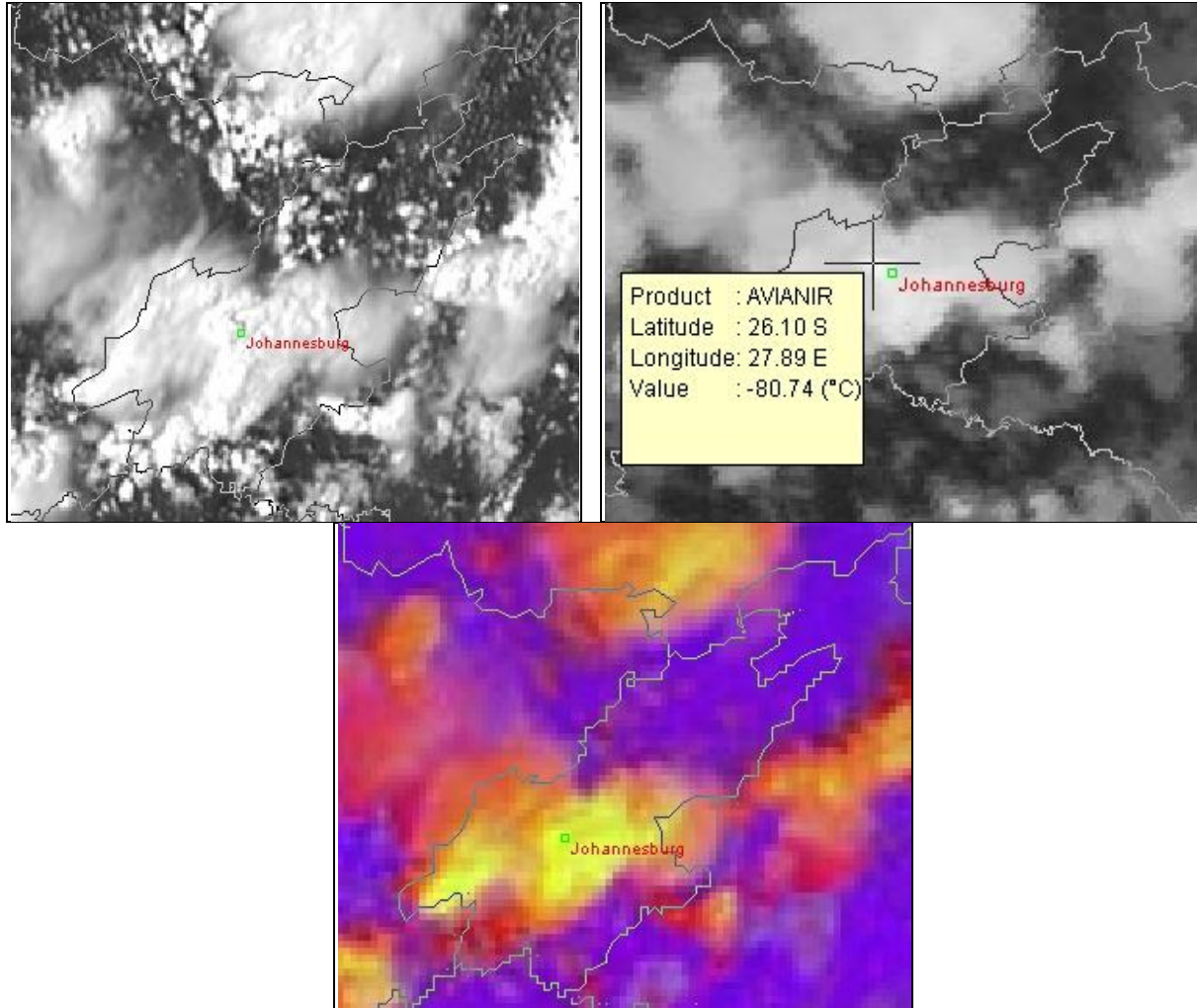


**FIGURE 4.13**

Meteosat Second Generation (MSG) satellite imagery over the Gauteng Province at 1330Z for 10 February 2009. The High Resolution Visible (HRV) satellite image, inverted Infra Red (IR) 10.8µm satellite image, convection channel combination are depicted from top left to the bottom center. Copyright (2013) EUMETSAT

In figure 4.14 the lowest CTT in storm B remained between 190K and 200K, in an orientation that was consistent with the area of small ice particles and strong updraft on the convection RGB in figure 4.13. Ice particles were still evident in a west to east orientation according to the BTD values in figure 4.14, similar to the orientation of CTT lower than 230K seen on the IR10.8µm image in figure 4.14.

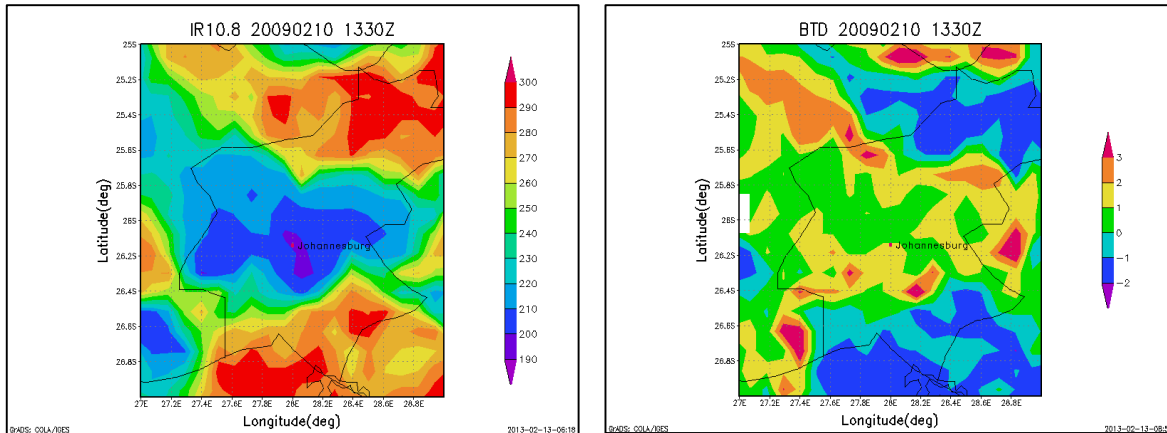


**FIGURE 4.14**

The Grid Analysis display system (GrAds) imagery of IR10.8 $\mu\text{m}$  measured in degrees Kelvin (K) is on the left hand side and the Brightness Temperature Difference (BTD) of IR8.7 $\mu\text{m}$  – IR10.8 $\mu\text{m}$  measured in K is on the right hand side, for 10 February 2009 at 1330Z. Copyright (2013) EUMETSAT

By 1345Z (figure 4.15) storm B had continued to develop and spread out over much of the central parts of Gauteng. Optical thickness in storm B was still very high as seen on the HRV image, while the lowest CTT was measured as 193K (-80.13°C) on the IR10.8 $\mu\text{m}$  image. The convection RGB still shows small ice particles dominating in both CB clouds in figure 4.15. The area of the small ice particles in storm B expanded significantly since 1300Z (figure 4.9), suggesting that the period of first icing occurred closer to 1300Z.

The bright yellow colour persisting in storm A could be the influence of cirrus cloud which dominated above the dissipating CB cloud. The orange colour on the western edge of storm A is indicative of large ice particles in the CB. The northern and southern fringes of the anvil from storm B also show up as a bright yellow colour.



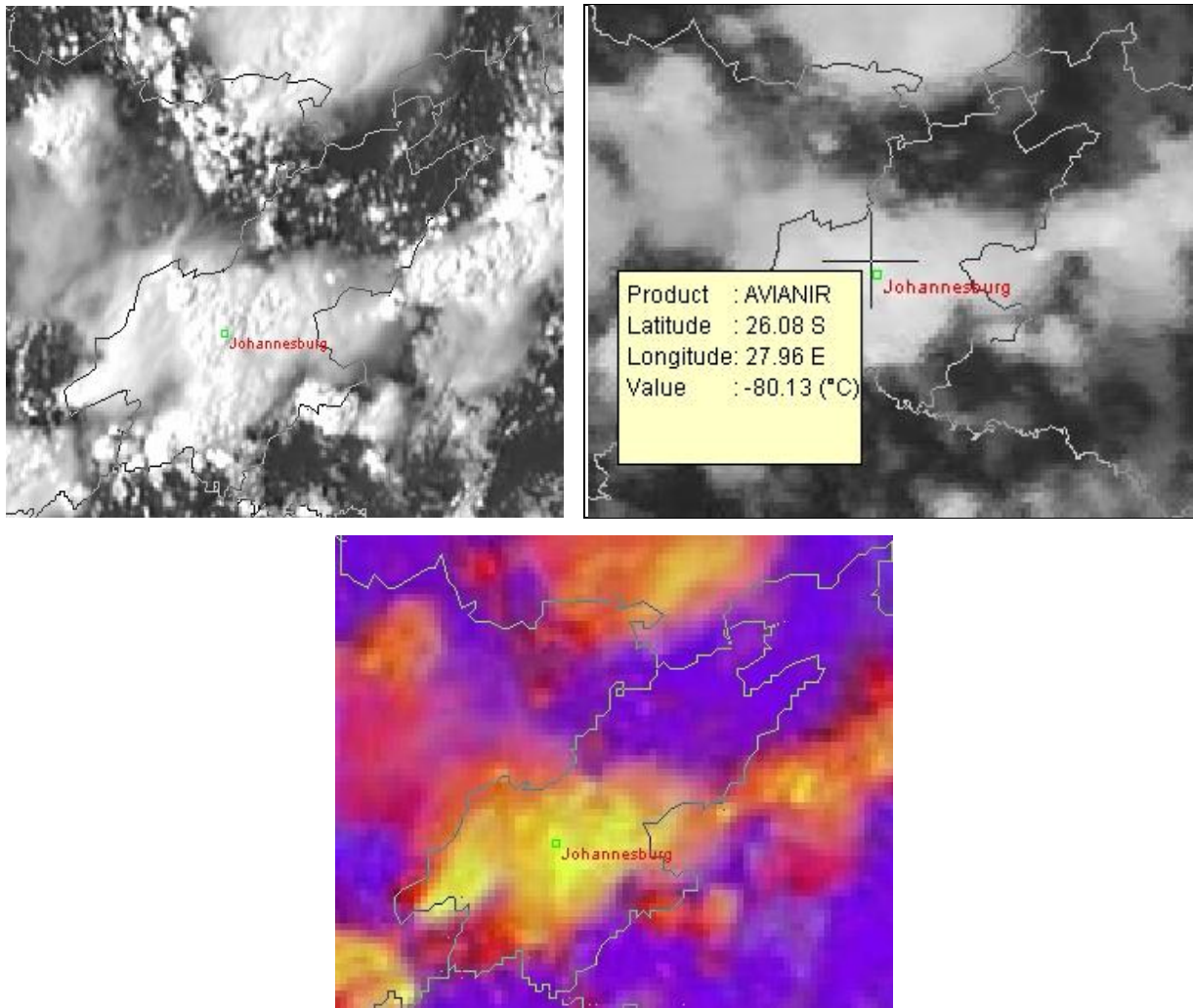


**FIGURE 4.15**

Meteosat Second Generation (MSG) satellite imagery over the Gauteng Province at 1345Z for 10 February 2009. The High Resolution Visible (HRV) satellite image, inverted Infra Red (IR) 10.8µm satellite image, convection channel combination are depicted from top left to the bottom center. Copyright (2013) EUMETSAT

The IR10.8µm image in figure 4.16 depicted that the lowest CTTs were located north of Johannesburg with values between 190K and 200K at 1345Z, which correlated well with the data from the IR10.8µm satellite image in figure 4.15. Ice particles were still dominated according to the BTd data in figure 4.16, the north-to-south extent of which had increased substantially since 1300Z.

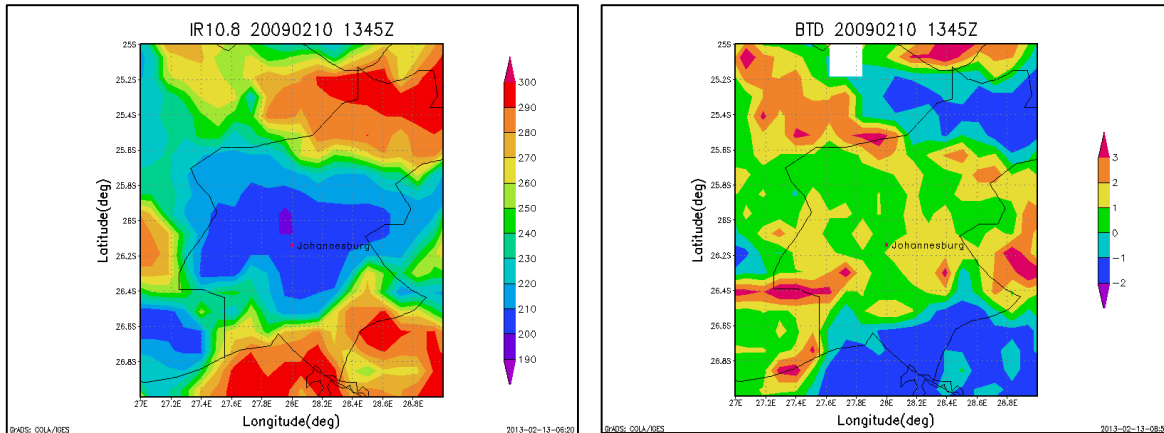


**FIGURE 4.16**

The Grid Analysis display system (GrAds) imagery of IR10.8 $\mu\text{m}$  measured in degrees Kelvin (K) is on the left hand side and the Brightness Temperature Difference (BTD) of IR8.7 $\mu\text{m}$  – IR10.8 $\mu\text{m}$  measured in K is on the right hand side for 10 February 2009 at 1345Z. Copyright (2013) EUMETSAT

By the end of the period at 1400Z, convection was still very active over Johannesburg and central Gauteng with storm B maintaining its uneven texture and high optical thickness (figure 4.17). The lowest CTT measured on the IR10.8 $\mu\text{m}$  image in figure 4.17 is 196K (-76.64°C), which was slightly warmer than at 1345Z (figure 4.15).

The area of small ice particles on the convection RGB had reduced in size since 1345Z (figure 4.15). New convective development, which started on the border of Gauteng with Mpumalanga at 1345Z and, at 1400Z (figure 4.17), is more noticeable as a relatively small cell with a high reflectance. The convection RGB in figure 4.17 was depicting a light orange colour by 1400Z. When this CB experiences its first icing in the cloud tops, a bright yellow colour is expected to be seen.

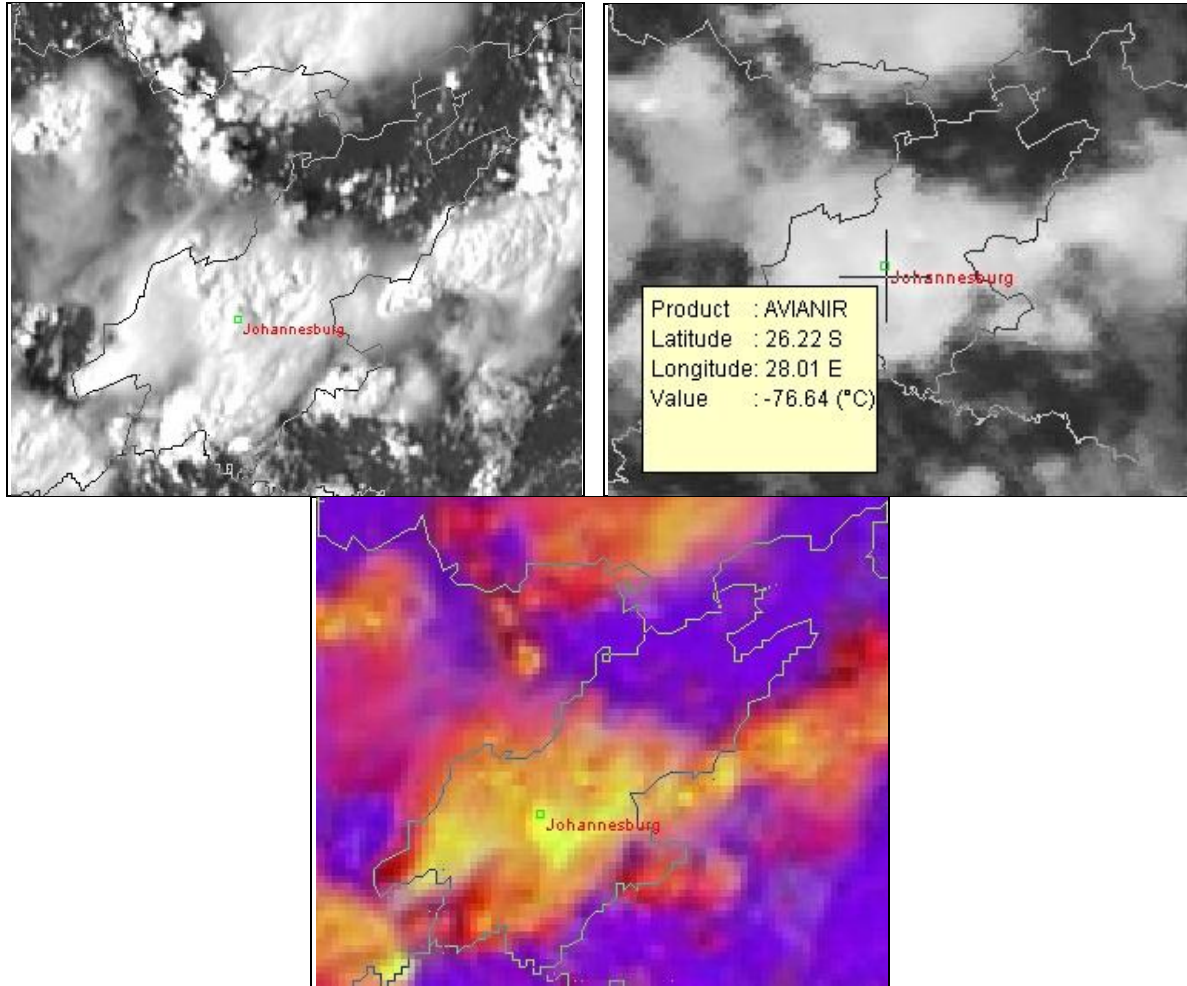


**FIGURE 4.17**

Meteosat Second Generation (MSG) satellite imagery over the Gauteng Province at 1400Z for 10 February 2009. The High Resolution Visible (HRV) satellite image, inverted Infra Red (IR) 10.8µm satellite image, convection channel combination are depicted from top left to the bottom center. Copyright (2013) EUMETSAT

The horizontal extent of the CTTs lower than 210K spread further to the north and south between 1345Z and 1400Z as seen by comparing figure 4.17 with figure 4.15. Although ice particles were still dominant at 1400Z (figure 4.17), there was an area to the north-east of Johannesburg where the BTD values dropped closer to -1K, which borders on liquid water phase within the cloud.

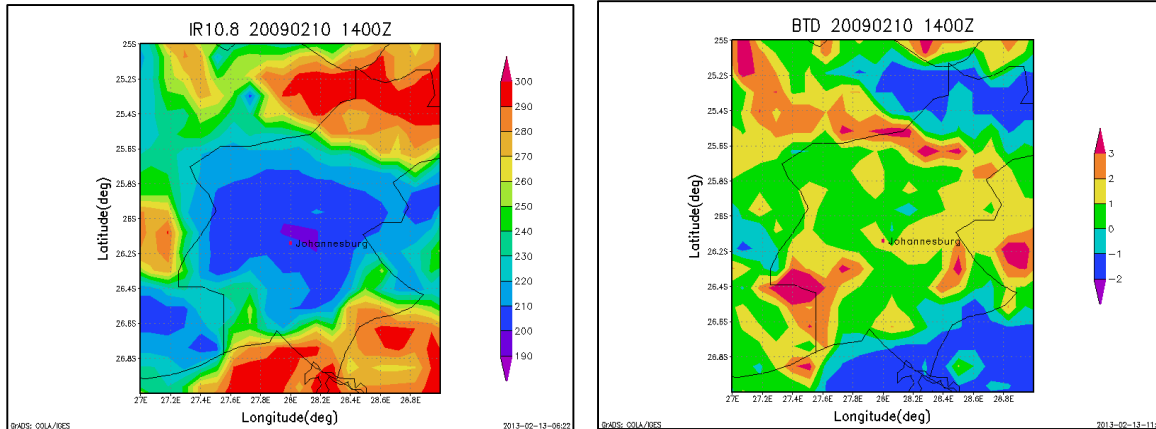


**FIGURE 4.18**

The Grid Analysis display system (GrAds) imagery of IR10.8 $\mu$ m measured in degrees Kelvin (K) is on the left hand side and the Brightness Temperature Difference (BTD) of IR8.7 $\mu$ m – IR10.8 $\mu$ m measured in K is on the right hand side for 10 February 2009 at 1400Z. Copyright (2013) EUMETSAT

### *Lightning data*

The amount of lightning strokes detected in this case study was significantly higher than in the previously discussed primary cases. As seen from the satellite imagery and satellite derived data sets in figures 4.9 to 4.18, there were two thunderstorms over the area of interest, one of which over 1 hour seemed to develop and spread out in horizontal extent. The period between 1330Z and 1400Z produced the most lightning and this 30 minute period was focused on in the discussion of the case.

For the 60 minute accumulation period between 1300Z and 1400Z, there were between 100 and 300 cloud-to-ground strokes in a north-to-south oriented band located west of Johannesburg, with a maximum amount of 600 to 1000 strokes detected just to the north-west of Johannesburg (figure 4.19). During the 60 minute accumulation period, the percentage of positively charged lightning strokes were between 7% and 9% in the band of maximum activity west of Johannesburg (figure 4.19). The area where more than 10% of the lightning strokes were positively charged lies west of the main band of lightning activity as seen in figure 4.19. More than 10% of the lightning strokes were positively charged over the south-western

corner of Gauteng, west of the CB cloud which developed over the south-western parts of the Province between 1300Z and 1400Z (figures 4.9 to 4.18).

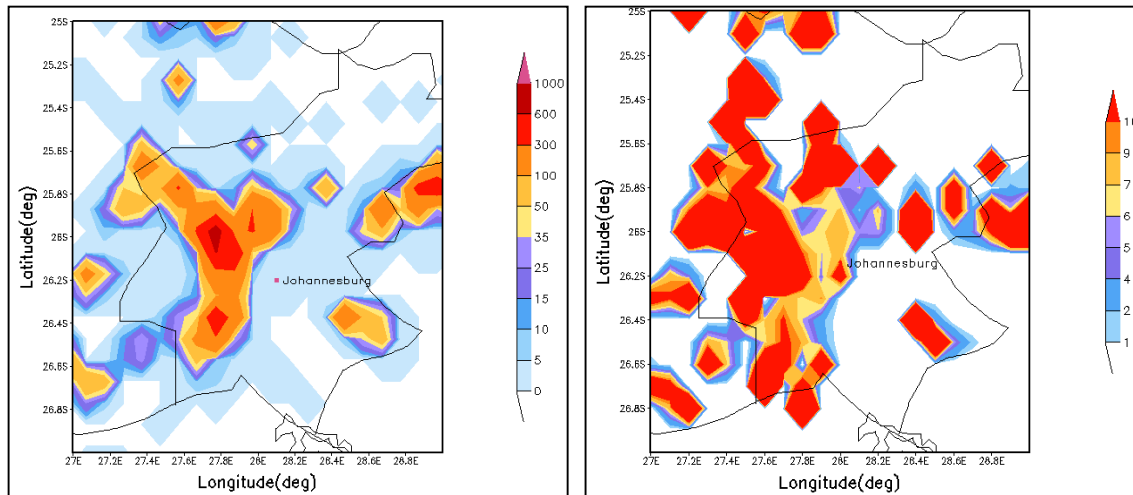


**FIGURE 4.19**

Total lightning strokes detected over the Gauteng Province for 10 February 2009 between 1300Z and 1400Z are on the left hand side and the percentage (%) of positively charged lightning strokes detected during the corresponding time period are depicted on the right hand side.

Figure 4.20 is valid for the 30 minute time period between 1330Z and 1400Z, where the maximum amount of cloud-to-ground lightning was detected west of Johannesburg in a band similar in orientation to what was observed in figure 4.19. The accumulation of lightning between 1330Z and 1400Z in figure 4.19 fell between 50 and 300 strokes with more than 300 strokes having been detected north-west of Johannesburg. The percentage of positively charged strokes during the corresponding time period in figure 4.19 was higher than 10% in, and to the west of the band of highest total amounts of lightning. This pattern was consistent with the orientation of the percentage of positive strokes found in figure 4.19. Associated with the band of lightning stretching west to east across central Gauteng high percentage of positively charged strokes extended into Mpumalanga.



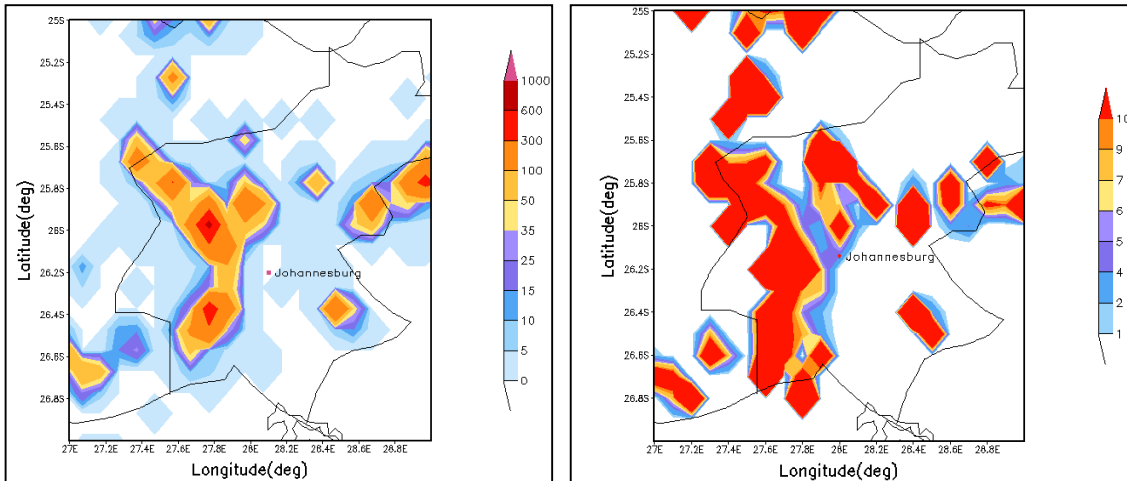


**FIGURE 4.20**

Total lightning strokes detected over the Gauteng Province for 10 February 2009 between 1330Z and 1400Z are on the left hand side and the percentage (%) of positively charged lightning strokes detected during the corresponding time period are depicted on the right hand side.

By breaking the 30 minute time period between 1330Z and 1400Z into two 15 minute periods, it is seen in figure 4.21 that 100 to 300 strokes accumulated between 1330Z and 1345Z to the west and north-west of Johannesburg. Between 5% and 6% of the strokes over Johannesburg were positively charged while more the 10% of the lightning strokes were positively charged in a location just west of the band of highest accumulation discussed in figures 4.19 and 4.20.

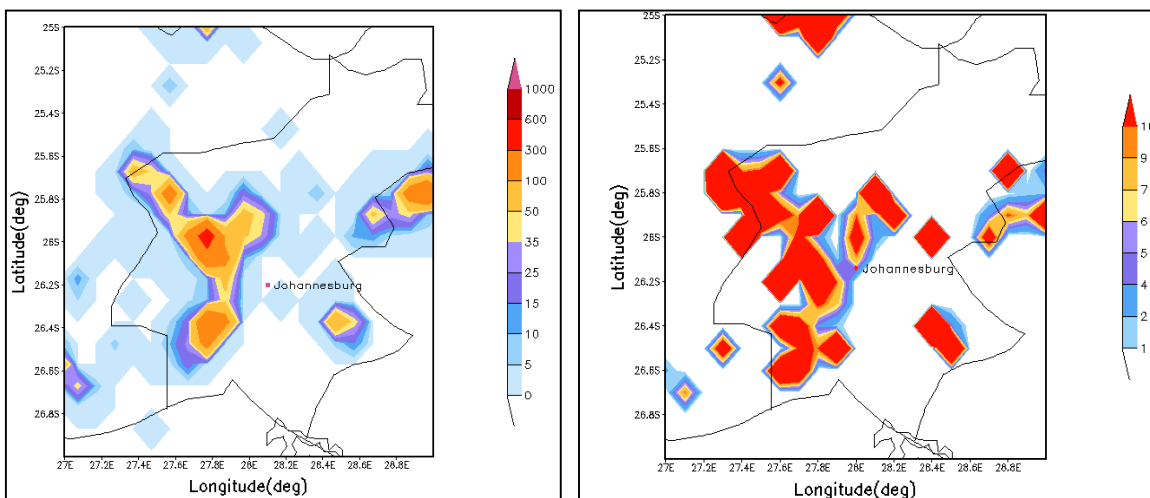


**FIGURE 4.21**

Total lightning strokes detected over the Gauteng Province for 10 February 2009 between 1330Z and 1345Z are on the left hand side and the percentage (%) of positively charged lightning strokes detected during the corresponding time period are depicted on the right hand side.

In figure 4.22 the 15 minute lightning accumulation between 1345Z and 1400Z is given, where the orientation of the band of highest accumulation was consistent with the band discussed in figures 4.19 to 4.21. In figure 4.22 there were fewer lightning strokes detected during the 15 minute period as compared to results in figure 4.21 but the percentage of positively charged strokes remained above 10% in the north-to-south band situated west of Johannesburg.

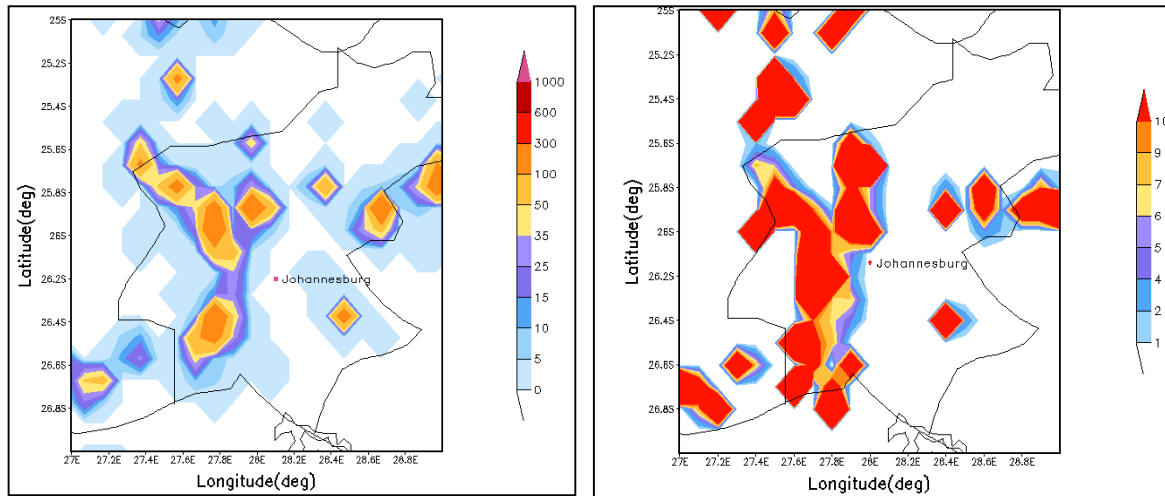


**FIGURE 4.22**

Total lightning strokes detected over the Gauteng Province for 10 February 2009 between 1345Z and 1400Z are on the left hand side and the percentage (%) of positively charged lightning strokes detected during the corresponding time period are depicted on the right hand side.

## 4.2 Secondary case study

### 4.2.1 Secondary case study: 29 October 2009 between 1500Z and 1600Z

This case study was identified and selected for inclusion by consulting the insurance claim data base obtained from Absa. According to the database, the average number of insurance claims over the 4 year period of interest from January 2007 to December 2010 was 28.2 claims per month. The month of October 2009 had an average of 29 claims per day. 29 October 2009 was selected as there were 24 insurance claims for the day, which was closest to the monthly average of 29. There were no lightning or weather related incidents reported on this day but it was not assumed that these

could not possibly have occurred. The results gathered for this case study were compared with results from the primary cases in an attempt to find any similarities between cloud microphysics and lightning occurrence.

The satellite data for 29 October 2009 were scrutinized and it was found that between 1500Z and 1600Z was when most of the convective activity occurred. The majority of convective activity took place over Mpumalanga (figure 1.1). The southern and central parts of Mpumalanga fall within the high ground density region of South Africa according to figure 1.3.

### *Satellite Imagery*

HRV satellite imagery was not available for use in this case as the data are not disseminated for this sector of South Africa after 1500Z daily. For this purpose, the VIS0.6 $\mu$ m was used to determine optical thickness and other relevant cloud features.

The VIS0.6 $\mu$ m image in figure 4.23 depicted convective cloud over the southern parts of Limpopo, northern Gauteng and the southern half of Mpumalanga at 1500Z. There was an area of high reflectance just to the south and south-west of the town of Ermelo where the uneven texture and cellular structure of the clouds were evidence that there was also convection taking place there. The high reflectance means that the clouds in the area were optically thick. The lowest CTT measured from the IR10.8 $\mu$ m image in figure 4.23 was 203K (-69.97°C). The area where the lowest CTT were detected (on the north-eastern border of Gauteng with Mpumalanga) was coincident with an optically thick area of convection identified on the VIS0.6 $\mu$ m image and the convection RGB depicted small ice particles in the same area (figure 4.23).



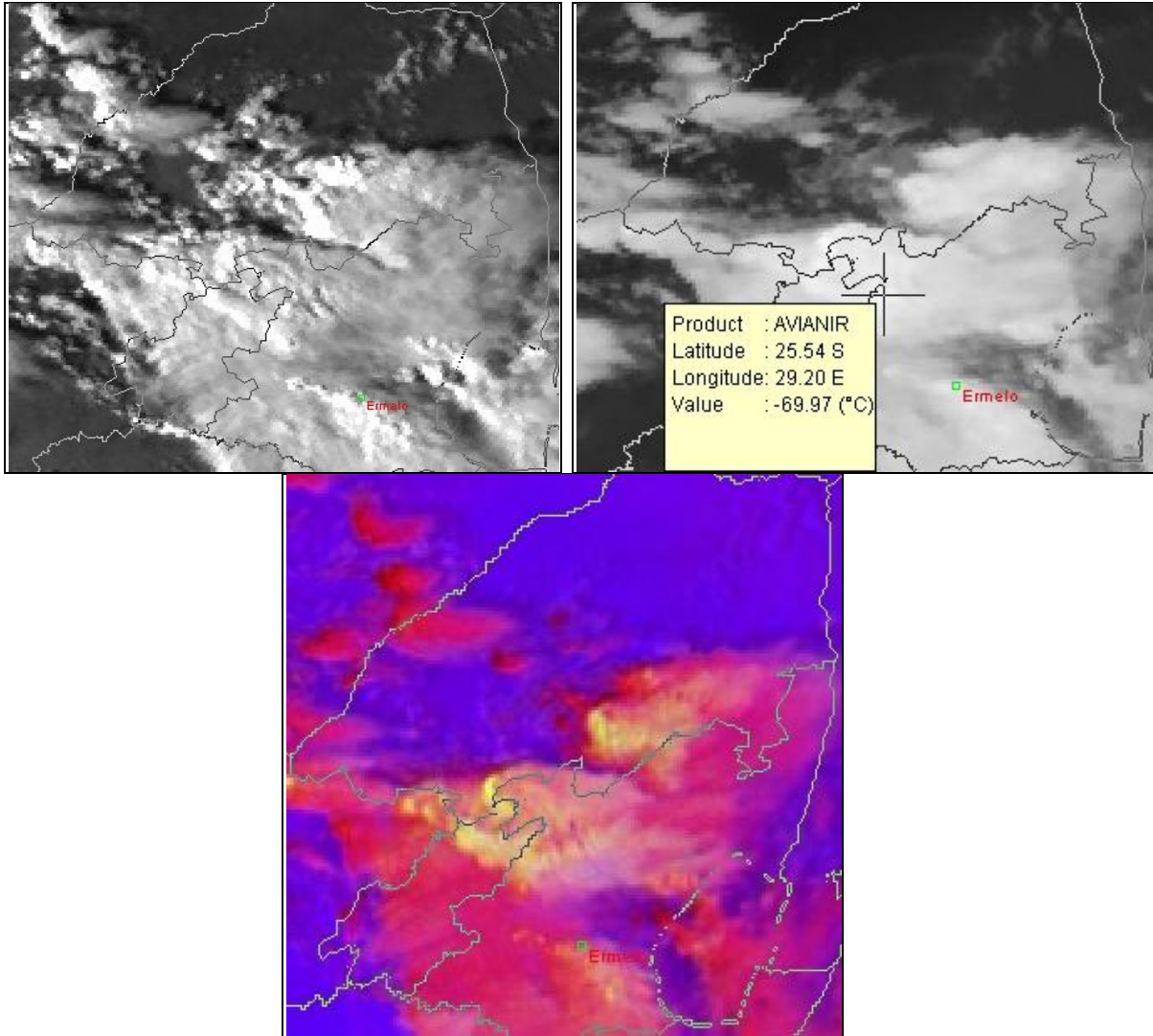


**FIGURE 4.23**

Meteosat Second Generation (MSG) satellite imagery over the Mpumalanga Province at 1500Z for 29 October 2009. The High Resolution Visible (HRV) satellite image, inverted Infra Red (IR) 10.8µm satellite image, convection channel combination are depicted from top left to the bottom center. Copyright (2013) EUMETSAT

The CTT data at 1500Z shown in figure 4.24 indicated a broad band of CTTs lower than 230K, with CTTs of between 200K and 210K found over northern Gauteng extending to the north-western parts of Mpumalanga, as well as in two small patches south-east of Ermelo.

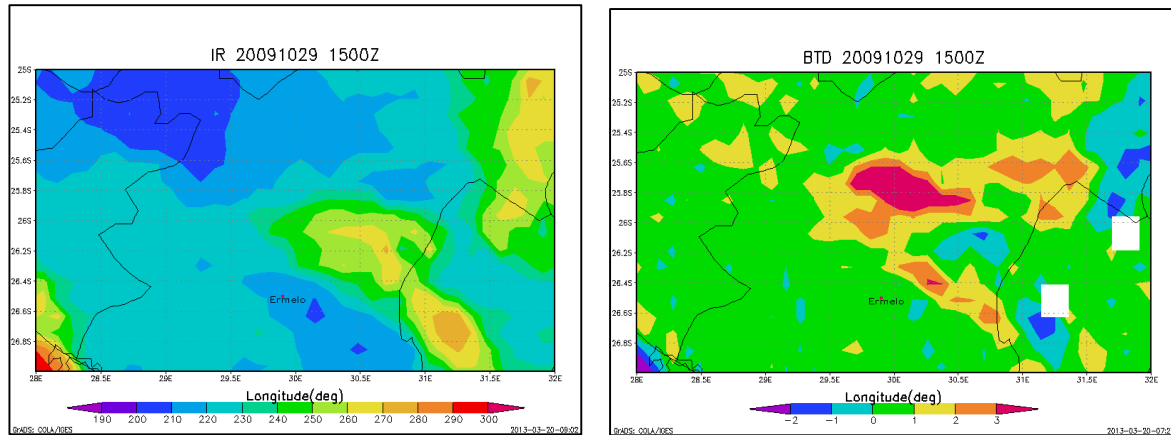


**FIGURE 4.24**

The Grid Analysis display system (GrAds) imagery of IR10.8µm measured in degrees Kelvin (K) is on the left hand side and the Brightness Temperature Difference (BTD) of IR8.7µm – IR10.8µm measured in K is on the right hand side for 29 October 2009 at 1500Z. Copyright (2013) EUMETSAT

By 1515Z in figure 4.25 the convective development had persisted in the north-western parts of Mpumalanga and south-east of Ermelo, while the CTT on the IR10.8µm image decreased significantly to 197K (-76.09°C) over the north-western parts of Mpumalanga. Small ice particles were only just identifiable on the convection RGB in figure 4.25, over the area of lowest CTT seen on the IR10.8µm image. The grey coloured cloud in the VIS0.6µm image in figure 4.25 is thinner mid level cloud and possibly the remnants of anvils from dissipated CB clouds from earlier during the afternoon. The ripple effect observed in the cloud band on the VIS0.6µm image could have resulted from gravity waves emanating from the active convection in the area as it seemed to originate in the thick convective cloud west of Gauteng.

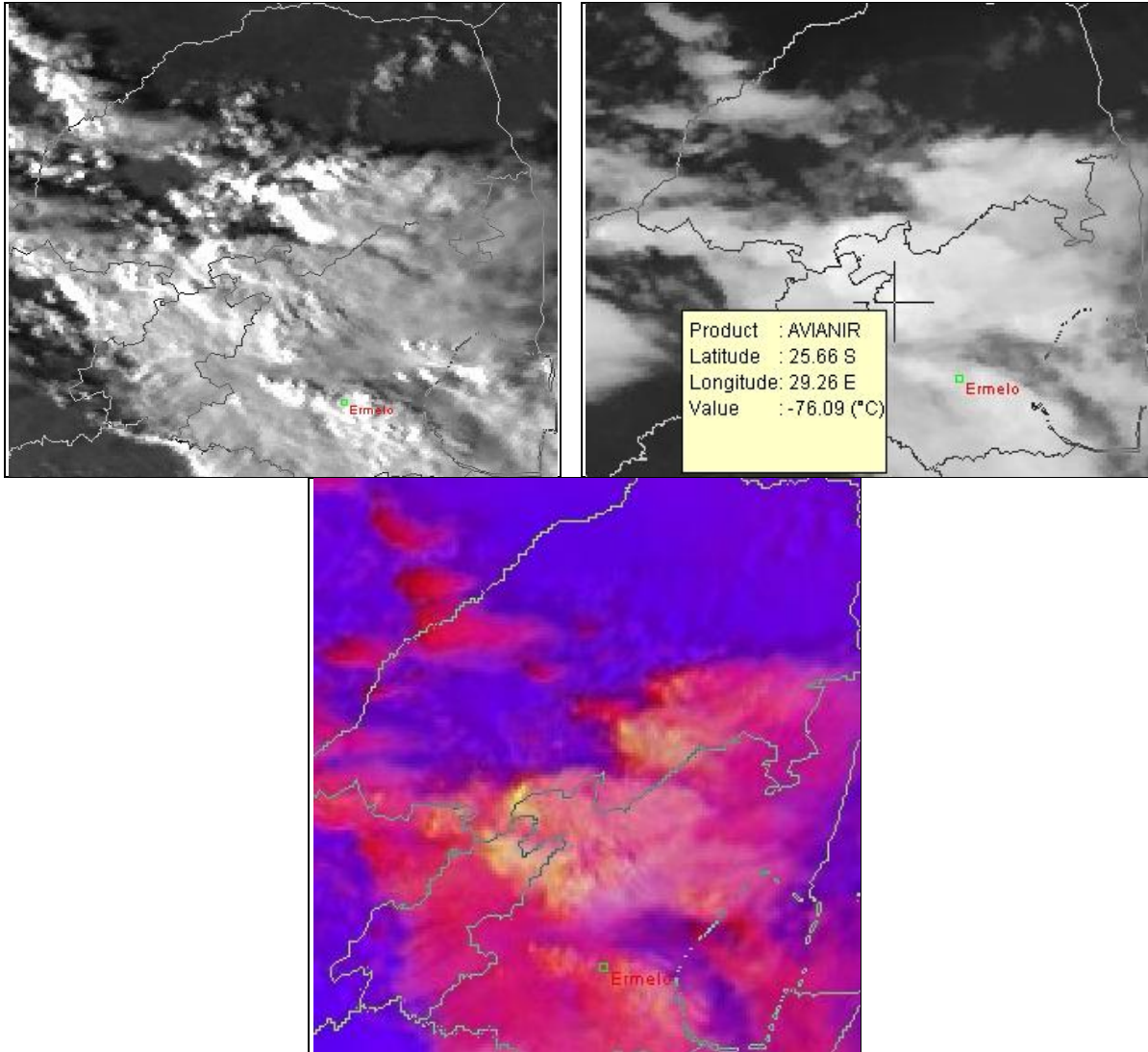


**FIGURE 4.25**

Meteosat Second Generation (MSG) satellite imagery over the Mpumalanga Province at 1515Z for 29 October 2009. The High Resolution Visible (HRV) satellite image, inverted Infra Red (IR) 10.8µm satellite image, convection channel combination are depicted from top left to the bottom center. Copyright (2013) EUMETSAT

The lowest CTT on the IR10.8µm image in figure 4.26 was between 190K and 200K which correlated well with the lowest CTT on the IR10.8µm satellite image in figure 4.25. Ice particles were dominant over the area where convection had been identified at 1515Z according to the BTD values in figure 4.26 although small pockets of possible liquid water were present as well.

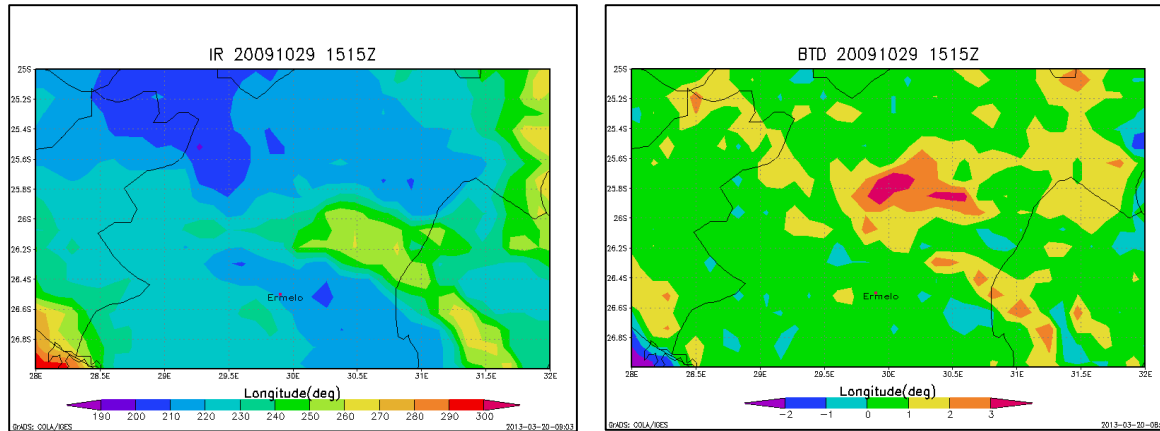


**FIGURE 4.26**

The Grid Analysis display system (GrAds) imagery of IR10.8µm measured in degrees Kelvin (K) is on the left hand side and the Brightness Temperature Difference (BTD) of IR8.7µm – IR10.8µm measured in K is on the right hand side for 29 October 2009 at 1515Z. Copyright (2013) EUMETSAT

By 1530Z the convection RGB was no longer a reliable image to interpret due to the low angle of the sun. For this reason, only the VIS0.6µm and IR10.8µm imagery was considered from 1530Z until 1600Z. Figure 4.27 depicts satellite imagery at 1530Z where optically thick, convective cloud was still evident south of Ermelo and over the north-western parts of Mpumalanga on the VIS0.6µm image. The lowest CTT measured on the IR10.8µm image in figure 4.27 was 199K (-73.95°C), located over the north-western parts of the Mpumalanga Province.

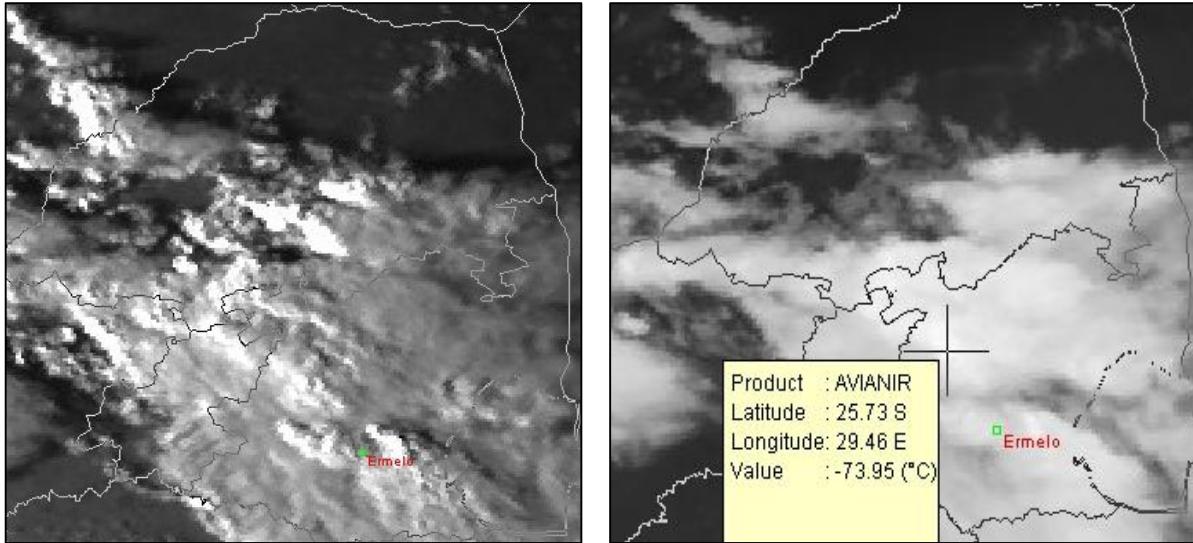


**FIGURE 4.27**

Meteosat Second Generation (MSG) satellite imagery over the Mpumalanga Province at 1530Z for 29 October 2009. The High Resolution Visible (HRV) satellite image on the left hand side and inverted Infra Red (IR) 10.8µm satellite image on the right hand side. Copyright (2013) EUMETSAT

The GrAds imagery in figure 4.28 correlated well with the satellite imagery in figure 4.27 where the lowest CTT in figure 4.28 fell between 200K and 210K. There is an extremely small area of CTTs below 200K on the IR10.8µm image in figure 4.28 which was where the CTT of 199K was measured on the IR10.8µm satellite image in figure 4.27. The BTD values in figure 4.28 gave evidence of potential pockets of liquid water being found east and north-east of Ermelo.

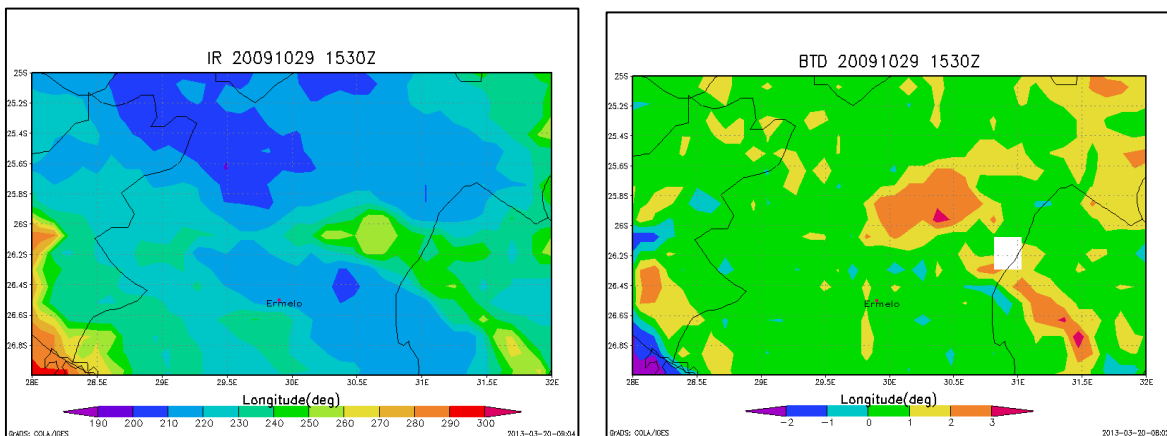


**FIGURE 4.28**

The Grid Analysis display system (GrAds) imagery of IR10.8µm measured in degrees Kelvin (K) is on the left hand side and the Brightness Temperature Difference (BTD) of IR8.7µm – IR10.8µm measured in K is on the right hand side for 29 October 2009 at 1530Z. Copyright (2013) EUMETSAT



The setting sun at 1545Z accentuated the shadows cast by the uneven cloud top structure in the CB clouds over Mpumalanga and the southern parts of Limpopo (figure 4.29). The lowest CTT measured on the IR10.8 $\mu$ m image in figure 4.29 was 197K (-75.54°C) which was the lowest CTT measured since 1500Z. The lowest CTTs consistently occurred in the CB cloud over north-western Mpumalanga, despite the apparent development of a CB cloud north-east of Ermelo.

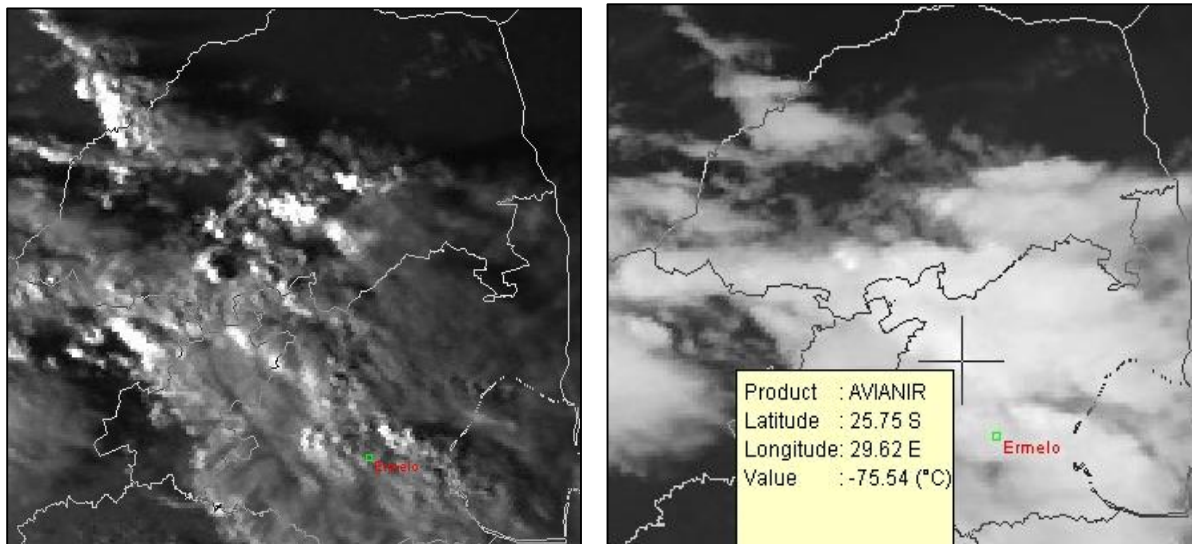


**FIGURE 4.29**

Meteosat Second Generation (MSG) satellite imagery over the Mpumalanga Province at 1545Z for 29 October 2009. The High Resolution Visible (HRV) satellite image on the left hand side and inverted Infra Red (IR) 10.8 $\mu$ m satellite image on the right hand side. Copyright (2013) EUMETSAT

The GrAds image of the CTT on the IR10.8 $\mu$ m image in figure 4.30 showed temperatures only dropped as low as 200K, where it was seen in figure 4.29 that the CTT dropped below that value over the north-western parts of Mpumalanga. Although ice particles were still the dominant water phase in the CB clouds in figure 4.30 there were more pockets of possible liquid water droplets appearing north-east of Ermelo and over the north-western parts of Mpumalanga. This suggested that the CB clouds were no longer increasing vertically but that the clouds were rather starting to dissipate by 1545Z.

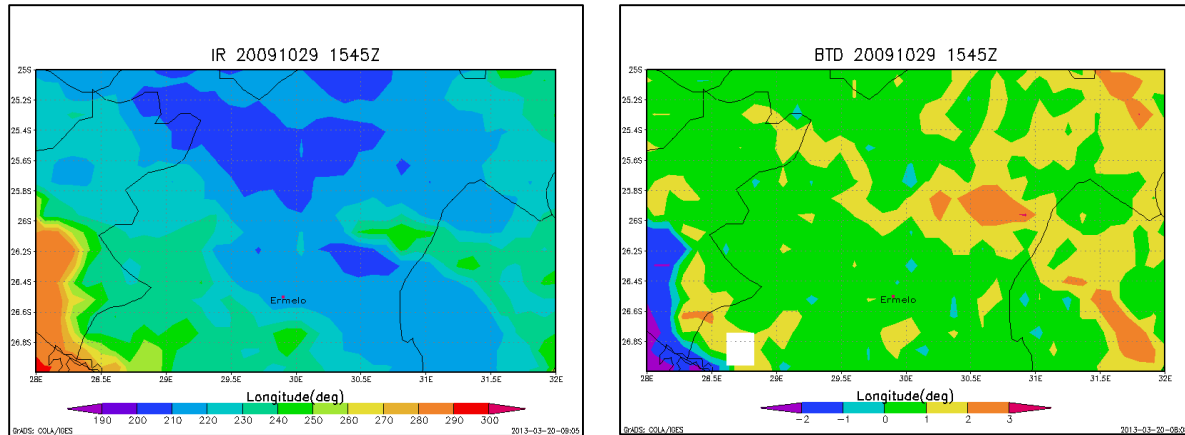


**FIGURE 4.30**

The Grid Analysis display system (GrAds) imagery of IR10.8µm measured in degrees Kelvin (K) is on the left hand side and the Brightness Temperature Difference (BTD) of IR8.7µm – IR10.8µm measured in K is on the right hand side for 29 October 2009 at 1545Z. Copyright (2013) EUMETSAT

By 1600Z the satellite imagery in figure 4.31 showed little detail on the VIS0.6µm image, besides high reflectance on the cloud tops north-east of Ermelo, which suggested that the CB cloud in that area was still active. The CTT on the IR10.8µm image had started increasing over the north-western parts of Mpumalanga by 1600Z and the lowest value was measured to be 202K (-70.93°C).

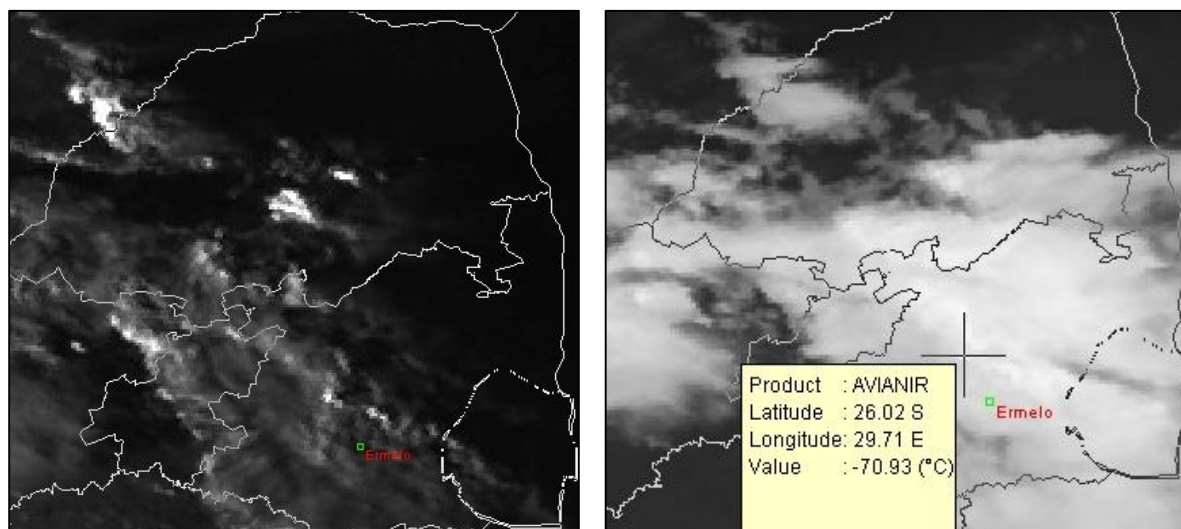


**FIGURE 4.31**

Meteosat Second Generation (MSG) satellite imagery over the Mpumalanga Province at 1600Z for 29 October 2009. The High Resolution Visible (HRV) satellite image on the left hand side and inverted Infra Red (IR) 10.8µm satellite image on the right hand side. Copyright (2013) EUMETSAT

The band of lowest CTT on the GrAds display of IR10.8 $\mu$ m in figure 4.32, were found over the northern and north-western parts of Mpumalanga. The BTD values over that area at the corresponding time (figure 4.32) were indicative of mostly ice particles, with possible pockets of liquid water persisting since 1515Z.

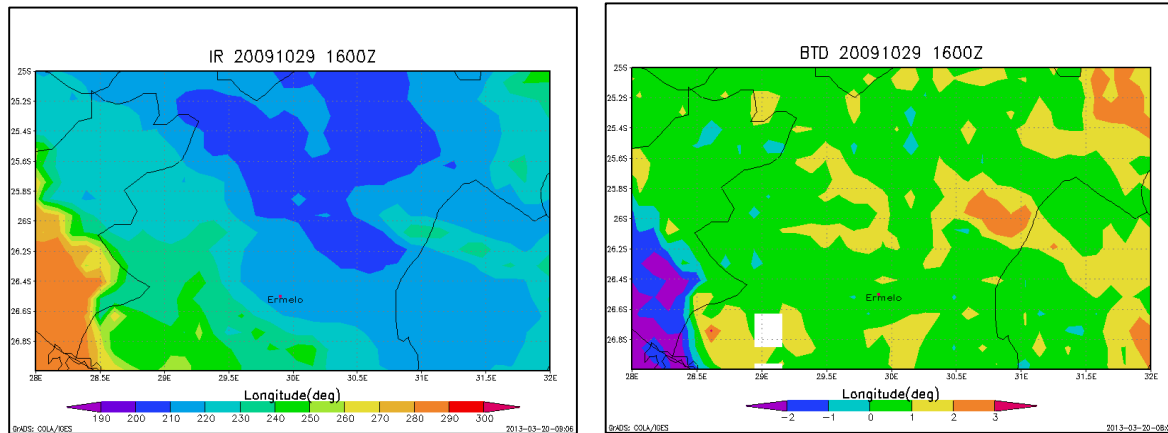


**FIGURE 4.32**

The Grid Analysis display system (GrAds) imagery of IR10.8 $\mu$ m measured in degrees Kelvin (K) is on the left hand side and the Brightness Temperature Difference (BTD) of IR8.7 $\mu$ m – IR10.8 $\mu$ m measured in K is on the right hand side for 29 October 2009 at 1600Z. Copyright (2013) EUMETSAT

### *Lightning Data*

The accumulation of cloud-to-ground lightning strokes was calculated for 60 minute, 30 minute and 15 minute periods between 1500Z and 1600Z on 29 October 2009. In figure 4.33 the 60 minute accumulation of lightning strokes between 1500Z and 1600Z is given, with 100 to 300 strokes detected in a band oriented north to south over the western and north-western parts of Mpumalanga, extending eastwards over the central parts of the province. Within this band of highest accumulation there are small pockets where between 300 and 600 strokes were detected during the 60 minute period. In the area where the highest accumulation of lightning occurred, over the western and north-western parts of Mpumalanga, between 2% and 4% of the strokes were positively charged (figure 4.33). Areas on figure 4.32 where more than 10% of the lightning was positively charged, lie to the west of the band of maximum accumulation as well as in a band south-east of Ermelo.



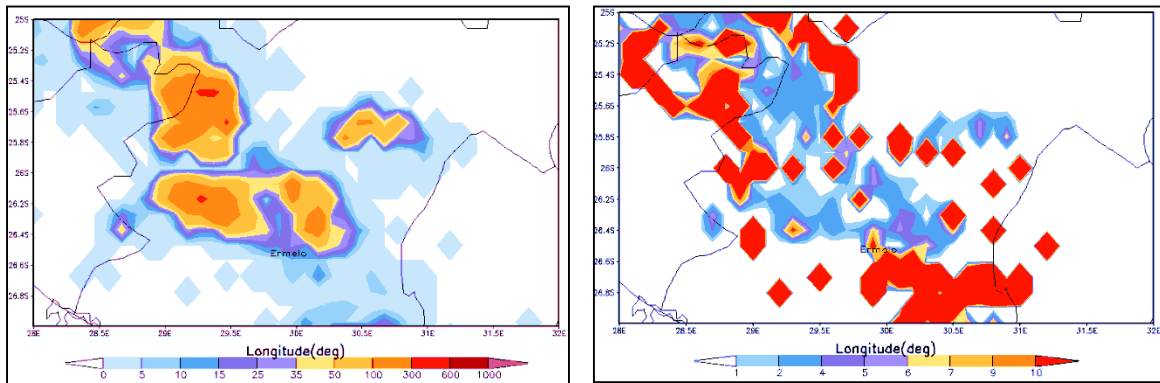


**FIGURE 4.33**

Total lightning strokes detected over the Mpumalanga Province for 29 October 2009 between 1500Z and 1600Z are depicted on the left hand side. The percentage (%) of positively charged lightning strokes detected at the corresponding time are depicted on the right hand side.

During the first 30 minute accumulation period from 1500Z to 1530Z between 50 and 100 strokes were detected in a band extending south from the north-western border of Mpumalanga and Gauteng (figure 4.34). There were small pockets within the band where 100 to 300 strokes were detected in figure 4.34 and the percentage of those strokes which carried a positive charge was as low as 2% to 4% of the total. The area south-east of Ermelo, and north-west of the band of highest accumulation, experienced more than 10% positively charged strokes (figure 4.34).

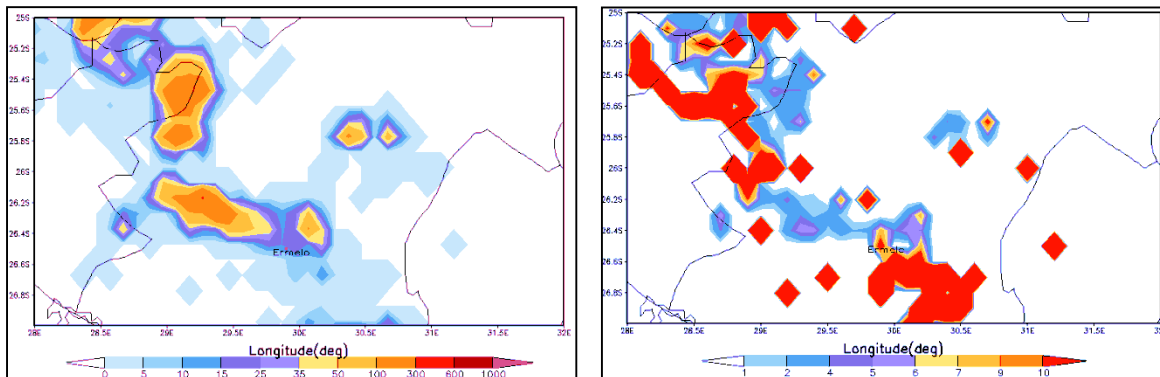


**FIGURE 4.34**

Total lightning strokes detected over the Mpumalanga Province for 29 October 2009 between 1500Z and 1530Z are depicted on the left hand side. The percentage (%) of positively charged lightning strokes detected at the corresponding time are depicted on the right hand side.

Between 50 and 100 lightning strokes accumulated between 1500Z and 1515Z as seen in figure 4.35. Of these strokes the percentage of them that carried a positive charge was mostly between 2% and 6% with more than 10% of the strokes detected

as being positively charged south-east of Ermelo and over northern Gauteng (figure 4.35).

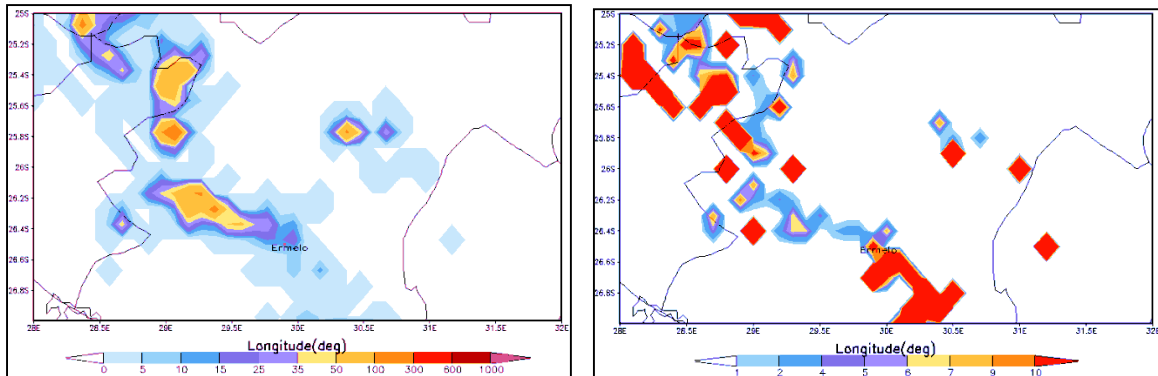


**FIGURE 4.35**

Total lightning strokes detected over the Mpumalanga Province for 29 October 2009 between 1500Z and 1515Z are depicted on the left hand side. The percentage (%) of positively charged lightning strokes detected at the corresponding time are depicted on the right hand side.

During the subsequent 15 minute accumulation period, very similar amounts of lightning were detected in figure 4.36 as was seen in figure 4.35, although the percentage of positive strokes detected in figure 4.36 was slightly higher.

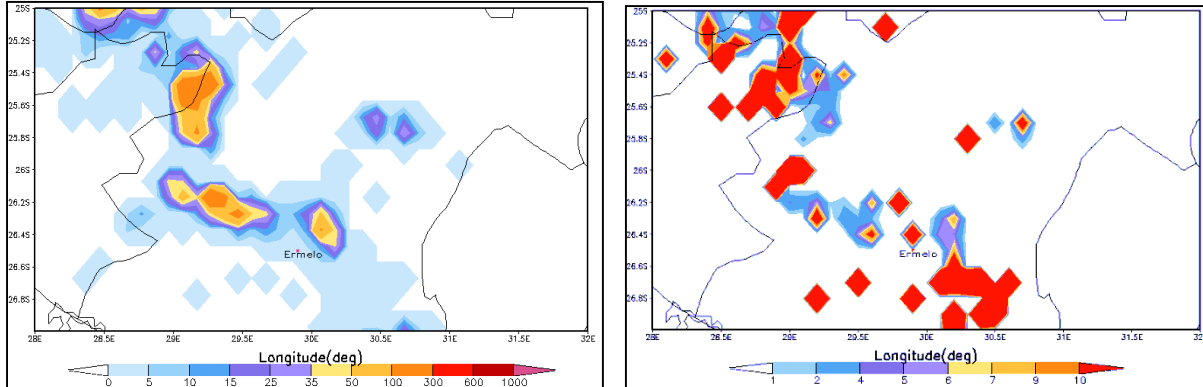


**FIGURE 4.36**

Total lightning strokes detected over the Mpumalanga Province for 29 October 2009 between 1515Z and 1530Z are depicted on the left hand side. The percentage (%) of positively charged lightning strokes detected at the corresponding time are depicted on the right hand side.

The lightning accumulation over the latter half of the period, seen in figure 4.37, was less than was detected between 1500Z and 1530Z in figure 4.34. The percentage of positively charged lightning strokes between 1530Z and 1600Z was highest to the east of the band of maximum accumulation in figure 4.37. This result was opposite to what was found in figure 4.34. During the latter 30 minutes of the period, the area

south-east of Ermelo continued to receive more than 10% positively charged strokes (figure 4.37).

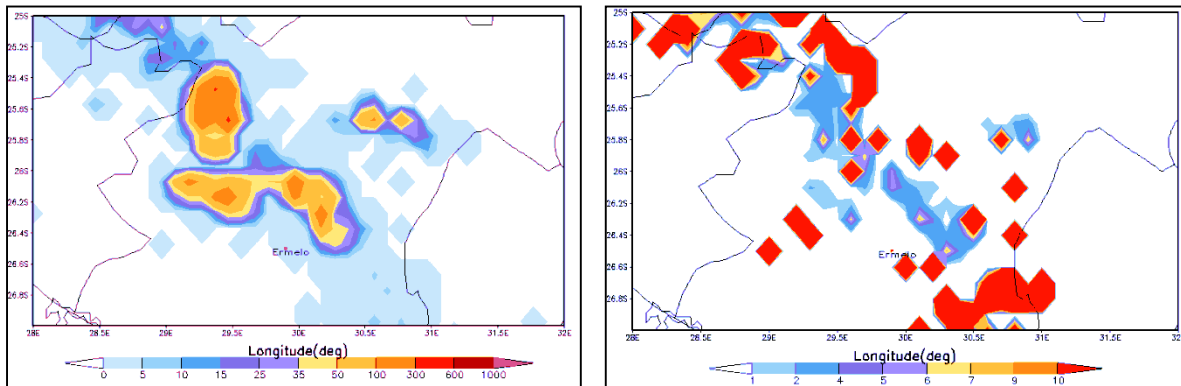


**FIGURE 4.37**

Total lightning strokes detected over the Mpumalanga Province for 29 October 2009 between 1530Z and 1600Z are depicted on the left hand side. The percentage (%) of positively charged lightning strokes detected at the corresponding time are depicted on the right hand side.

Between 1530Z and 1345Z (figure 4.38) 100 to 300 lightning strokes were detected over the north-western part of Mpumalanga as well as over a small area north-east of Ermelo. The percentage of positive strokes as shown in figure 4.38 lay between 2% and 4% with isolated pockets where higher values of between 6% and 7% were found.

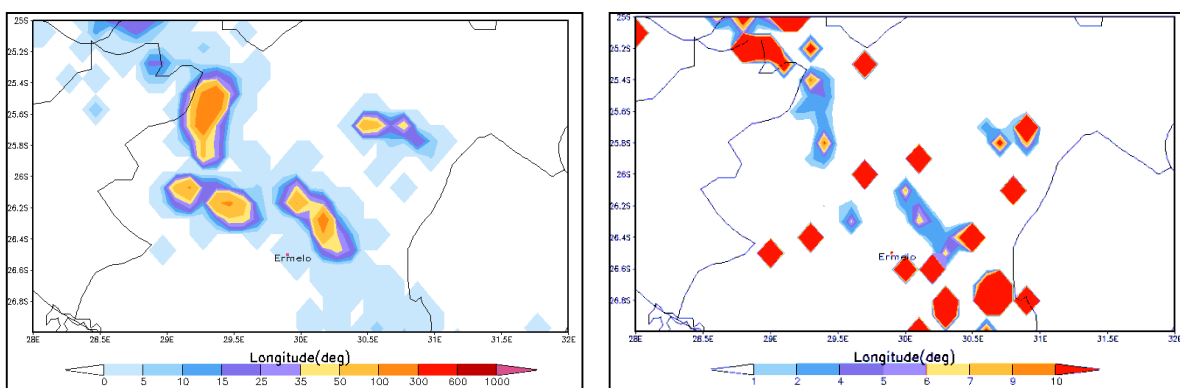


**FIGURE 4.38**

Total lightning strokes detected over the Mpumalanga Province for 29 October 2009 between 1530Z and 1545Z are depicted on the left hand side. The percentage (%) of positively charged lightning strokes detected at the corresponding time are depicted on the right hand side.

The final 15 minutes of the period of interest saw the north-western parts of Mpumalanga receive between 100 and 300 lightning strokes (figure 4.39) with between 4% and 6% of them being positively charged. There is an area in figure 4.39 where more than 10% of the strokes were positively charged, lying north-east of the band of highest accumulation.

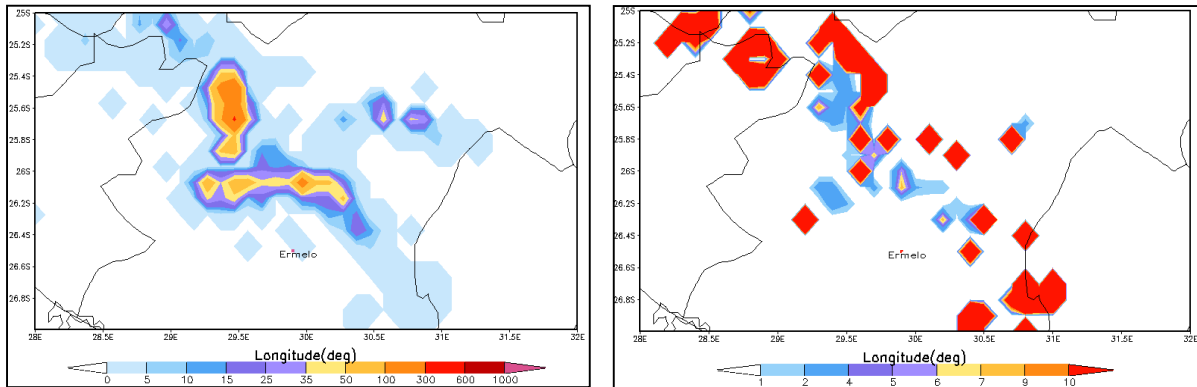


**FIGURE 4.39**

Total lightning strokes detected over the Mpumalanga Province for 29 October 2009 between 1545Z and 1600Z are depicted on the left hand side of the figure. The percentage (%) of positively charged lightning strokes detected at the corresponding time are depicted on the right hand side of the figure.

## **CHAPTER 5**

### Case study summaries and combined results

#### **5.1 Case study summaries**

##### *5.1.1 22 November 2007 at 1414Z*

The cloud microphysical properties observed over the Randfontein area between 1400Z and 1415Z were consistent with clouds containing small ice particles. These small ice particles had also recently undergone a phase change from water to ice, evidence by the BTD falling between 0K and 1K. The area of small ice particles coincides with the area of CTT of approximately 210K. The coldest CTT in the thunderstorm was found east of Randfontein with values between 190K and 200K. The area of small ice particles was coincident with the thickest part of the CB cloud.

The CB cloud investigated produced lightning with 5% to 6% of the total cloud-to-ground strokes measured between 1400Z and 1415Z carrying a positive charge. A narrow band stretching from north of Randfontein to the south-western parts of Gauteng received more than 10% positively charged lightning strokes. This band not only coincides well with the location of lowest CTT and an area of ice particles according to the convection RGB and the BTD values but it is also in extremely close proximity to Randfontein and needs to be noted as being significant. At the time of the lightning stroke which resulted in the fatality, the most active part of the thunderstorm was already east of the location where the woman was struck.

### *5.1.2 22 November 2007 at 1503Z*

The cloud microphysical properties over the Northcliff area at 1500Z were consistent with clouds containing ice particles. This data were confirmed by the output from the IR10.8 $\mu$ m satellite image in figure 4.5 in which the CTT was 202K (-70.93°C), and in the convection RGB (figure 4.5) and BTD values in figure 4.6 which both depicted ice particles over Northcliff. The overshooting tops in the HRV image in figure 4.5 suggested the presence of strong updrafts which were also confirmed by the output from the convection RGB. The total amount of detected cloud-to-ground lightning strokes during the 15 minute period of accumulation from 1500Z to 1515Z was comparatively very low.

The areas of lowest CTTs and ice particles were observed east of Northcliff at the time of the fatality and this was coincident with where the highest amount of cloud-to-ground lightning strokes were detected during the same period.

### *Comparing both cases*

The sequence of events shown in appendices B and C suggest that the same thunderstorm moved from Randfontein to Northcliff between 1400Z and 1515Z on 22 November 2007. The storm progressed from the west, passing over Randfontein between 1400Z and 1415Z, and was positioned over the Northcliff area from 1445Z to 1515Z. The development of an overshooting top at 1500Z in figure 4.5 suggested that the storm was in fact still developing when it moved over Randfontein and reached its peak development while moving towards and over Northcliff. The coldest CTTs were reached while the storm moved between Randfontein and Northcliff, indicating that the storm was still growing vertically and that it was not yet mature. The CB cloud in both cases had cloud water which was in the ice phase and small in size. In both cases the position of the most active (coldest CTT, overshooting top)

portion of the thunderstorms are located east and north-east of Randfontein and Northcliff respectively, at the time when the fatal lightning strokes occurred.

Regarding the lightning data, the 15 minute accumulated lightning totals were significantly lower at the respective points of interest between 1500Z and 1515Z (Northcliff) compared to totals between 1400Z and 1415Z (Randfontein). The percentage of positively charged strokes was, however, higher at Northcliff than over Randfontein. This makes sense as the most lightning is expected to occur during the development phase of a thunderstorm.

### *5.1.3 10 February 2009 between 1300Z and 1400Z*

From the HRV satellite imagery, two thunderstorms were clearly discernible over Gauteng, one over the western parts of Gauteng and a second over the city of Johannesburg. Consistently high reflectance in the storm over Johannesburg is evidence that the CB cloud developed and reached its mature stage between 1300Z and 1400Z. This is also supported by the fact that the CTT decreased during the same time, reaching their maximum cold value at 1345Z. This is evidence of a thunderstorm which is still developing and finally reaching its mature stage.

When looking at the CTT displayed in GrAds, the narrow band of CTTs below 210K remained very consistent in its orientation over central Gauteng, extending from the western to the eastern side of the province. The area spread to the north and south during the latter half of the period as the zone of CTTs lower than 200K remained very much over the Johannesburg area. The BTd data depicted that over the Johannesburg area and the central parts of Gauteng, the cloud water had already undergone a phase change from liquid water to ice particles.

The total amount of lightning was highest between 1330Z and 1400Z, which correlates well with the time when the lowest CTT was detected and when it is suggested the CB cloud had reached maturity. The highest amount of cloud-to-ground lightning strokes was found on the western edge of the thunderstorm over Johannesburg, and this orientation persisted throughout the period. The area of positively charged strokes greater than 10% was found to have a similar orientation from 1300Z until 1400Z located on the western edge of the thunderstorm. This orientation of the positively charged strokes relative to the CB cloud is in line with the theory of positively charged cloud-to-ground strokes often being detected in the stratiform cloud trailing a CB cloud.

#### *5.1.4 29 October 2009 between 1500Z and 1600Z*

After analyzing the satellite data it was found that convective activity developed over the northern parts of Gauteng and moved eastwards and south-eastwards into Mpumalanga during the afternoon of 29 October 2009. There was also convective development over Ermelo during the period of interest, which moved north-eastwards with time. VIS and IR satellite imagery showed that the convective clouds were indeed thick ice clouds, with small ice particles and CTTs which were mostly below 200K. The orientation of the lowest CTTs was in band stretching west to east from Gauteng and over the western and central parts of Mpumalanga. The CB cloud on the border between Gauteng and Mpumalanga was still developing between 1500Z and 1515Z as CTTs continued to decrease while the cloud was still growing vertically with an updraft.

The BTD values for the 60 minutes from 1500Z to 1600Z indicated ice particles for the majority of the area where the convection was found. There were, however, pockets of possible liquid water that were identified around Ermelo towards the middle and end of the period along with increasing CTTs. This suggested that the CB clouds in that area were possibly dissipating after 1530Z.



Total amounts of lightning detected throughout the period were fairly consistent. The first 30 minute accumulation period and the second 30 minute accumulation period in figures 4.34 and 4.36 respectively, showed that between 300 and 600 strokes were detected in a band over the western and north-western parts of Mpumalanga at first, progressing eastwards in the latter half of the period. This is due to CB clouds moving from west to east with the prevailing atmospheric winds.

The percentage of lightning strokes which were positively charged was mostly between 2% and 4% in the band where highest lightning totals were detected. There were pockets within the band where between 4% and 6% of the strokes were positively charged although these areas were comparatively very small. The area south-east of Ermelo received more than 10% positively charged strokes throughout the period of interest. This higher percentage was associated with a low count of total lightning strokes with less than 10 strokes during each 30 minute period. Over the western parts of Mpumalanga, more than 10% of the lightning was positively charged in a band to the west of where highest accumulations were recorded.

Most positive lightning was detected where the convective cloud was thickest but not where the lowest CTT were measured. During the latter half of the period, most positive lightning strokes were found to occur east of the lowest CTT's.

## **5.2 Combined results**

Considering the case studies investigated in chapter four, correlations were found between the various parameters used, including the timing and location of satellite based data and the lightning detection data. The results from the individual case

studies have been tabled. The first two case studies, where fatalities were reported, have been grouped together for comparison, as the exact time and location of the fatalities were known. The last two case studies are compiled from data which spanned 60 minutes without a fixed location. These last two case studies have therefore been tabled separately. The results from the lightning data and satellite data have been separately tabulated for the initial results.

### 5.2.1 Satellite data

Comparing the first two case studies, very similar results emerge from the satellite based data, as seen in table 5.1. It was ascertained in the initial discussion of each case that the same thunderstorm which resulted in the fatality in Randfontein at 1414Z, moved north-eastwards and was the cause of the fatality at 1503Z in Northcliff as well. The two cases will be referred to hereafter as Case 1 and Case 2.

**TABLE 5.1** Results based on satellite imagery obtained for Case 1 and Case 2 on 22 November 2007 at 1414Z and 1503Z respectively.

Case study date	Location of highest reflectance values relative to reported fatality	CTT (K) At the location	Location of lowest CTT relative to reported fatality	BTD Value (K)	Location relative to reported fatality	Particle size and phase	Location of small ice particles relative to reported fatality
22/11/2007 1414Z (Case 1)	Directly over Randfontein	205	Slightly north-west	0-1 Ice	Directly over Randfontein	Small ice	Directly over Randfontein and South-east
22/11/2007 1503Z (Case 2)	West and NW of Northcliff	202	North-west	0-1 Ice	Directly over Northcliff	Small ice	West and north-west of Northcliff

From the CTT measured manually using SUMO, the temperatures decreased between the two events, from 205K to 202K. The thickest cloud was detected to be directly over Randfontein at the time of the incident at 1414Z, whereas by 1503Z, the thickest clouds were found west and north-west of Northcliff. It is therefore suggested that the most active part of the thunderstorm was still approaching when the fatality

occurred, which is reinforced by the fact that the lowest CTT were also found north-west of Northcliff at the same time. Highest reflectance, and hence the thickest part of the CB cloud, was found in the same location where the convection RGB detected small ice particles.

In both cases, the area of small ice particles extended beyond the location of the reported fatalities. The area of lowest CTTs measured from the IR10.8 $\mu$ m imagery were in fact located east of where the fatal lightning stroke occurred in both cases. In Case 1 the lowest CTTs depicted in the GrAds imagery were less than 190K, whereas the lowest CTTs in Case 2 were between 190K and 200K.

As the second two cases studies did not have any point of reference for a single incident, the results are discussed by looking at the orientation of the satellite and lightning data to one another within the active CB clouds identified. Table 5.2 presents the results for the case studies of 10 February 2009 and 29 October 2009, referred to hereafter as Case 3 and Case 4.

**TABLE 5.2** Results based on satellite imagery obtained for Case 3 and Case 4 on 10 February 2009 and 29 October 2009.

Case Study Date	Location of highest reflectance values relative to convective activity	Lowest CTT (K)	Location of lowest CTT relative to convective activity	BTD value (K)	Location of ice particles relative to convective activity	Particle size and phase	Location of small ice particles relative to convective activity
10/02/2009 1300Z to 1400Z Case 3	On the western edge of the CB cloud associated with overshooting Tops	192	North-west	0-1 Ice	Over activity and to the north-west	Small ice	Over the central and western parts of the thunderstorm
29/10/2009 1500Z to 1600Z Case 4	West and south-west of identified CB cloud	197	South-west	1-2 Ice	Over activity and to the east	Small ice	In the west and south-west

Highest reflectance from the HRV and VIS imagery were found on the western and south-western edge of the thunderstorms identified in the above tabled case studies, with an overshooting top seen in Case 3. The CTT of 192K correlates well with the identification and location of the overshooting top. The location of the lowest CTTs relative to the thickest part of the thunderstorm, were displaced to the north-west in Case 3, and to the south-west in Case 4.

In both cases small ice particles were identified, coincident with the thickest part of the thunderstorm in Case 4 and with the area of lowest CTT as well. In Case 4, there were pockets of liquid water droplets found within the broader area of ice particles towards the end of the time period. This result suggested that the CB cloud was in fact dissipating during the latter part of the case study.

Comparing the first three primary case studies, it is important to be cognizant of the fact that the cases involving fatalities are related to a point of reference, where the third case is related to a thunderstorm cell. In each of the primary cases the lowest CTT measured occurred north-west of the point of interest. In Case 3 the lowest CTTs were on the north-western edge of the thunderstorm. Although the CTT in Case 3 is markedly lower than in Case 1 and 2 in all three cases the CTT fell to between 190K and 200K. The thickest part of the thunderstorm in Case 3 was located on the western or north-western part of the thunderstorm and west or over the point of interest in Case 1 and Case 2. Ice was found to be the dominant particle phase in each case with the area of small ice particles corresponding with the thickest part of the thunderstorms.

In Case 4, the lowest CTTs were found on the south-western edge of the identified convection, and the ice particles were located towards the eastern parts of the thunderstorm, as well as over the central areas. The zone of small ice particles was coincident with the lowest CTTs, displaced to the south-western edge of the

thunderstorm. This orientation of parameters deviates from the first three cases discussed above.

### 5.2.2 Lightning data

The lightning data are tabled for the case studies where fatalities were reported, in table 5.3. For the 15 minutes around the time, and at the location of the reported fatalities, less than 25 cloud-to-ground lightning strokes were detected in both cases. In Case 2, less than 10 strokes were detected during the period of interest. The highest 15 minute accumulation of cloud-to-ground lightning strokes during the events ranged from 100 to 300 for Case 1, and 50 to 100 for Case 2. In both instances, the area over which the highest total strokes were detected lies east and north-east of where the fatality occurred. Fairly low percentages of positive cloud-to-ground strokes were detected at the point of interest in both cases, falling below the accepted average of 10%, as stated by Malan (1963). The highest amount of positive cloud-to-ground strokes were detected south-east of the location of the fatality in both cases.

**TABLE 5.3** Results based on lightning data obtained for Case 1 and Case 2 on 22 November 2007 at 1414Z and 1503Z respectively.

Case study Date	Total amount of cloud-to- ground lightning strokes at point of interest	Highest total cloud-to-ground lightning strokes	Location of highest accumulation of lightning strokes relative to reported fatality	% Positive cloud-to-ground lightning strokes at the point of interest	Location of highest % positive strokes relative to reported fatality
22/11/2007 1414Z (Case 1)	15-25	100-300	East and north-east	5-6	South-east
22/11/2007 1503Z (Case 2)	5-10	50-100	East and north-east	6-9	South-east

In the second two cases, the results of which are given in table 5.4, 60 minute accumulations of cloud-to-ground lightning strokes were calculated. By scrutinizing

the 60 minutes of data in 15 minute and 30 minute segments, the highest 15 minute accumulation was observed to deliver between 300 and 600 strokes in both cases. Results from Case 3 show an accumulation of 600 to 1000 strokes during the 60 minute time period compared to the 300 to 600 strokes accumulated in Case 4. The highest 15 minute accumulations were located on the north-western edge of the thunderstorm in Case 3, while in Case 4 the highest lightning totals were displaced to the southern and eastern parts of the thunderstorm.

**TABLE 5.4** Results based on lightning data obtained for Case 3 and Case 4 on 10 February 2009 and 29 October 2009.

Case Study Date	Highest 60 minute total cloud-to-ground lightning strokes	Highest 15 minute total cloud-to-ground lightning strokes	Location of highest accumulation of lightning strokes relative to active convection	% Positive cloud-to-ground lightning strokes during the most active 15 minutes	Location of highest % positive strokes relative active convection
10/02/2009 1300Z to 1400Z (Case 3)	600-1000	300-600	North-west	>10	West
29/10/2009 1500Z to 1600Z (Case 4)	300-600	300-600	South and east	2-4	West

Another obvious difference between the two cases was the percentage of positive cloud-to-ground strokes detected during the most active 15 minutes of each of the thunderstorms. In Case 3 close to 10% of the lightning strokes were positively charged, while only 2% to 4% were positively charged in Case 4. In both cases, the highest percentage of positive cloud-to-ground lightning was detected on the western side of the convective activity.

Lightning data from Case 1, Case 2 and Case 3 were compared with one another as they were for the satellite data. In each case the percentage of positive lightning strokes was above 6% and approaching 10% in Case 3. Case 3 also had significantly higher total amount of lightning in a 15 minute accumulation period than the first two cases. The location of the highest lightning totals in Case 3 were displaced to the

north-western edge of the thunderstorm, while in the cases involving fatalities, the lightning strokes were concentrated more to the east and north-east of the reported events.

## **CHAPTER 6**

### Conclusion and recommendations

#### **6.1 Conclusion**

The installation of the new LDN in South Africa in 2005 provided a dataset which could be used to increase understanding of lightning distribution, intensity, frequency and polarity. With each passing year the LDN data archive has increased and with it the understanding of the data.

The Highveld falls within the austral summer rainfall region of South Africa and is known for its thunderstorm activity. The Highveld receives the highest ground flash density of cloud-to-ground lightning in South Africa per annum, with 4% to 6% of the lightning strokes being positively charged, according to data collected between 2006 and 2010 from the SAWS LDN. Positive cloud-to-ground lightning is known to carry a higher charge and as being more severe than negatively charged lightning strokes. Not every country can boast having its own LDN, being able to find correlations between satellite data (which is more widely available) and LDN data can provide valuable guidance in understanding what identifiable cloud microphysical properties could produce above average amounts of positively charged cloud-to-ground lightning.

The cloud water phase associated with most active lightning is generally accepted as being ice particles at the cloud top level. This is indicative of a thunderstorm with an active updraft which can lift newly formed ice to the top of the CB cloud. By looking at BTD values at the cloud top level, the distribution of liquid water and ice particles can be ascertained. The convection RGB is another very helpful tool in determining the phase and size of the water particles within a CB cloud.



Although only two of the case studies investigated were linked to reported fatalities as a direct result of a lightning stroke, the reader must not assume that: 1) there were no fatalities linked to the other two cases just because it was not reported in the media or that 2) there were not more than two fatalities resulting from lightning in the first two cases studies for the same reason. The lightning related insurance claims were obtained from only one institution, which limited the case studies of 10 February 2009 and 29 October 2009 to a restricted amount of information instead of for a representative distribution of data.

### *6.1.1 Comparing cloud particle phase with lightning polarity*

The cloud particle phase of each of the CB clouds identified as being directly responsible for the fatal lightning stroke or large amount of lightning related damage was scrutinized with the use of GrAds display software. The BTD of the CB clouds were calculated both at the time of interest and for the time period of interest in the case where large amounts of lightning related damage were reported. In all three of these primary cases the BTD values were indicative of ice particles being the dominant water phase in the CB clouds, with BTD values falling between -1K and 1K in each case study. The information displayed in the convection RGB in each of the primary case studies clearly showed CB clouds with small ice particles.

Together with the BTD values of between -1K and 1K, lowest CTTs which dropped to between 190K and 200K and the small ice particles detected with the use of the convection RGB, the outputs of the data were in agreement that small ice particles were dominant in the CB clouds for the three primary case studies.

The accepted global average for positively charged cloud-to-ground lightning is 10% but LDN data from 2006 to 2010 showed that over the Highveld regions of South Africa (including the Gauteng and Mpumalanga Provinces) the average percentage of positively charged strokes lies between 4% and 6%. The polarity of the cloud-to-ground lightning for each of the three primary cases was calculated from the total

strokes detected, with the use of Fortran code, Microsoft Excel and GrAds display software. It was shown in each of the three primary case studies that more than 6% of the cloud-to-ground lightning strokes were positively charged over the point or area of interest, which is above average for the region. There were instances in each case study where more than 10% of the strokes were positively charged in the vicinity of the reported fatalities. The highest percentage ( $\geq 10\%$ ) of positively charged strokes did, however, occur simultaneously with the concentration of small ice particles in CB clouds. The location of this zone of greater than 10% positively charged strokes was not coincident with the point where the fatalities were reported.

### *6.1.2 Positive polarity compared to negative polarity*

The lightning polarity in each case study was calculated from the total number of cloud-to-ground lightning strokes detected for the various time periods of interest. In each case study there were areas over which more than 10% of the total cloud-to-ground lightning was positively charged, although these areas did not coincide with either of the points of interest in the primary case studies. The area over which more than 10% positively charged strokes were detected was displaced east or south-east of the point of interest for the two cases involving fatalities. In the case study of 10 February 2009 areas of more than 10% positively charged lightning strokes were displaced to the western edge of the most active convection identified.

In the secondary case study of 29 October 2009, the percentage of positively charged strokes over the area of most active convection fell between 2% and 4%. In this secondary case study, there were areas where more than 10% of the lightning strokes were positively charged. These areas were located south-east of Ermelo as well as in a north-to-south band over the western parts of Mpumalanga. Neither of these areas were coincident with where the most active convection occurred at the time.

Considering that there were instances in all four case studies where more than 10% of the total cloud-to-ground strokes were positively charged, is evidence that there were areas in each of the thunderstorms where severe lightning could have occurred. Although the percentage of positively charged lightning over the points and areas of interest were lower than 10%, the positively charged strokes in each case study fell within the range of between 4% and 6% expected for the Highveld and Gauteng.

Negatively charged cloud-to-ground lightning dominated in both the primary and secondary case studies. In the case studies of 10 February 2009 and 29 October 2009, where a large accumulation of cloud-to-ground lightning was detected over a 15 minute period, the percentage of positive strokes did not show a marked increase from what was found in the two cases involving fatalities, where a relatively low accumulation of cloud-to-ground lightning was detected. It was only in the case of 10 February where there was an area of greater than 10% positively charged strokes displaced to the western edge of the CB cloud.

### *6.1.3 Consistency between particle phase and lightning polarity in a secondary case study*

After the particle phase in the CB clouds was determined for each of the four cases by displaying the BTM data with GrADS display software, the results were compared with the polarity of the lightning occurring simultaneously over identified areas of interest. By comparing the findings from the three primary cases, with those from the secondary case study it was found that despite the presence of small ice particles at the cloud top level the percentage of positively charged lightning strokes was only between 2% and 4% during the most active 15 minute period of convection in the secondary case study, as compared to above 5% for the primary case studies. The presence of potential pockets of super-cooled water located within the larger area of ice particles in the secondary case study may have been the cause of a lower percentage of positively charged lightning strokes in those areas.

Even though the secondary case study had a higher 15 minute total of accumulated cloud-to-ground lightning strokes than the two case studies involving fatalities, the percentage of positively charged strokes was lower than in the three primary case studies.

## **6.2 Recommendations**

1. It is recommended that a broader analysis of BTD values versus lightning polarity needs to be performed in future for a larger data set in order to create a reliable bench mark for when most positive lightning can be expected to result in large amounts of damage or a possible fatality.
2. Mixed phased CB clouds could be investigated to ascertain the effect of liquid water droplets on lightning polarity.
3. Parameters could be developed for SUMO to highlight CB clouds which display characteristics which are indicative of relatively high percentages of positively charged cloud-to-ground lightning strokes.
4. Thunderstorms over the entire interior region of South Africa could be investigated to determine whether there are cloud microphysical properties linked with more damaging and fatal lightning events, particularly over the Eastern Cape and KwaZulu-Natal Provinces, where many fatalities are reported each year.

## References

- Arakawa, A. and Schubert, W. H., 1974: Interaction of cumulus cloud ensemble with the large scale environment. Part I. *J. Atmos. Sci.*, **31**, 671–701
- Bader, M.J., Forbes, G.S., Grant, J.R., Lilley, R.B.E. and Wolters, A.J., 1995: Images in weather forecasting: *A Practical guide for interpreting satellite and radar imagery*. Cambridge University Press pp. 499
- Berger, K., 1977: Lightning, *Volume 1: Physics of Lightning*, Academic Press 121-190
- Blumenthal, R., 2005: Lightning Fatalities on the South African Highveld: A Retrospective Descriptive Study for the period 1997 to 2000, *The American Journal of Forensic Medicine and Pathology*, **26**, 66 – 69.
- Blumenthal, R., 2007: A retrospective descriptive study on the pathology of trauma of lightning fatality cases in Gauteng 2001 – 2004. Paper Presented at the *International Congress of Lightning and Static Electricity (ICOLSE)* Paris, France, 2007.
- Carey, L.D. and Buffalo, K.M., 2006: Environmental control of cloud-to-ground lightning polarity in severe storms, Department of Atmospheric Sciences, Texas A&M University, College Station, Texas
- Cotton, W.R. and Anthes, R.A., 1989: *Storm and Cloud Dynamics*, Academic Press, California, pp. 881
- Dent, M.C., Lynch, S.D., and Schulze, R.E., 1989: *Mapping Mean Annual and other Rainfall Statistics over Southern Africa*. Water Research Commission, Pretoria. WRC Report, 109/1/89. pp230
- Gijben, M., 2012: The Lightning Climatology of South Africa. *S. Afr J of Sci.* 2012:108(3/4), Art. #740, 10 pages.  
<http://dx.doi.org/10.4102/sajs.v108i3/4.740>
- Gill, T., *Initial steps in the development of a comprehensive lightning climatology of South Africa*. MSc Thesis, Johannesburg, University of the Witwatersrand, 2008
- Glossary of Meteorology, 2000: American Meteorological Society, Second Edition, Boston, Massachusetts, United States of America. pp694.

- Google Earth, 2010: Location of Lightning strikes 22 November 2007 – South Africa-26°02'04.01"S 28°06'07.14"E, 5101ft
- Holle, R.L. and Lopez, R.E., 2003: A comparison of current lightning death rates in the U.S with other locations and times. Int. Conf. on Lightning and Static Electricity, Blackpool, England, Royal Aeronautical Soc., paper 103-34 KMS, 7pp.
- Holle, R.L., 2008: Annual Rates of Lightning Fatalities by Country. 20<sup>th</sup> Annual Lightning Detection Conference, Tucson, Arizona, U.S.A., pp.14
- Kerkmann, J., 2005: *RGB composites with channels 01-11 and their interpretation*, Accessed on 9<sup>th</sup> June 2012.  
[http://oiswww.eumetsat.org/WEBOPS/msg\\_interpretation/msg\\_channels.php](http://oiswww.eumetsat.org/WEBOPS/msg_interpretation/msg_channels.php)
- Krehbiel, P.R., 1986: *The Electrical Structure of Thunderstorms. The Earth's Electrical Environment*, eds. E. P. Krider and R. G. Roble, Washington DC: National Academy Press., 90–113
- Kruger, A.C., 2004: *Climate of South Africa. Climate Controls. WS44*, South African Weather Service, South Africa
- Latham, J. and Mason B.J., 1961: Electric charge transfer associated with temperature gradients in ice. *Proc., Roy., Soc., London A March 21 1961*, **260**, 1303 523 – 536
- Lindsey, D.T., Hillger, D.W., Grasso, L., Knaff, J.A. and Dostalek, J.F., 2006: GOES climatology and analysis of thunderstorms with enhanced 3.9- $\mu$ m reflectivity. *Mon. Wea. Rev.*, **134**, 2342-2353
- Lindsey, D.T., 2008: Examining a Possible Relationship between Positive Dominated Storms and Cloud Top ice Crystal Size. Paper presented at the *Third Conference on Meteorological Applications of Lightning Data* in Atlanta, GA, in 2008
- LIS Global lightning image obtained from  
<http://thunder.nsstc.nasa.gov/data/query/mission.png>, maintained by NASA EOSDIS Global Hydrology Resource Center (GHRC) DAAC, Huntsville, AL. 2011. Data for the image were provided by the NASA EOSDIS GHRC DAAC
- Malan, D.J., 1963: *Physics of Lightning*, English University Press, London, pp. 170

MSG-2, *Successfully Launched*. (2005).

Retrieved on June 9, 2011, from EUMETSAT Press Releases Web Site:

[http://www.eumetsat.int/Home/Main/News/Press\\_Releases/005023?I=en](http://www.eumetsat.int/Home/Main/News/Press_Releases/005023?I=en)

Netcare 911, 2007: Road Safety and Arrive alive Blog, accessed 4 February 2007,

<http://roadsafety.wordpress.com/2007/11/23/2-killed-in-3-separate-lightning-strikes-in-49-minutes-during-storm/>

Prieto, J., 2008: *Applications of the SEVIRI window channels in the infrared*, Accessed on 9<sup>th</sup> June 2012.

[http://oiswww.eumetsat.org/WEBOPS/msg\\_interpretation/msg\\_channels.php](http://oiswww.eumetsat.org/WEBOPS/msg_interpretation/msg_channels.php)

Proctor, D. E., 1993: *Lightning and its relation to precipitation*, Report to the WRC by Ematek, CSIR, WRC Report No 279/1/93.

Pruppacher, H.R. and Klett J.D., 1978: *Microphysics of clouds and Precipitation*. D Reidel, pp.714

Rakov, V. A. and Uman, M.A., 2003: *Lightning, physics and effects*, Cambridge University Press, pp. 687

Reynolds, S. E., Brook, M. and Gourley, M.F., 1957: Thunderstorm charge separation. *J. Meteor.* **14**, 426- 436

Rosenfeld, D., and Lensky, I. M., 1998: Satellite based insights into Precipitation formation processes in continental and maritime convective clouds. *Am. Meteorol. Soc.*, **79**, 2457–2476

Rutledge, S. A. and MacGorman, D.R., 1988: Cloud-to-ground Lightning activity in the 10-11 June 1985 Mesoscale Convective System Observed during the Oklahoma-Kansas PRE-STORM Project, *Mon. Wea. Rev.*, **116**, 1393-1408

Saunders, C. P. R., 1992: *A Review of Thunderstorm Electrification Process*, *Journal of Applied Meteorology*, **32**, 642-655

Schmetz, J. S., Govaerts, Y., König, M., Lutz, H., Ratier, A. and Tjemkes, S., Eumetsat, 2003: *A Short Introduction to Meteosat Second Generation (MSG)*, Accessed on 9<sup>th</sup> June 2012.

<http://rammb.cira.colostate.edu/wmovl/vrl/pptlectures/eumetsat/index.html>





Sherwood, S. C., Phillips, V. T. J. and Wettlaufer, J. S., 2006: Small ice crystals and the climatology of lightning. *Geoph. Res. Let.*, **33**, L05804, doi: 10.1019/2005GL025242



- Taljaard, J.J., 1994: Atmospheric circulation systems, Synoptic Climatology and Weather Phenomena of South Africa. Part 1: Controls of the weather and climate of South Africa. *S. Afr. Weath. Bur. Technical Pap.* **27**, 45pp. S. Afr. Weather Service., Pretoria, South Africa.
- Taljaard, J.J., 1996: Atmospheric circulation systems, Synoptic Climatology and Weather Phenomena of South Africa. Part 6: Rainfall in South Africa. *S. Afr. Weath. Bur. Technical Pap.* **32**, 45pp. S. Afr. Weather Service., Pretoria, South Africa.
- Uman, M.A., 1969: *Lightning: Advanced Physics Monograph series*. McGraw-Hill Inc. pp. 264
- VAISALA, 2004: Introduction to Lightning Detection, *CP Series: CP7000 Cp8000 Users Guide*, M210557EN-A, Vaisala Oyj, Helsinki, Finland, pp243
- Watson, A. I., Lopez, R. E. and Holle, A. L., 1994: Diurnal Cloud-to-ground Lightning Patterns in Arizona during the Southwest Monsoon, *Mon. Wea. Rev.*, **122**, 1726-1739
- Wetli, C.V., 1996. Keraunopathology: An analysis of 45 fatalities. *Amer. J. Forensic Med. Pathol.* 1996; **17**:89-98
- Wolters, E. L. A., Robert, A. and Feijt A. J., 2008: Evaluation of Cloud-Phase retrieval methods for SEVIRI on Meteosat-8 Using Ground-Based Lidar and Cloud Radar Data, *American Meteorological Society*, DOI: 10.1175/2007JAMC1591.1
- Zajac, B. A. and Rutledge, S. A., 2001: Cloud-to-ground lightning in the Contiguous United States from 1995 to 1999, *Mon. Wea. Rev.*, **129**, 999-1-19.
- Zwartz-Meise, V., Zentral Anstalt für Meteorologie und Geodynamik (ZAMG), 2004: *Introduction into the window channels*, Accessed on 9<sup>th</sup> June 2012.  
[http://oiswww.eumetsat.org/WEBOPS/msg\\_interpretation/msg\\_channels.php](http://oiswww.eumetsat.org/WEBOPS/msg_interpretation/msg_channels.php)

## APPENDIX A

The colour scheme and interpretation of the convection RGB obtained from Kerkmann (2005) is shown below.

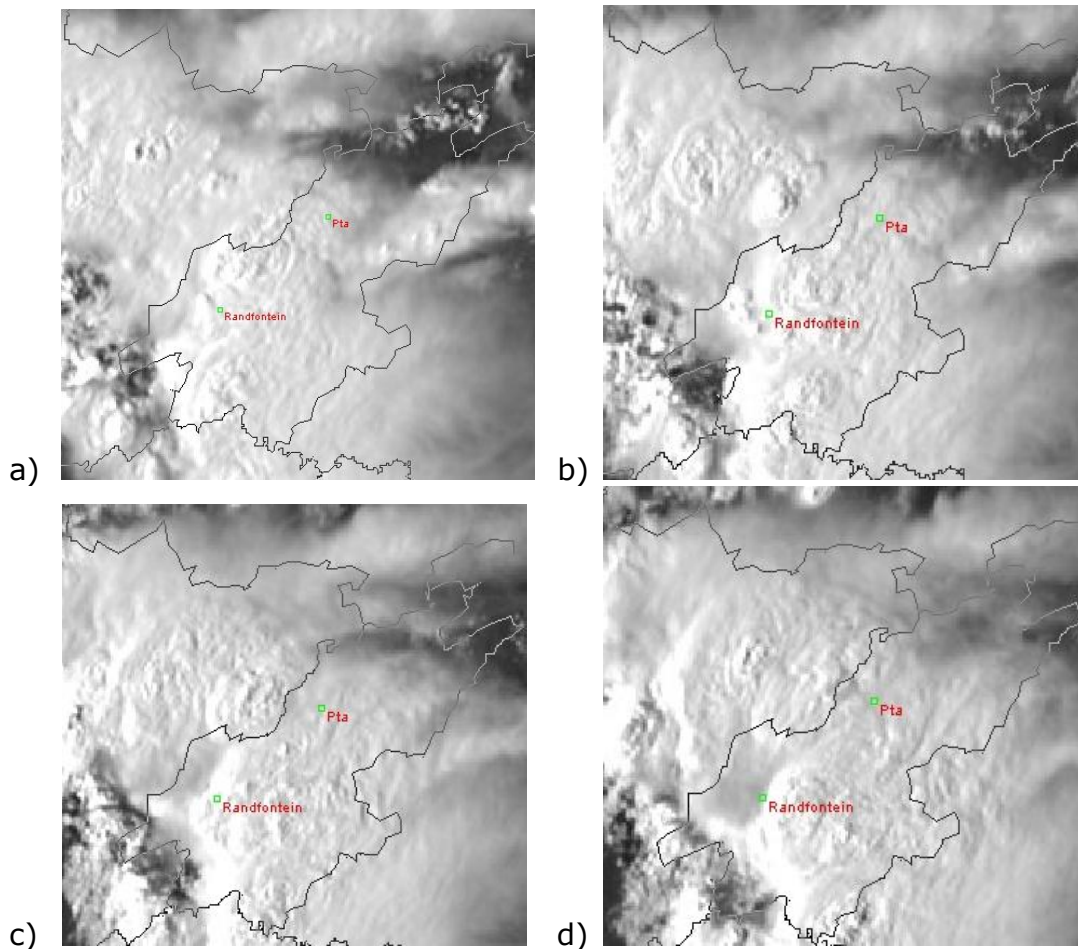
			
<p>Deep precipitating cloud (precip. not necessarily reaching the ground) - high-level cloud - large ice particles</p>	<p>Deep precipitating cloud (Cb cloud with strong updrafts and severe weather)* - high-level cloud - small ice particles *or thick, high-</p>	<p>Thin Cirrus cloud (large ice particles)</p>	<p>Thin Cirrus cloud (small ice particles)</p>

## **APPENDIX B**

This appendix contains the imagery for the case study of 22 November 2007 at 1414Z, where a woman was killed by lightning in Randfontein, Gauteng. The figures that follow are of the sequence of events from 1345Z until 1430Z for both satellite and lightning data.

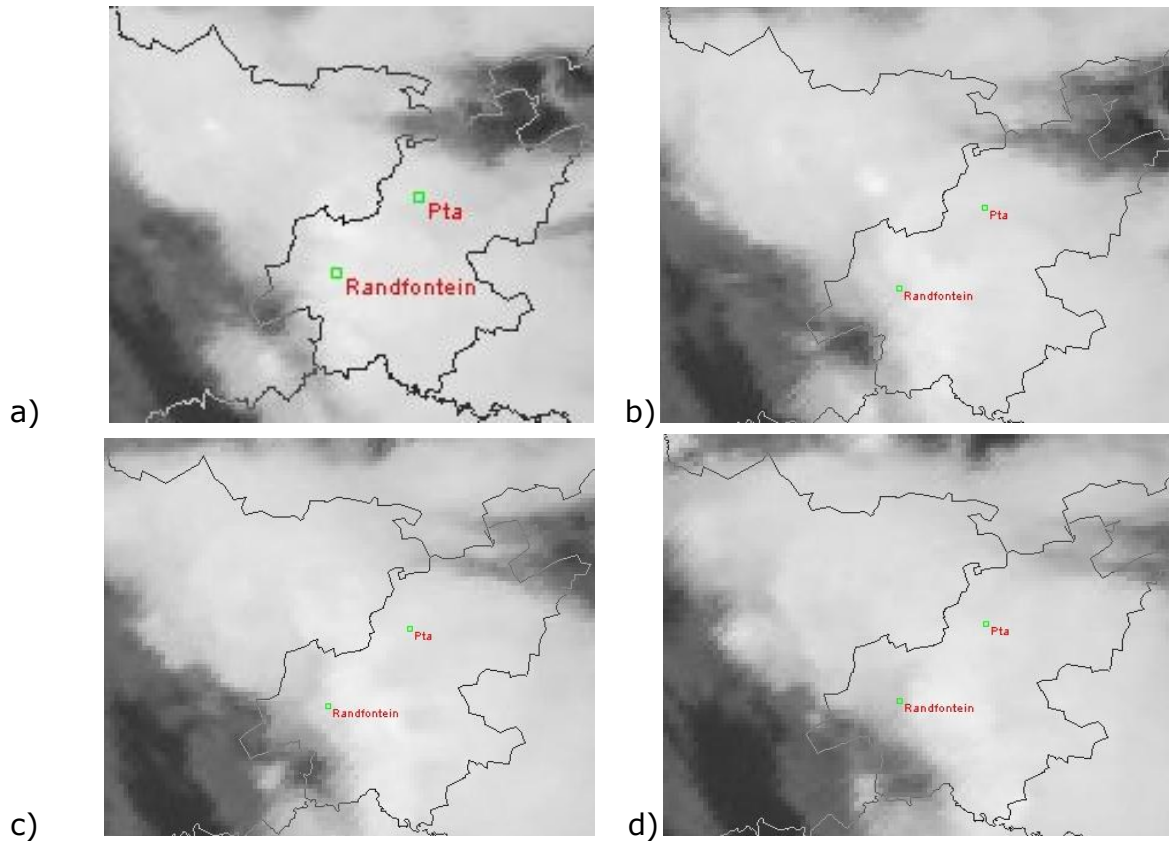
### **Satellite data**

#### HRV satellite imagery



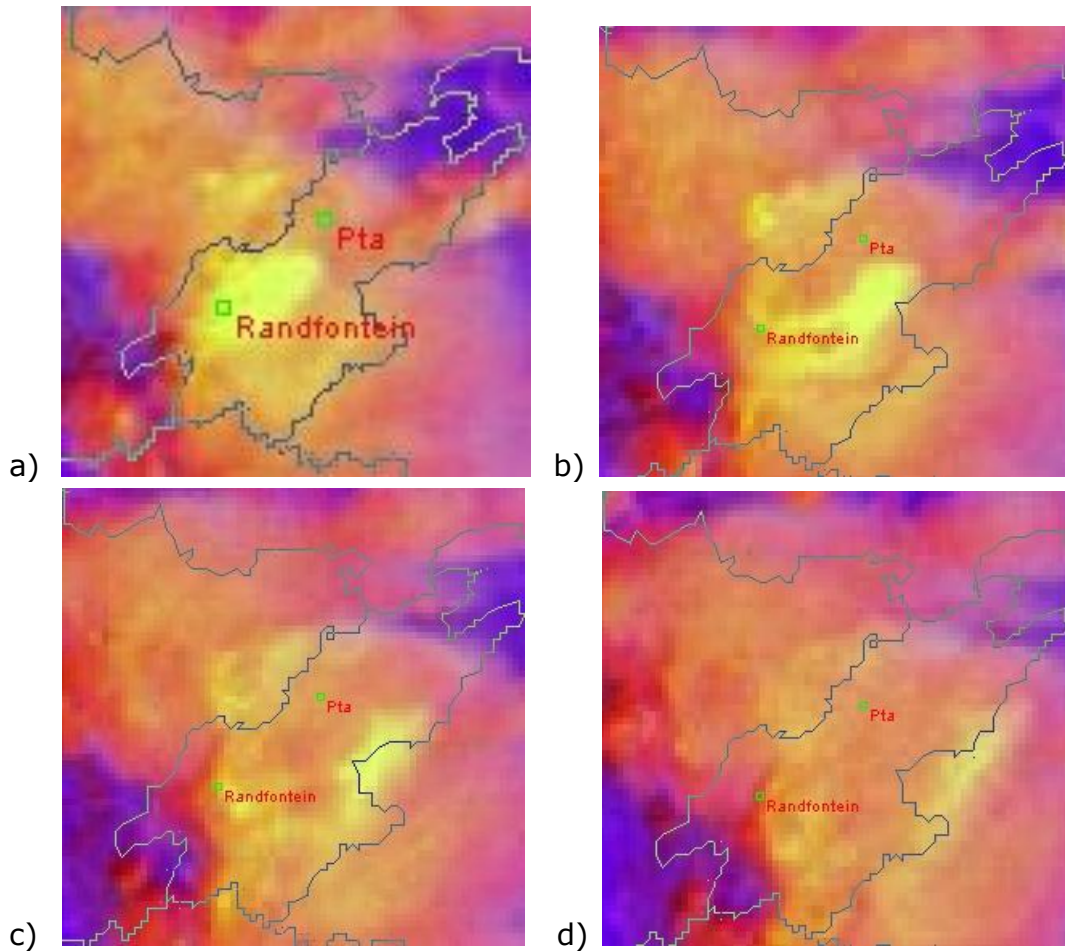
The High Resolution Visible (HRV) Meteosat Second Generation (MSG) satellite images for a) 1345Z, b) 1400Z, c) 1415Z and d) 1430Z are depicted from top left to the bottom right, for 22 November 2007. Copyright (2013) EUMETSAT

IR10.8 $\mu$ m satellite imagery



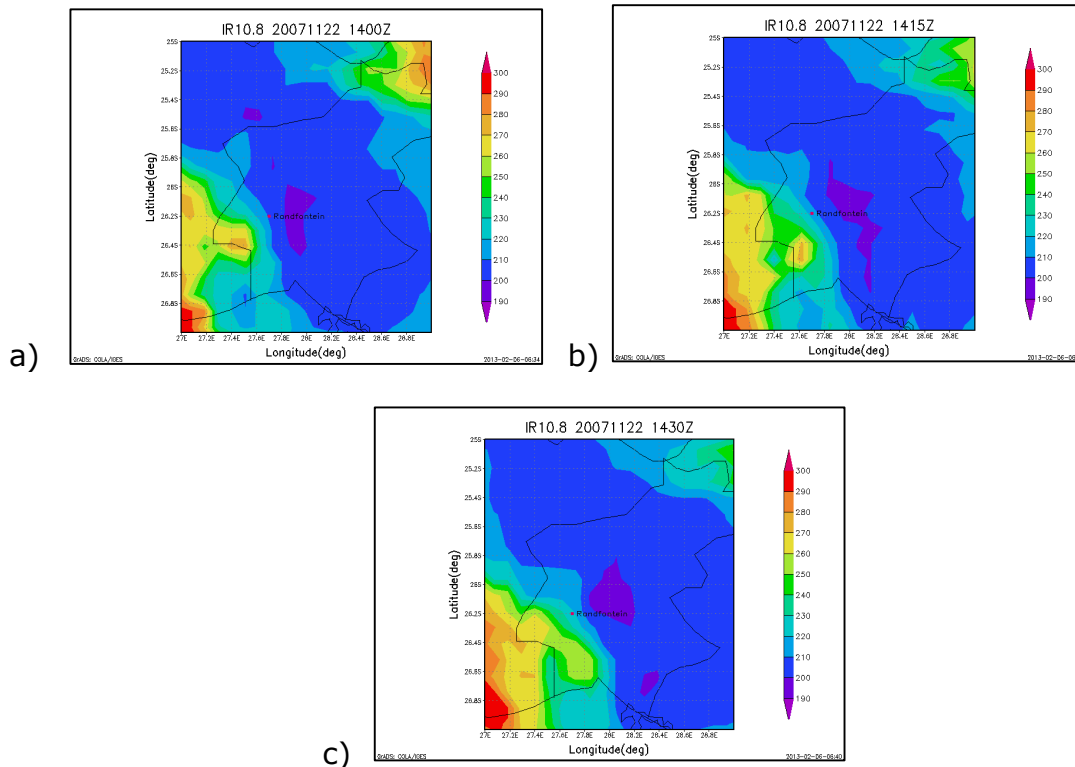
The Infra Red (IR) 10.8 $\mu$ m Meteosat Second Generation (MSG) satellite images for a) 1345Z, b) 1400Z, c) 1415Z and d) 1430Z are depicted from top left to the bottom right, for 22 November 2007. Copyright (2013) EUMETSAT

Convection RGB



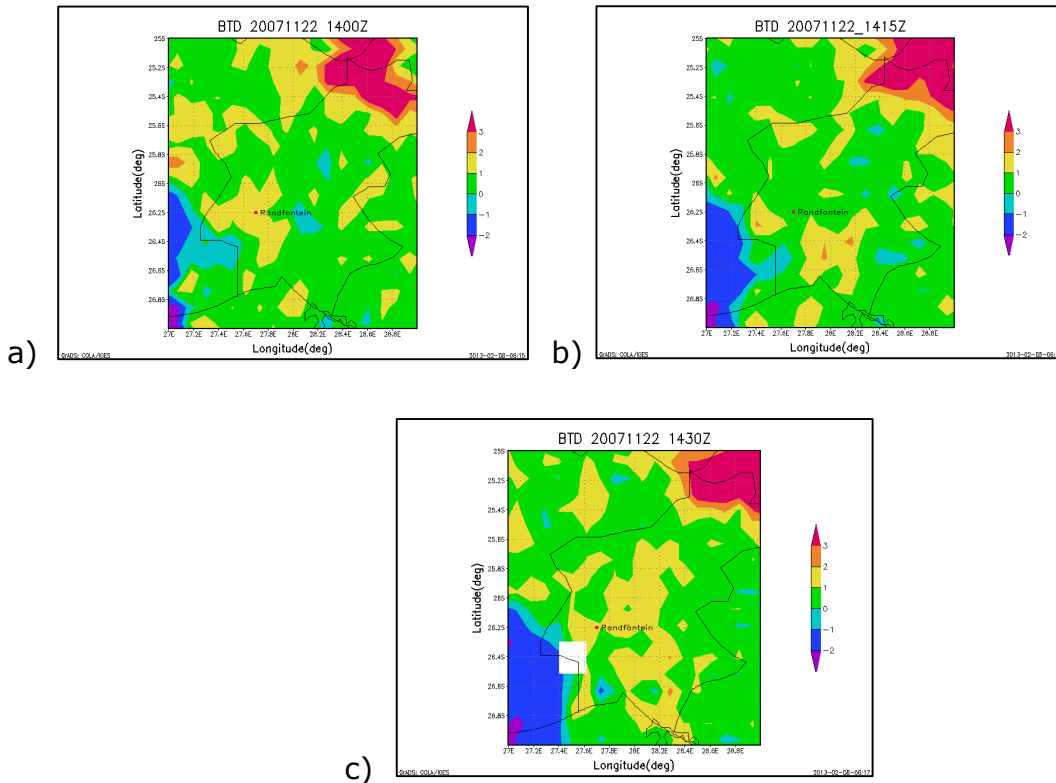
The convection combination (RGB) Meteosat Second Generation (MSG) satellite images for a) 1345Z, b) 1400Z, c) 1415Z and d) 1430Z are depicted from top left to the bottom left, for 22 November 2007. Copyright (2013) EUMETSAT

GrAds display of IR10.8 $\mu$ m satellite data



Grid Analysis display system (GrAds) imagery of Infra Red (IR) 10.8 $\mu$ m data in degrees Kelvin (K) at a) 1400Z, b) 1415Z and c) 1430Z on 22 November 2007. Copyright (2013) EUMETSAT

BTD data

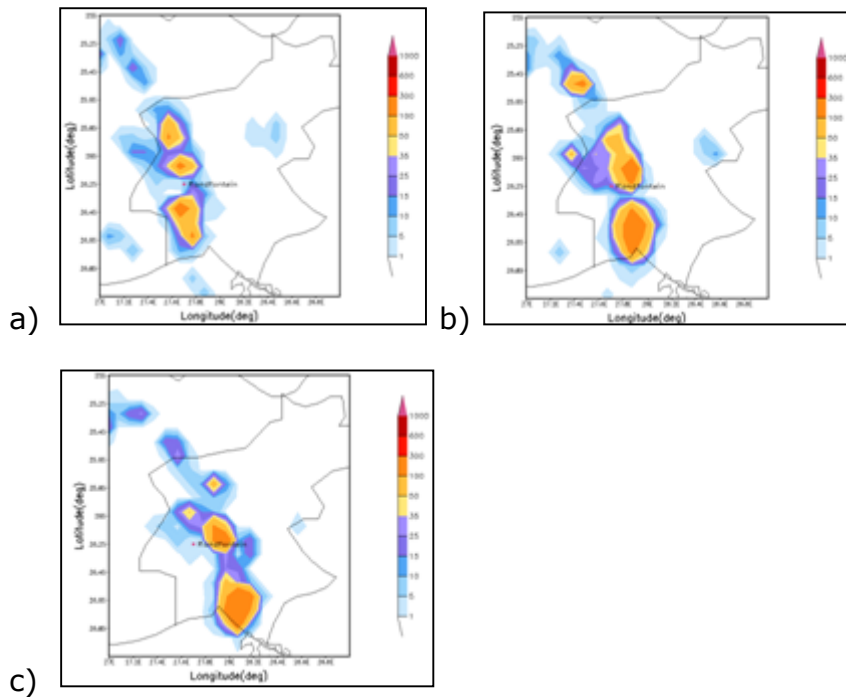


Grid Analysis display system (GrAds) imagery of Brightness Temperature Difference (BTD) of IR8.7µm-IR10.8µm measured in K at a) 1400Z, b) 1415Z and c) 1430Z on 22 November 2007. Copyright (2013) EUMETSAT



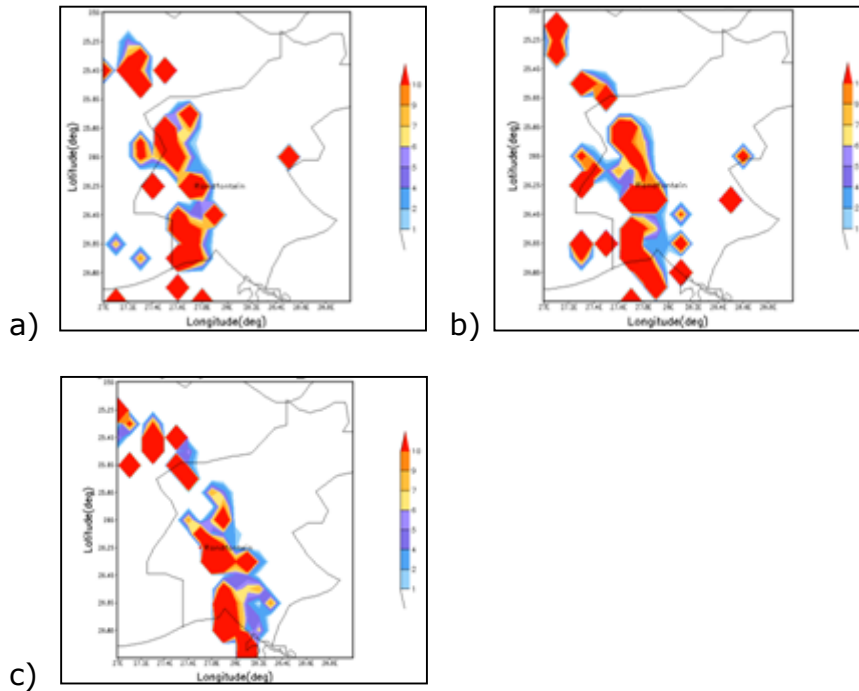
## Lightning data

### Stroke accumulation



Sum of the lightning strokes detected over the Gauteng Province are depicted between a) 1345Z and 1400Z, b) 1400Z and 1415Z and c) 1415Z and 1430Z on 22 November 2007.

## Percentage positive strokes



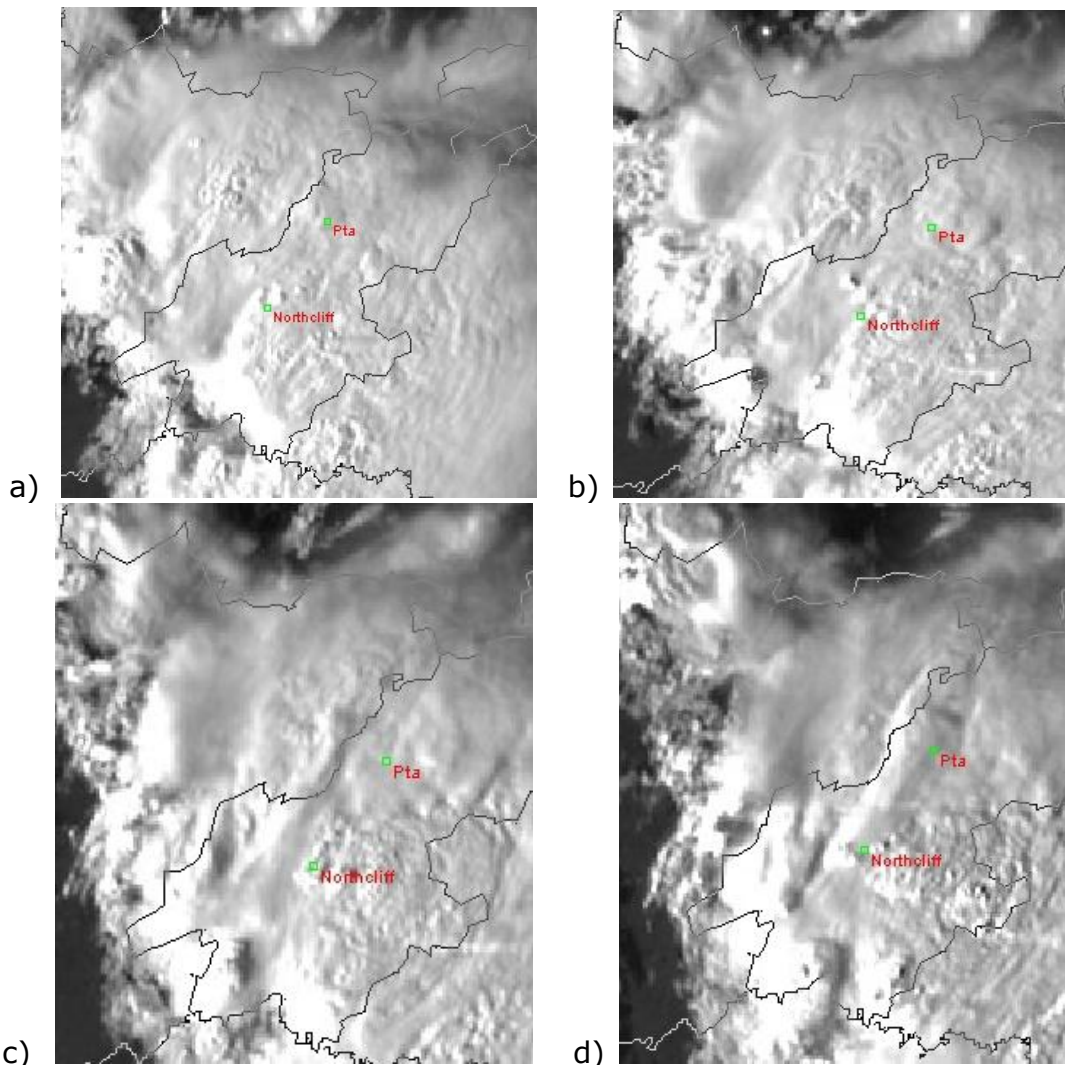
The percentage (%) of positively charged lightning strokes over the Gauteng Province are depicted between a) 1345Z and 1400Z, b) 1400Z and 1415Z and b) 1415Z and 1430Z on 22 November 2007.

## **APPENDIX C**

This appendix contains the imagery for the case study of 22 November 2007 at 1503Z, where a woman was killed by lightning in Northcliff, Gauteng Province. The figures that follow are of the sequence of events from 1445Z until 1530Z for both satellite and lightning data.

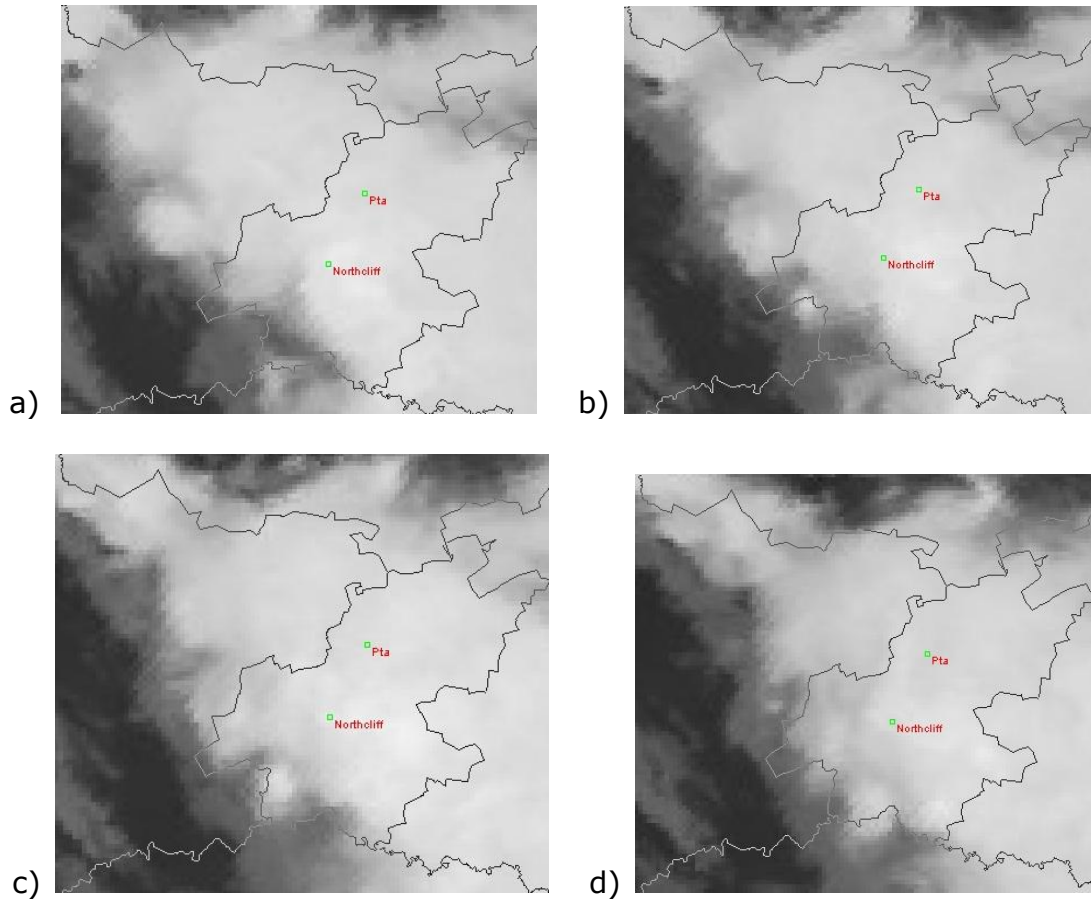
### **Satellite data**

#### HRV satellite imagery



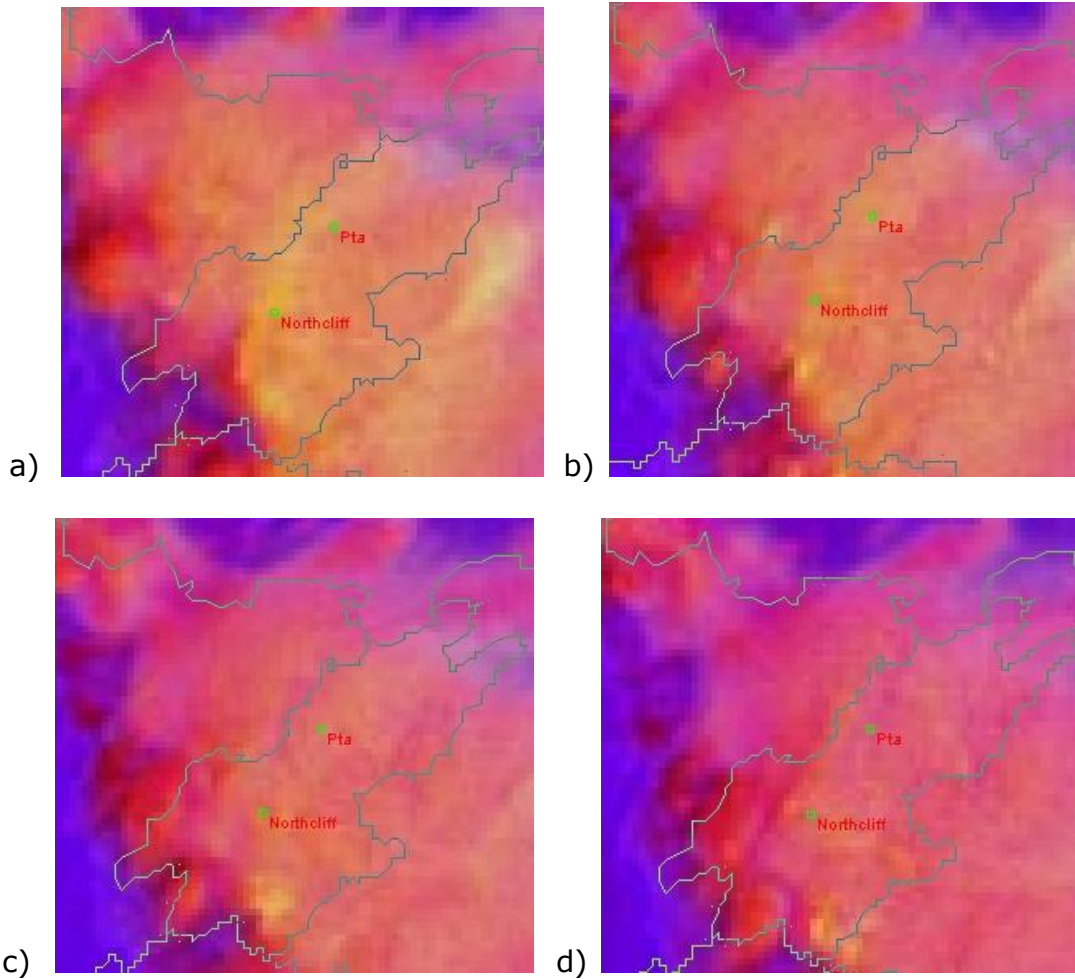
The High Resolution Visible (HRV) Meteosat Second Generation (MSG) satellite images for a) 1445Z, b) 1500Z, c) 1515Z and d) 1530Z are depicted from top left to the bottom right, for 22 November 2007. Copyright (2013) EUMETSAT

## IR10.8 $\mu$ m Satellite Imagery



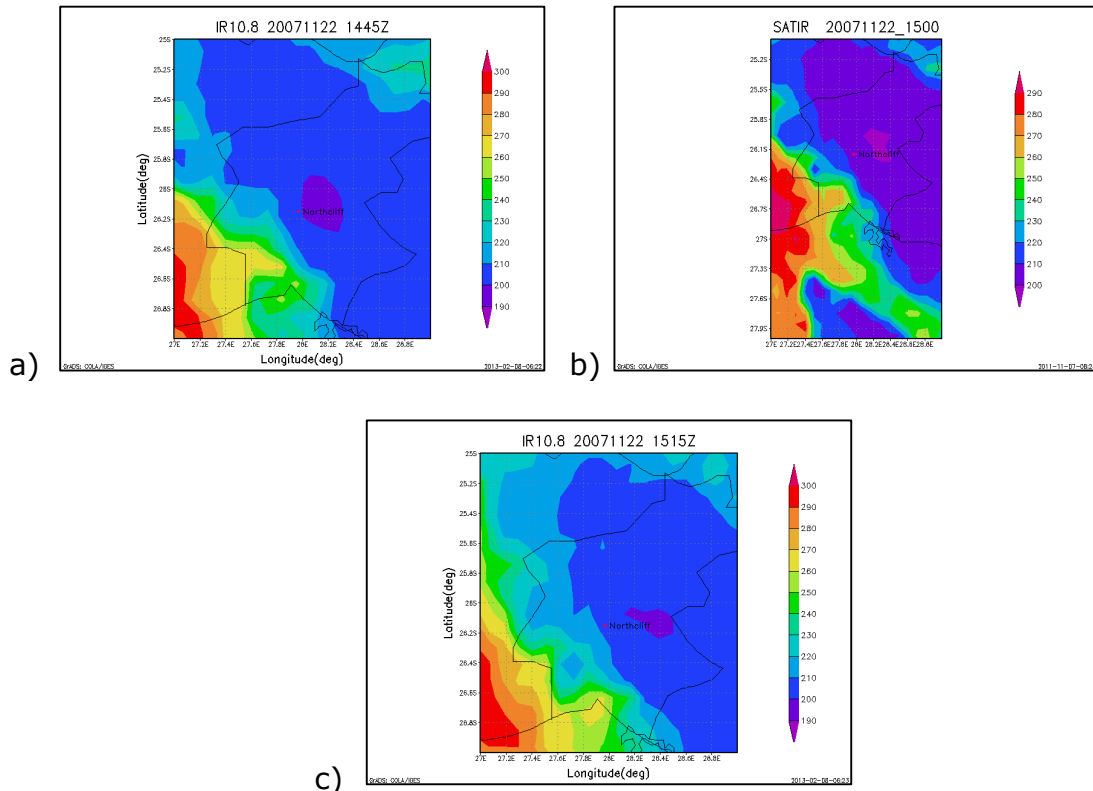
The Infra Red (IR) 10.8 $\mu$ m Meteosat Second Generation (MSG) satellite images for a) 1445Z, b) 1500Z, c) 1515Z and d) 1530Z are depicted from top left to the bottom right, for 22 November 2007. Copyright (2013) EUMETSAT

## Convection RGB



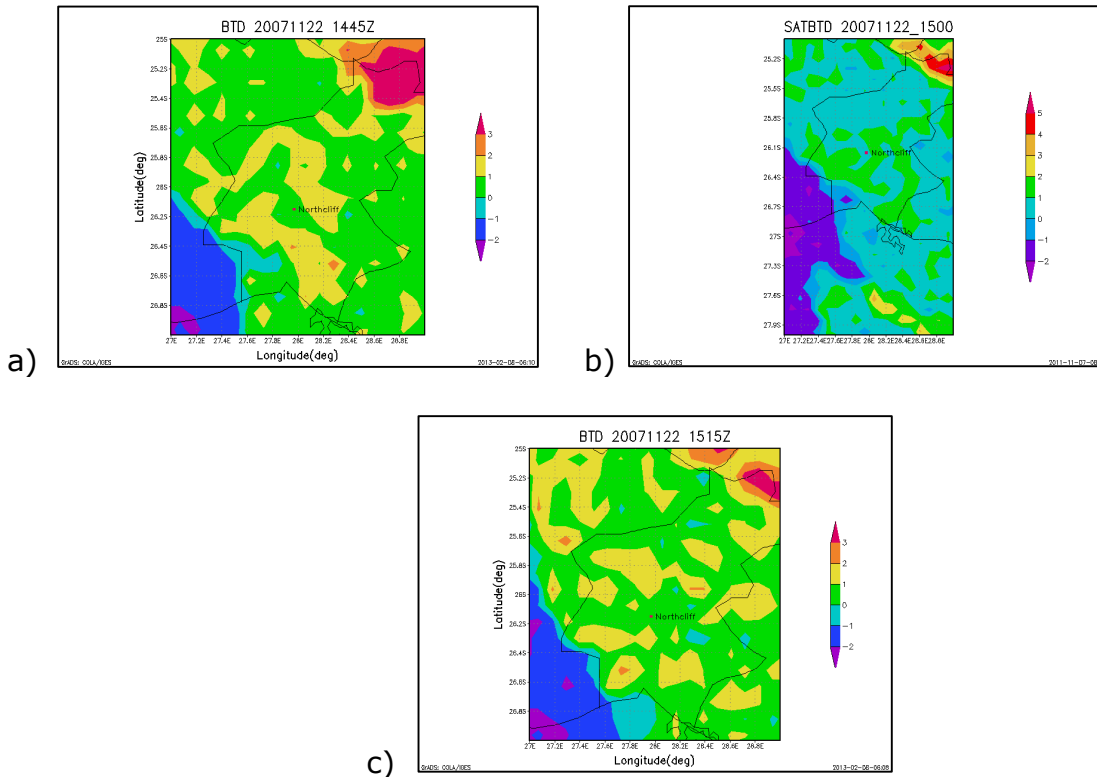
The convection combination (RGB) Meteosat Second Generation (MSG) satellite images for a) 1445Z, b) 1500Z, c) 1515Z and d) 1530Z are depicted from top left to the bottom right, for 22 November 2007. Copyright (2013) EUMETSAT

IR10.8 $\mu$ m Satellite Data



Grid Analysis display system (GrAds) imagery of Infra Red (IR) 10.8 $\mu$ m data in degrees Kelvin (K) at a) 1445Z, b) 1500Z and c) 1515Z on 22 November 2007. Copyright (2013) EUMETSAT

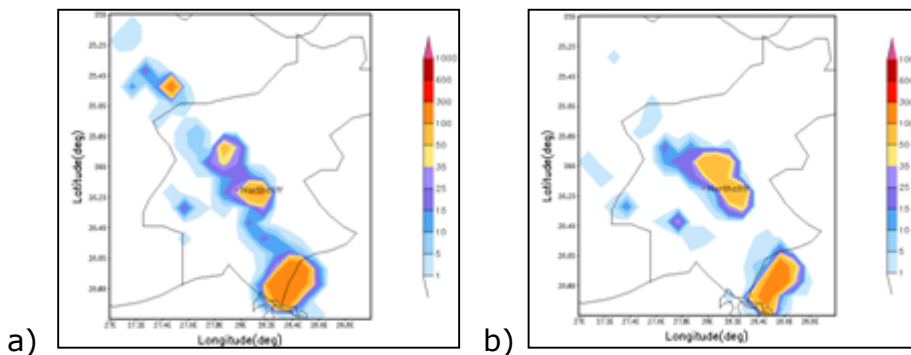
## BTD data



Grid Analysis display system (GrAds) imagery of Brightness Temperature Difference (BTD) of IR8.7µm-IR10.8µm measured in K at a) 1445Z, b) 1500Z and c) 1515Z on 22 November 2007. Copyright (2013) EUMETSAT

## Lightning Data

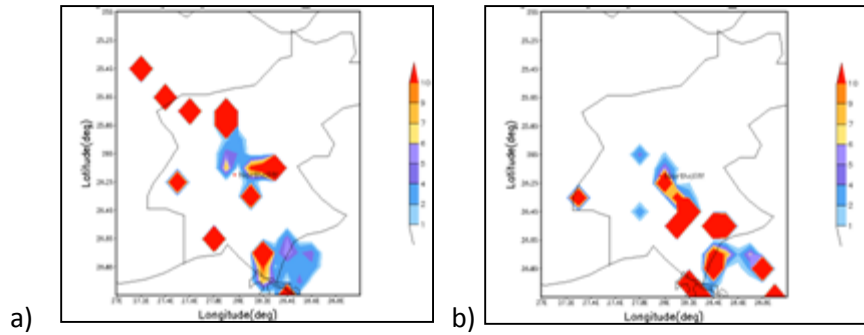
### Total Strokes



Sum of the lightning strokes detected over the Gauteng Province are depicted between a) 1445Z and 1500Z and b) 1500Z and 1515Z on 22 November 2007.



## Percentage Positive strokes



The percentage (%) of positively charged lightning strokes over the Gauteng Province are depicted between a) 1445Z and 1500Z and b) 1500Z and 1515Z on 22 November 2007.